LAPPEENRANTA-LAHTI UNIVERSITY OF TECHNOLOGY LUT
School of Energy Systems
Energy Technology
Master's Thesis

Ilari Kosonen

Operation and Dynamics of Cogeneration in Microgrids; Mitigation of the Challenges with Uninterruptible Power Systems

Examiners: Professor, D.Sc. Esa Vakkilainen
Research Assistant, M.Sc. Kari Luostarinen

Instructors: Technology Manager, B.Eng. Janne Paananen

ABSTRACT

Lappeenranta-Lahti University of Technology LUT
School of Energy Systems
Energy Technology

Ilari Kosonen

Operation and dynamics of cogeneration in microgrids; mitigation of the challenges with uninterruptible power systems

Master's Thesis
2020
112 pages, 33 figures, 22 tables, and 1 appendix
Examiners: Professor, D.Sc. Esa Vakkilainen and Research Assistant, M.Sc. Kari Luostarinen
Instructors: Technology Manager, B.Eng. Janne Paananen

Keywords: CHP, UPS, microgrids, distributed generation, system dynamics, adjusting power, energy investments

This thesis analyzes the challenges of distributed combined heat and power (CHP) in microgrids and utilizes uninterruptible power systems (UPS) to mitigate the problems. The objectives are to examine the system's operational and dynamical stability when the microgrid is islanded, find configuration parameters for the UPS grid regulation, and assess the overall feasibility of different CHP and UPS combinations.

The research consists of a literature review, CHP supplier interviews, modeling and simulation, and profitability assessment. The primary challenges of CHP in islanded microgrids are slow adjustability, leading to problems in meeting power generation and load, and the low rate of change of frequency (ROCOF) toleration of 2.0 Hz/s. UPS can meet the load imbalances and ensure low ROCOF, but the CHP technologies with small inertia or long time constants will require more continuous support during islanded.

Feasible CHP and UPS systems in under the 5 MW power range are biomass-fueled organic Rankine cycle and gasification technologies, and gas-powered spark-ignition engine. The biomass-fueled systems are especially profitable if the peak operating time is high and all thermal energy can be utilized efficiently.

TIIVISTELMÄ

Lappeenrannan-Lahden teknillinen yliopisto LUT

Energiajärjestelmien osasto

Energiatekniikan koulutusohjelma

Ilari Kosonen

Yhteistuotannon toiminta ja dynamiikka mikroverkoissa; haasteiden lieventäminen keskeytymättömien virransyöttöjärjestelmien avulla

Diplomityö

2020

112 sivua, 33 kuvaa, 22 taulukkoa ja 1 liite

Tarkastajat: Professori TkT Esa Vakkilainen ja tutkimusassistentti DI Kari Luostarinen

Ohjaajat: Teknologiajohtaja ins. Janne Paananen

Hakusanat: CHP, UPS, mikroverkot, hajautettu tuotanto, järjestelmädynamiikka, säätövoima, energiainvestoinnit

Työssä analysoidaan hajautetun sähkön ja lämmöntuotannon (CHP) haasteita mikroverkoissa ja hyödynnetään keskeytymättömiä virransyöttöjärjestelmiä (UPS) ongelmien lieventämiseksi. Tavoitteena on tutkia järjestelmän toimintakykyä ja vakautta mikroverkon saarekekäytössä, löytää konfigurointiparametrit UPS:n verkkotuelle, ja arvioida eri CHP- ja UPS-yhdistelmien toteutettavuutta.

Tutkimus koostuu kirjallisuuskatsauksesta, CHP-järjestelmätoimittajien haastatteluista, mallintamisesta ja simuloinnista sekä kannattavuuden arvioinnista. CHP:n ensisijaiset haasteet saarekeverkoissa ovat hidas säädettävyys, mikä johtaa ongelmiin tuotannon ja kulutuksen tasapainottamisessa, ja taajuuden muutosnopeuden (ROCOF) matala 2.0 Hz/s sietokyky. UPS pystyy vastaamaan sähköjärjestelmän epätasapainoon ja varmistamaan alhaisen ROCOF:n, mutta vähäisen inertian tai pitkät aikavakiot omaavat tekniikat tarvitsevat jatkuvatoimisempaa tukea saarekekäytössä.

Toteutettavissa olevat alle 5 MW:n tehoalueella toimivat CHP- ja UPS-järjestelmät ovat biomassapohjaiset orgaaniseen Rankine prosessiin ja kaasutukseen perustuvat tekniikat, ja kaasukäyttöinen kipinäsytytteinen iskumäntämoottori. Biomassaa käyttävät järjestelmät ovat erityisen kannattavia, jos huipunkäyttöaika on korkea ja kaikki lämpöenergia saadaan hyödynnettyä tehokkaasti.

PREFACE

This thesis was made for Eaton as part of the business development project named Helios. The project is designed to research innovative ideas for utilizing uninterruptible power and energy storage systems in the future of growing renewables. Thank you, Eaton, for the opportunity.

I would like to thank my instructor Janne Paananen for the subject and great conversations throughout the process. I value the time and sharing insights on the energy industry both inside and outside the research boundaries. I would also like to express my gratitude to Mika Lindén for the possibility to perform a thesis within the Helios-project.

From the university, I would like to thank my examiners Esa Vakkilainen and Kari Luostarinen for the guidance and fast responses when needed. I feel the thesis obligations were always clear and the process went smoothly.

The best thanks also to the whole project engineering team and my manager. I believe time management was one of the key factors for finishing the thesis, and you made it possible.

I enjoyed my time in LUT and the five years went rapidly. I made lifelong friends, had the privilege to go to student exchange, and the chance to apply the learned knowhow in the working life. In this context, I would like to thank the people who have enabled the career development.

Finally, I appreciate the continuous support from my family, friends, and of course, the better half.

Espoo, December 2020

Ilari Kosonen

TABLE OF CONTENTS

NOMENCLATURE

Greek symbols

η	efficiency	%
ω	angular velocity	rad/s

Roman symbols

C	cost	€
D	frequency sensitivity of the load	%
E	energy	J
f	frequency	Hz
F	transfer function	s
H	inertia constant	s
i	interest rate	%
I	investment	€
J	moment of inertia	kgm^2
P	active power	W
p	pressure	Pa
Q	reactive power	var
r	ramping rate	%/s
R	speed regulation	p.u.
s	entropy	J/K
S	generator power	W
T	temperature or torque	°C or Nm
t	time or time constant	s
U	voltage	V
Y	valve position	%

Sub-indices

a	annual
anc	ancillary
bat	battery
c	control
ch	chest and the inlet piping
co	crossover
d	demand
e	electric
f	fuel
g	generator

gv	governor
hp	high pressure
ip	intermediate pressure
k	kinetic
l	load
lfc	load frequency control
lp	low pressure
m	mechanical
max	maximum
meas	measured
net	net
nom	nominal
om	operation and maintenance
ref	reference
rh	reheater
s	synchronous
set	set
ss	steady-state
sys	system
t	turbine
tg	turbine-generator
th	thermal
tie	tie-line
tot	total
ups	uninterruptible power supply
v	variable

Compounds

CO	carbon monoxide
CO_2	carbon dioxide
HC	hydrocarbon
NO_x	nitrogen oxides
O_2	oxygen
R-HCO	aldehyde
SO_x	sulfur oxides
VOC	volatile organic compound

Abbreviations

AC	alternating current
AGC	automatic generation control

AVR	automatic voltage regulator
BAT	best available technology/techniques
BFB	bubbling fluidized bed
BMEP	brake mean effective pressure
BMS	battery management system
BREF	best reference
CB	circuit breaker
CFB	circulating fluidized bed
CHP	combined heat and power
CIGRE	International Council on Large Electric Systems
DC	direct current
DFIG	doubly-fed induction generator
DG	distributed generation
EEA	European Energy Agency
EMC	electromagnetic compatibility
EMEA	Europe, the Middle East, and Africa
ENTSO-E	European Network of Transmission System Operators
EPA	Environmental Protection Agency
ESS	energy storage system
ETN	European Turbine Network
FC	fuel cell
FCR	frequency containment reserve
FL	feeder line
GS	generator system
HHV	higher heating value
HP	high pressure
HV	high voltage
ICE	internal combustion engine
IEA	International Energy Agency
IEEE	Institute of Electrical and Electronics Engineers
IG	induction generator
IGBT	insulated gate bipolar transistor
IGV	inlet guide vane
IP	intermediate pressure
IRR	internal rate of return
LFC	load frequency control
LHV	lower heating value
LIB	lithium-ion battery
LP	low pressure
LV	low voltage
MG	motor-generator

MV	medium voltage
NPV	net present value
ORC	organic Rankine cycle
PCC	point of common coupling
PP	payback period
PV	photovoltaics
RES	renewable energy source
ROCOF	rate of change of frequency
ROI	return on investment
RV	residual value
SG	synchronous generator
SHP	separate heat and power
SI	spark-ignition
UHC	unburned hydrocarbons
UPM	uninterruptible power module
UPS	uninterruptible power system/supply
VRLA	valve-regulated lead-acid

1 INTRODUCTION

The global energy sector is in the transition towards more flexible and sustainable energy systems. The target of achieving a completely renewable energy based future has led governments, utility providers, and energy companies to change their perspective on conventional inflexible power generation capacity, directing more resources to clean energy innovations, technology, and infrastructure.

According to International Energy Agency (IEA) statistics, the share of renewables in global electricity generation was nearly 28% in the first quarter of 2020, including 9% of variable renewables in the form of solar photovoltaics and wind power (IEA 2020, 27-35). As renewable energy sources reach high competitiveness even without subsidies, the resulting challenge is not any more feasibility, but the lack of flexible power generation and energy storage capacity to enable stable electricity grids.

This thesis utilizes uninterruptible power systems (UPS) in combined heat and power (CHP) production, attempting to create more flexible and sustainable power generation. From an environmental standpoint, microgrids with renewable energy and CHP are an effective solution in reducing greenhouse gas emissions and primary energy use during the current decade (Ray et al. 2020, 22). Still, especially biomass-fueled plants are prone to operational difficulties, limiting their decentralized use drastically. If the challenges can be mitigated, it creates possibilities for replacing pollutant back-up or peaking generation with more efficient emission saving alternatives.

1.1 Background of the thesis

The initiative for this research originates from two business cases with challenges in integrating distributed CHP to microgrids. In the first business case, the CHP plant wanted to be operated in an islanded microgrid, but it could not fulfill the distribution network's stability and power quality requirements. Since the load deviations were rapid, the lack of operational flexibility would have caused issues in maintaining grid frequency and damage to the system components.

In the second business case, the CHP plant wanted to be connected to a distribution network with a strong share of wind energy, but the connection was prohibited due to excessive fault current levels. The grid connection required a fault current limiter, but this led to an idea of connecting converter-based energy storage in series with the CHP system. The solution would solve stability and power quality issues of the plant with a price of converter efficiency losses, but in turn, provide flexibility in operating the prime mover.

The third key driver for this research is the fact that data center clients are actively seeking ways to eliminate diesel generators from future sites. As they are pollutant, expensive and restricted only to emergency situations, other solutions would be preferred, but not by compromising the safety of the critical electrical loads.

1.2 Purpose and objectives of the thesis

The purpose of this thesis is to utilize UPS technology to overcome the challenges of CHP in the microgrids operational framework. The issues in the first business case are grid stability and system reliability in the islanded mode of operation, while in the second business case, the converter coupling would isolate the CHP unit from the grid, thus solving the power quality issues of the system. In the end, the objective is to find feasible solutions that can replace currently installed alternative technologies from future sites.

To achieve the objective, CHP technologies are studied from technical, operational, and economic perspectives, and the findings are compared. The dynamic response of CHP to load steps is simulated to find parameters for the UPS system. The profitability of different design options is assessed by using investment calculation methods. Finally, the feasibility is evaluated against alternative solutions. The primary research questions for this thesis are presented below.

(1) What are the challenges of CHP in islanded microgrids?

(2) How should EnergyAware UPS be configured to mitigate the emerged operational and dynamical problems?

(3) In which circumstances different CHP and UPS systems are feasible compared to the alternative solutions?

1.3 Structure and delimitations of the thesis

This thesis consists of theoretical and assignment phases. The theoretical part studies microgrids, CHP, and UPSs based on literature review and supplier interviews. The intention is to lead to the topic and gather data, which is processed in the next phase. The assignment phase consists of simulation and profitability assessment. The research plan and methodology are presented in Figure 1.1.

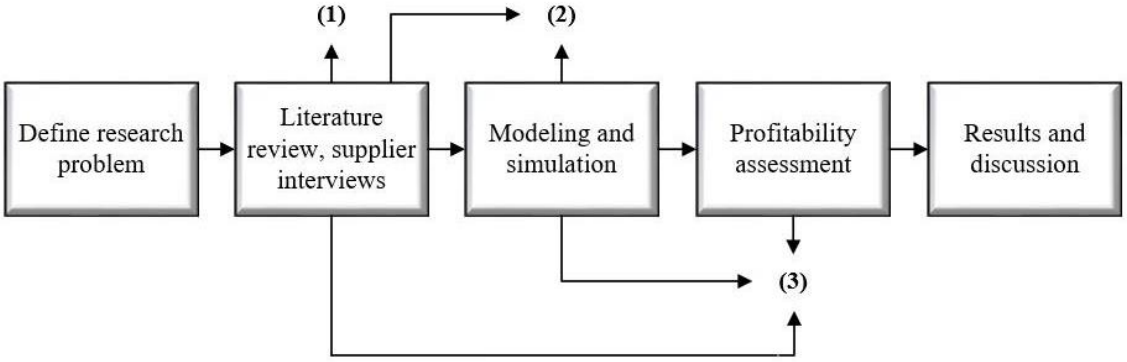

Figure 1.1: Research plan and methodology.

Chapter 2, Microgrids, studies microgrid operational modes, distributed generation, and control. Profound study regarding control methods, electrical circuits, and grid elements is delimited from the research. Also, it does not review smart grids.

Chapter 3, Combined heat and power, studies biomass-, biogas-, and natural gas-fueled CHP technologies. The primary focus is on operational characteristics, adjustability, and part-load performance. The electric power is delimited to 5 MW_e, but the main interest is 100 kW_e to 2 MW_e. In the end, the technologies are compared by also considering emissions and costs. Technologies without combustion are not studied.

Chapter 4, Uninterruptible power systems, studies double-conversion UPS's operation and its secondary applications in grid support. Other topologies are delimited from the research. The focus is on Eaton EnergyAware UPS technology enabling the secondary functions.

Chapter 5, Dynamics of CHP and UPS parallel system, studies the operational framework, reviews critical limitations for CHP operation, and analyzes the dynamics of the different design options. A turbine-generator system's frequency response to load steps is modeled and simulated in Matlab Simulink through transfer function analysis. The dynamics of engine-generator systems are delimited from the study as Eaton has already researched them.

Chapter 6, Profitability assessment, evaluates payback of the selected CHP technologies compared to diesel generator back-up system. The investment needed for the different CHP and UPS parallel systems is calculated based on CHP ramping capabilities and start-up time. The payback time for the investments is calculated using investment calculation methods as opposed to purchased electricity and heat.

Chapter 7, Results and discussion, answers to the research questions and analyzes their meaning. The CHP and UPS series system's feasibility, related to the second business case, is only presented in this part of the thesis based on the research findings. In addition, suggestions for future research are made.

2 MICROGRIDS

Microgrids are electricity distribution systems containing various distributed energy resources and electrical loads that are connected to the main power network or islanded. They can enhance power quality and reliability, allow broad utilization of localized generation, and provide operational benefits in conjunction with the primary grid.

This chapter defines the concept and functionality of microgrids by going through operational modes, distributed generation, and control methods. The focus is on managing the power balance and stability in the network as this research works with vulnerable applications, such as medical services and information technology, both containing critical electrical loads.

2.1 Fundamentals of microgrids

A microgrid is composed of energy generation, energy storage system (ESS), protection system, and control system or central controller, connected to each other in a single grid structure. Depending on the power generation and form of power consumption, the microgrids function with alternating current (AC) or direct current (DC) between the grid elements. Microgrids have two operation modes, the grid-connected mode and islanded mode, allowing more flexibility compared to the traditional power network. (Ray et al. 2020, 18.)

Microgrids are installed near the load, allowing beneficial use of local energy resources while also reducing the utility transmission and distribution losses. Compared to large conventional power generation with pollutant primary fuels like coal, microgrids are great platforms to integrate higher amounts of more environmentally friendly production such as renewable energy sources (RES) or decentralized combined heat and power to the energy system. From an environmental standpoint, RES and CHP based microgrids are considered as an effective solution in reducing greenhouse gas emissions and primary energy use during the current decade. (Ray et al. 2020, 19-22.)

In addition to energy generation and environmental aspects, microgrids provide functional and power quality benefits to users. As microgrids can isolate from the primary

distribution grid, it creates an additional layer of reliability for critical loads and helps to maintain continuity of the power supply. In the grid-connected mode, microgrids can transfer surplus power to utility or vice versa, enhancing power system stability with a better balance between generation and load demand. (Marnay et al. 2015, 25-29.)

2.1.1 Classification and structure

Microgrids can be classified based on generation capacity, load type, structure, and connection to the grid. Generally, when the generation is over 20 MW, the grid is named substation microgrid, whereas under 2 MW capacity is called simple microgrid. Between these sizes are corporate microgrids with 2-5 MW and feeder microgrids with 5-20 MW capacity. The load and installation further classify microgrids to military, campus, community, island, and remote microgrid categories. (Ray et al. 2020, 18-19.)

Grid connection and structure determine the best operational microgrid for each of the categories. For instance, in a remote microgrid, the AC structure is suitable in supplying the local load, while the DC type microgrid is more suited for heating purposes in universities and organizations. In military and corporate microgrids, the hybrid AC and DC arrangement is preferred to maintain reliability and increase load flexibility. Depending on the utility that the microgrid is connected to, they can also be classified as large grid-connected microgrids or small grid-connected microgrids. (Ray et al. 2020, 18-20.)

The hybrid microgrid consists of both AC and DC systems connected to each other through a bi-directional converter located between AC-DC busbars. Parallel to DC busbar can be DC power generation through DC-DC booster circuits, such as solar photovoltaics (PV) and fuel cells (FC), or AC power generation through a rectifier, for instance, wind turbine (WT) systems. Usually, the DC busbar also has ESS with a bi-directional DC-DC circuit. The AC system is structured similarly to the DC system, with direct AC power generation parallel to the AC busbar and possible ESS. Electric loads can be directly connected to either AC or DC busbar depending on the application. The utility power grid is connected to the AC busbar through a feeder line (FL). Figure 2.1 shows a hybrid AC-

DC microgrid structure with two points of common coupling (PCC). (Majumder 2014, 252-254.)

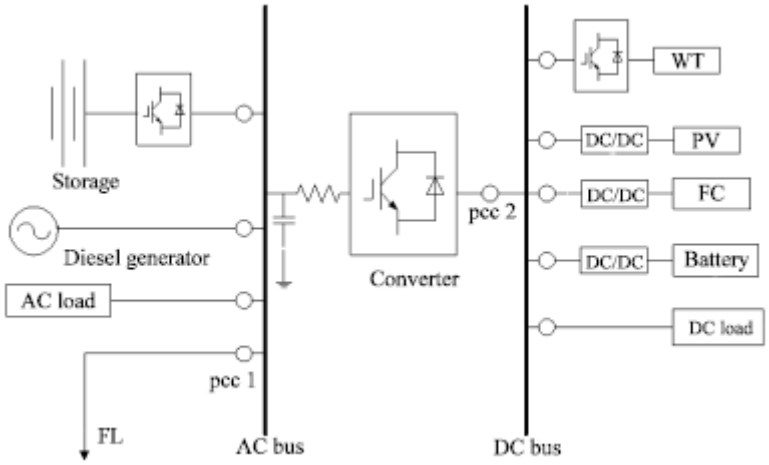

Figure 2.1: Structure of a hybrid AC-DC microgrid (Majumder 2014, 253).

As shown in Figure 2.1, the utility grid is connected to the AC bus via the feeder line, which has PCC1 breaker to change the microgrid operating mode. If the PCC2 breaker is open, the microgrid would work as a grid-connected AC microgrid and islanded DC microgrid. The microgrid could be modified to a plain DC microgrid by ignoring the AC bus and directly connecting the utility grid to a bi-directional AC-DC converter. (Majumder 2014, 252-254.)

The main disadvantages with DC-only microgrids are that most of the loads work on AC, requiring inverters to convert the current to a suitable form. However, DC microgrids have a more efficient supply to the load, grid connection is simple, and generation and load fluctuations can be easily managed using ESS to supply deficient power. Considering RES integration, the DC microgrid can easily handle controlling based on voltage, and the circulating current can be damped between the production sources. Additionally, rotating generators can operate at an optimal level as there is no need for synchronization. (Ray et al. 2020, 25.)

The main disadvantages with AC only microgrids are difficulties in grid operation and control. However, AC microgrids are preferable because almost all electrical loads work on the AC supply system, and they function without a bi-directional converter. DC

generation can also be connected to the AC bus by using converters. (Ray et al. 2020, 25-26.)

The hybrid microgrid, shown in Figure 2.1, has the advantages of both AC and DC microgrids while also avoiding the disadvantages of both structures. As a result, the most suitable generation, loads, and storage are connected to either AC or DC bus without unnecessary converters. The communication between AC and DC bus enables demand management, storage for excess generation, and performing of grid support functions. (Majumder 2014, 252-254.)

2.1.2 Grid-connected and islanded mode

In the grid-connected mode of operation, the microgrid exchanges power with the utility distribution network. Considering Figure 2.1, then PCC1 switch is closed. If PCC1 switch is disconnected, the microgrid isolates from the primary grid and goes to islanded mode with no power transfer with the utility. In hybrid microgrids, other parts of the network can be islanded while others are grid-connected, or both can be islanded, depending on the PCC connections. (Majumder 2014, 253.)

The prerequisite of all electricity grids is to maintain a constant power balance between power generation and consumption. If the utility grid is large enough, changes in loads caused by disconnecting individual applications will not significantly affect the voltage level or frequency. In the grid-connected operation, the utility stabilizes these changes in the microgrid, providing operational reliability. Secondly, the surplus power generation from a microgrid can be fed straight to other loads within the larger grid, reducing the stored energy and avoiding unnecessary power conversion losses. (Bordons et al. 2020, 20-25.)

The islanded mode of operation is preferred if the utility experiences grid-fault, affecting the protection of the loads. Maintaining power balance in an island network requires rapid voltage and frequency adjustment because fluctuations in consumption are higher in relation to the grid’s rated power. Generally, microgrids have some sort of rotating machines and equipment, at least back-up generators, together with energy storage to maintain the power balance. If the island network is supplied solely by power electronics,

the grid's maximum short circuit current can be significantly reduced, causing protection issues. In turn, the rotating mechanical masses involve large amounts of inertia, stabilizing the grid and increasing the allowed short circuit current limits. (Bordons et al. 2020, 20-25.)

2.2 Distributed energy production

As national networks were built, electric power was generated in large power stations and distributed long distances through the hierarchically constructed transmission system, featuring high voltage (HV), medium voltage (MV), and low voltage (LV) wiring with numerous substations. Because voltage and frequency balance had to be ensured, conventional fossil-fueled baseload generation was supported with faster, generally gas-fired, peaking, and load-following power plants. (Breeze 2014, 6-7.)

Most forms of current energy production methods do not fit into this traditional operational structure. Renewable energy, such as wind and solar, consists of relatively small units, often providing intermittent and unpredictable generation. Microgrids utilize more localized energy sources by integrating other power generation such as biomass-based CHP to the transmission network. The use of distributed generation (DG) allows meeting demand in a particular area with cleaner energy alternatives while also increasing efficiency due to reduced transmission losses. As the microgrid can be self-sufficient in terms of primary energy, the dependence of the main utility reduces, providing reliability during natural disasters or other grid anomalies. (Breeze 2014, 6-9.)

Despite the advantages, DG creates difficulties for the electrical networks. This section goes through the grid connection technologies for distributed energy production and reviews some of the posed stability and protection challenges, while Section 2.3 focuses on microgrid operational characteristics and controllability.

2.2.1 Stability of distributed power systems

The European Network of Transmission System Operators (ENTSO-E) describes future generation system to consist of numerous distributed and power electronics based generators, which provide intermittent and only partially transferable power.

Traditionally, network stability has relied on the characteristic and availability of conventional power generation through active and reactive power control, but the generation from RESs often does not contribute to energy reserves, system inertia, and grid voltage control on a larger scale. Consequently, the crucial challenge is the reliable balancing of power generation and load. (Klimstra et al. 2017, 60-62.)

The difficulty of managing energy production varies based on the distributed energy resource (DER). RESs are mostly intermittent, but forecasting has become better, and some areas indicate very predictable daily patterns, especially for solar PV. Wind energy is less predictable, but the power output can be regulated or even stored to some extent with the advanced grid connection technologies. The power output of conventional energy generation, such as steam and gas turbines or reciprocating engines, can be controlled directly with speed and load controllers, which regulate the fuel intake based on assigned frequency threshold. (Breeze 2014, 8-12.)

In addition to active and reactive power control, the inertial response of power generation is essential. Inertia in a power system limits the frequency deviation in the first seconds after an unexpected imbalance between generation and load, where the rate of change of frequency (ROCOF) is highly based on DER. As the main source of inertia is the kinetic energy stored in rotating masses, particularly generators and motors, the decrease in conventional generation will require rapid frequency response and higher ramping capability from the grid-connected generators to respond to the steep frequency dips or rises. One of the solutions from power converter connected generation is virtual inertia, which mimics the standard synchronous power generation and counteracts the deviations by controlling the systems' active power. (Tielens & Van Hertem 2016, 999-1003.)

Ensuring power quality in islanded microgrids is inherently more difficult compared to parallel operation with the primary grid. The Institute of Electrical and Electronics Engineers (IEEE) describes separated power systems as generally weak, underlining the higher probability of an islanded network experiencing high, abrupt, and more frequent frequency and voltage deviations from their nominal values. The combination of intermittent generation and small total inertia in the power system not only challenges power balance but especially grid protection. Maintaining the same parameters as in the

grid-connected operation would often lead to disconnecting DG and loads due to over and under frequency restrictions, which in the worst case causes system blackout. On the other hand, if too high deviations are allowed, it damages various equipment and devices, especially sensitive AC motors and electronics. Therefore, the critical design question is how large frequency and voltage variations are permitted to maintain grid stability without compromising the power quality and load protection. (Klimstra et al. 2017, 62; Sulla 2009, 25-26.)

2.2.2 Grid connection technologies

From the electrical system perspective, the grid connection technologies are not divided based on the prime mover or fuel source, but rather on how the electricity is produced. Generally, there are two major interconnection technologies: synchronously connected and indirectly or non-synchronously connected. The synchronous connection means that the mechanical energy is converted to the AC electrical power directly at the grid's voltage and frequency, while the indirect connection utilizes asynchronous generators, DC-generators, or power electronics to adapt to the requirements. (Klimstra et al. 2017, 49-51.)

The use of generator systems in the production of electrical energy is the foundation of power generation. Essentially all large conventional power plants use synchronous generators (SG), which consist of three essential components, the stator, the rotor, and the exciter system. The exciter system provides DC for the DC rotor winding, while the rotor winding produces a magnetic field, inducing AC in the stator winding. The electrical frequency of the stator voltage is interrelated to the mechanical speed of the rotor and the number of generator poles. As the rotational speed is directly related to frequency, in ideal conditions, the power generation system regulates the generator shaft to operate at a constant speed, producing steady AC power regardless of the load demand. SGs maintain good transient stability, but a large power imbalance can be problematic if the generation system has small inertia constant. (Jenkins et al. 2010, 46; Laaksonen et al. 2008, 499.)

Wind turbines, microturbines, hydro turbines, and reciprocating engines may use an induction generator (IG) or a more advanced doubly-fed induction generator (DFIG).

They consist of a squirrel-cage rotor and armature winding on the stator. In generator operation, a prime mover drives the rotor above the synchronous speed, which causes the induction motor to send power back to the electrical grid. The main advantage of IGs is that the frequency is independent of the prime mover speed variations. As a result, they do not require accurate speed control or synchronizing. However, during a voltage dip, an induction motor may stall and may not be able to accelerate its load when the supply voltage is restored to normal. During speed loss, the slip of the induction motor will increase with an increase in the line current. Constant loads with low inertia will rapidly decelerate, and the continuity of the output can be lost. The islanded operation and black start may also turn problematic in isolated power systems due to large current feed and voltage drop when starting the motor. (Jenkins et al. 2010, 50; Laaksonen et al. 2008, 499-500.)

Solar PV and fuel cells that generate DC electricity, or micro-turbines that provide electrical power with high-speed permanent magnet or induction, require adaptation to the mains frequency before connection to the electrical grid. Generally, power electronics is needed to convert the DC or high-frequency AC into mains AC frequency and voltage if the DC bus is not available. In the case of DC, the power electronics have an initial DC-DC stage for controlling the load and maintaining a stable voltage stack before the DC-AC converter generates ideal sinusoidal AC power. In the case of high-frequency AC, the power electronics have an AC-DC rectifier and DC-AC inverter to perform the power conversion. Figure 2.2 shows a schematic of the grid connection for a prime mover with an induction generator and requires power electronics to adapt to the grid requirements. (Klimstra et al. 2017, 58-59.)

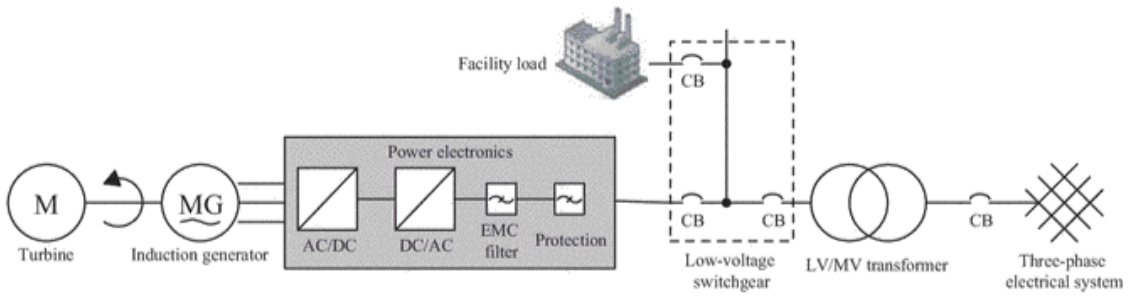

Figure 2.2: Schematic of grid connection with power electronics (Klimstra et al. 2017, 59).

As shown in Figure 2.2, power electronics typically utilizes active and passive electromagnetic compatibility (EMC) and protection filters for harmonics distortion control in the output. In addition, reactive power control or other protection features can be included. If needed, the generation system can be isolated from the LV switchgear by activating the circuit breaker (CB), or if the facility load cannot be met, the utility grid can transfer power through the LV/MV transformer. (Klimstra et al. 2017, 59.)

The stability of converter-connected DG is based on the used technology. Short duration voltage disturbances have typically led to tripping of the older frequency converter drives. However, modern self-commutated converters with fully controllable components come with higher stability and better power quality. For a voltage source converter based DG unit, a sudden decrease in grid voltage may trip the unit because of overcurrent as the control attempts to maintain steady power at the DC link. (Laaksonen et al. 2008, 501.)

The reconnection of the islanded microgrid back to the utility requires synchronization of DG sources in relation to mains. The balancing of voltage angle difference is not an issue for converter connection, but the SG interface cannot tolerate significant phase difference during microgrid reconnection without losing rotor angle stability. As a result, the mistimed reconnection with a large phase difference loses the islanded microgrid's frequency stability. (Laaksonen et al. 2008, 501-502.)

2.2.3 **Fault current from distributed generators**

Every rotating electrical machine, generators as well as motors produce fault current into a short circuit in the electrical grid. Short circuit current stability is essential, as excessive amounts will overload CBs and distort cables, whereas too low levels make the detection of over-currents difficult for the protection systems. As a result, it is important to assess the grid's short circuit rating and the fault current amount of the generator before the grid connection is acceptable. (Jenkins et al. 2010, 96.)

Achieving good power quality in a distribution system needs the short circuit level to be high, and it needs to approach the rating of the switchgear and other system components. This arrangement stabilizes the voltage variation in the grid when connecting large loads or starting large generators and ensures detection of the over-currents. If the short circuit

level is already high, then new grid connections may lead to excessive fault current and be prohibited. (Jenkins et al. 2010, 96-97.)

As distributed generators are relatively small and fault current is in line with the machine size and rating, the reliable and rapid detection of faults using short circuit current is difficult. Distribution networks are often protected with time-delayed over-current protection, which may require considerably high fault currents compared to the circuit's continuous rating to operate quickly. Therefore, a small generator's capability to deliver enough fault current needs to be evaluated in the microgrid design. (Jenkins et al. 2010, 97.)

Generally, SGs provide the highest fault current, whereas power electronics can deliver it only during the initial first few cycles and cannot tolerate high, long-lasting short circuit levels. The short circuit capability of an IG is mostly between these two types. Grid connection through power electronics is practical if the short circuit level is already high, for instance, in wind farms, because it limits the fault current from a generator, while microgrids with low short circuit levels can increase the stability of the electrical network by connecting SG. If needed, also separate fault current limiting equipment is available. (Klimstra et al. 2017, 61; Jenkins et al. 2010, 104.)

2.2.4 **Grid supporting capabilities of distributed generation**

Table 2.1 compares microgrid supporting capabilities of different distributed generator and DER combinations based on research conducted by the International Council on Large Electric Systems (CIGRE). The selected energy resources WT, PV, CHP, and ESS and their grid connection technologies SG, IG, DFIG, and inverter are in line with the assumed operational framework of the thesis. The comparison is indicative, assuming average performance characteristics in each category. (Marnay et al. 2015, 42.)

Table 2.1: Microgrid supporting capabilities of different DERs and their grid connection technologies (Marnay et al. 2015, 42).

Support function	Generator	WT	PV	CHP	ESS
Frequency control	All	+	+	++	++
Voltage control, congestion management, and grid loss optimization	SG	++		++	++
	IG	-		-	-
	DFIG	+			
	Inverter	++	++	++	++
Power quality control	SG	no		no	no
	IG	no		no	no
	DFIG	+			
	Inverter	++	++	++	++
Black start capability	SG	+		+	+
	IG	no		no	no
	DFIG	-			
	Inverter	+	+	++	++
Islanded operation capability	SG	+		++	++
	IG	no		no	no
	DFIG	-			
	Inverter	+	+	++	++
Fault ride through capability	SG	-		-	-
	IG	--		--	--
	DFIG	+			
	Inverter	++	++	++	++

Legend		
	++	indicates very good capabilities
	+	indicates good capabilities
	-	indicates small capabilities
	--	indicates very small capabilities
	no	indicates no capabilities without auxiliary equipment
	blank	indicates combination is not applicable

As seen from Table 2.1, inverter-coupled distributed generators can provide all types of grid support services regardless of DER. Other grid connection technologies are more dependent on the energy resource as the intermittency of WT and PV systems restricts the availability and the active power control capabilities. In contrast, CHP and ESSs are very good at regulating both active and reactive power. In the islanded mode of operation, SG and inverter-coupling provide very good operational capabilities, while direct IG coupling is not possible. Conceptually, all the generators can be de-coupled to the grid by an inverter interface. In that case, the machine dynamics are independent of the grid requirements, allowing advanced power conditioning, better controllability, and reduced fuel consumption if designed accordingly. (Marnay et al. 2015, 38-42.)

2.3 Operation and control of microgrids

The previous sections studied the functionality of microgrids and raised a concern regarding reliable power management of DG. The purpose of this section is to meet the identified challenges with the proper operation and control methods. This thesis focuses on the system-level functionality and only summarizes the control modes concerning the microgrid and the connected distributed energy sources.

2.3.1 Power balance at the system level

As defined, microgrids operate in two modes, which are the grid-connected and islanded mode. The grid-connected mode is divided into power-mismatched and power-matched operational modes based on the power flow between the microgrid and the utility grid. If active power and reactive power are not equal to zero, there is a power exchange between the microgrid and the utility grid, referred to as the power-mismatched operation. When $\Delta P > 0$, the power flows from the network to the microgrid to fulfill the load demand, and if $\Delta P < 0$, the microgrid generates surplus power, which is transferred to the utility. Similarly, reactive power is inadequate if $\Delta Q > 0$, and excessive if $\Delta Q < 0$. In the power-matched operation, active and reactive power is balanced, so the microgrid generation meets the load demand ideally, and no additional power exchange is required. (Ray et al. 2020, 25-27.)

In power-mismatched operation, the microgrid can rely on the utility network's stable frequency because of the vast number of directly grid-connected generators and electric motors that provide inertia. If energy production exceeds consumption, the rotational speeds of power generation equipment start to accelerate, increasing the network's frequency. However, with large amounts of inertia, the rate of change is reduced, and microgrid level consumption changes do not reflect notably to the grid frequency. (Ray et al. 2020, 25-27.)

In an island network, the situation is more challenging since the microgrid functions in power-matched operation and balances all the active and reactive power between the grid elements. Because microgrids have small rated power and usually less inertia due to lack

of synchronously-coupled generators, the disconnection of individual loads may substantially affect the power balance. Maintaining a stable frequency is dependent on the control and adjustability of power generation, together with mandatory energy storage solutions such as batteries, supercapacitors, or flywheels. When adjusting power generation by output control, the response is usually too slow as the microgrid's inertia does not provide enough time for the changes. Consequently, to ensure stability during islanded operation, ESS must mitigate the rapid voltage and frequency imbalance. (Tielens & Van Hertem 2016, 1001-1007.)

When energy storage is the primary back-up power source in an island network, its capacity needs to be dimensioned considerably large to deliver the power corresponding to the island network consumption in case of zero production. In the opposite situation, where production is at its peak and consumption is low, the balance problem can be solved by limiting power generation, but it is preferred to store the surplus energy in storage than let it go to waste. (Tielens & Van Hertem 2016, 1003-1008.)

2.3.2 **Microgrid control modes**

Microgrids commonly have three generic control modes to manage the overall system: master-slave, peer-to-peer, and combined control. The preferred control mode is chosen based on the microgrid size and capacity among its generation and load components. Apart from these, DERs have their control modes for the grid-connected inverters and prime movers with generators, including active-reactive power (P-Q) control, voltage-frequency (V-f) control, and droop control. (Ray et al. 2020, 27.)

In master-slave control mode, one or group of power generation units, such as wind turbine group or ESS, act as a master while others are signed as slaves. The signed master works in V-f control mode as a reference for the other generation units when islanded. In grid-connected operation mode, all the units work in P-Q control, and utility PCC functions as a reference point for the system power flow. The master unit regulates frequency and voltage in relation to load instabilities, resulting in fast control response throughout the microgrid. As the main disadvantage, the V-f controlled master needs to

keep constant output voltage, and if it breaks, the microgrid system may fail. (Ray et al. 2020, 27-28.)

Peer-to-peer control mode is mainly used on power electronics. This control mode assigns each unit equal, and all participate in maintaining the voltage and frequency by regulating active and reactive power via pre-set control functions. Whether in islanded or grid-connected operating mode, units function based on droop control. If fluctuation occurs, the voltage and frequency are distributed between the units with a droop factor, and power generation tries to find a new steady-state by adjusting its output frequency and voltage amplitude. Therefore, this control mode is only proportional control, but the main advantages include simple transitions between operational modes, no need for communication, and good reliability. (Ray et al. 2020, 28-29.)

Combined control mode combines advantages of master-slave and peer-to-peer control modes and overcomes the disadvantages. In practice, the combined control mode is used when a single control mode is not enough to meet the microgrid's operational requirements. Because of many control modes within a grid and different control functions between the generation, this mode can achieve the most stable and reliable microgrid but comes with the most complexity. (Ray et al. 2020, 29.)

Regarding control of DG, one of the main strategies is droop control. Here the grid frequency and voltage magnitude are measured to regulate active and reactive power based on predefined droop characteristics. Figure 2.3 presents the basic principle behind this approach. When the voltage or frequency deviates from the desired value, it can be controlled by changing the power generation unit's active or reactive power or inversed. (Ray et al. 2020, 31-33.)

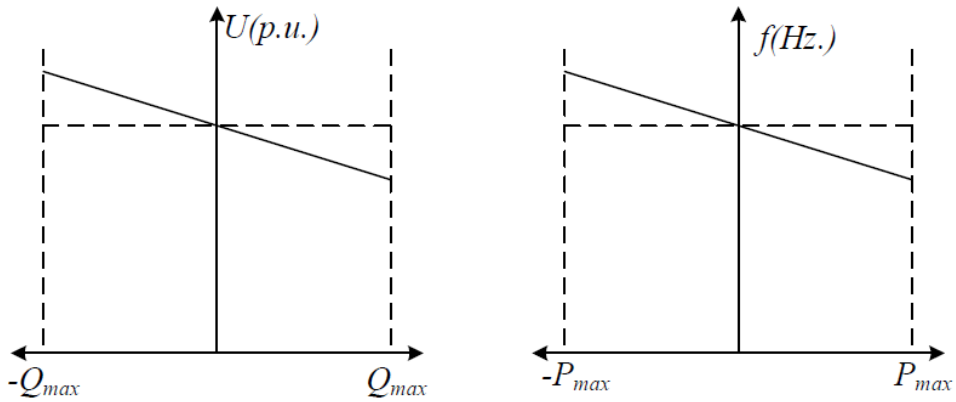

Figure 2.3: Microgrid droop control characteristics (Ray et al. 2020, 33).

By considering the horizontal dashed lines in Figure 2.3 as nominal for the grid voltage and frequency, a decrease in voltage and frequency requires an increase in reactive and active power to mitigate the change. The effort and time needed for the change are dependent on the grid-connected power generation, and thus ESSs are vital in ensuring sufficient adjusting time for the conventional generation or smoothing intermittent RESs. An example of a droop control response to a sudden decrease in grid frequency for a prime mover with a generator system is shown in Figure 2.4. (Klimstra et al. 2017, 65-66.)

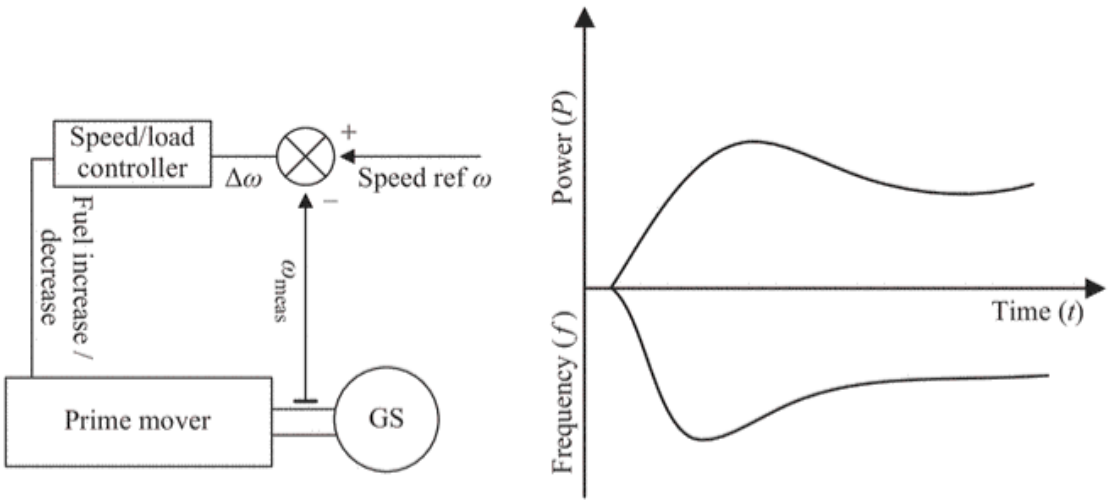

Figure 2.4: Droop control response to a decrease in frequency and the corresponding control schematic (Klimstra et al. 2017, 66).

As shown in Figure 2.4, the system senses a speed or frequency decrease of the generator and the speed or load controller regulates needed fuel input to stabilize the change. The

calculation is based on the rotational velocity difference (Δω) between the measured speed (ω_{meas}) and reference speed (ω). The frequency decline is prevented by increasing the system's active power, but the unit will not automatically bring the system to the nominal frequency and the time for the change depends on the prime mover characteristics. The droop control works similarly for reactive power control, but then voltage difference is used to calculate excitation increase or decrease for the generator system. (Klimstra et al. 2017, 65-66.)

Another active and reactive power control method for prime mover systems is isochronous control, so-called zero droop. Here the control schematic is the same, but the frequency or voltage is always controlled to a pre-set nominal level. Figure 2.5 presents isochronous control response to a change in grid voltage with reactive power parameters. (Klimstra et al. 2017, 68-71.)

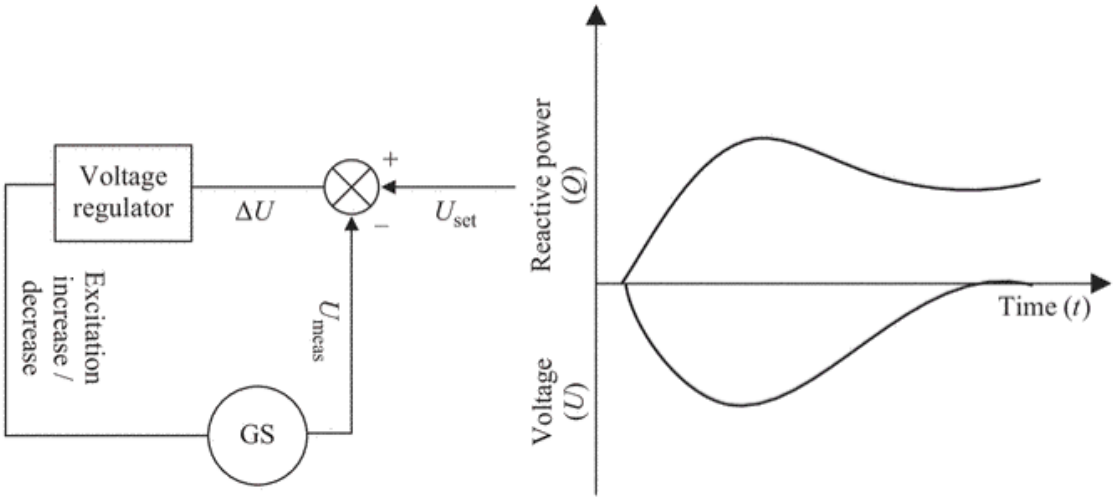

Figure 2.5: Isochronous control response to a decrease in voltage and the corresponding control schematic (Klimstra et al. 2017, 71).

As shown in Figure 2.5, the system senses a voltage decrease of the generator and the voltage regulator determines the needed excitation increase to achieve nominal voltage. The calculation is based on the voltage difference (ΔU) between the measured voltage (U_{meas}) and reference voltage (U_{set}). The voltage decline is equalized by creating a stronger magnetic field for the generator system, which provides more reactive power to the grid. (Klimstra et al. 2017, 71; Jenkins et al. 2010, 46-48.)

Both active and reactive power can be controlled with various other methods, especially when functioning parallel to the primary utility grid, but droop and zero droop control can be considered as the main prime mover control modes when islanded. The simple droop control has many advantages, including the possibility to parallel multiple generation units and do load sharing without the need for extensive communication. On the other hand, the isochronous control removes the need for additional control to reach nominal level requirements. (Klimstra et al. 2017, 65-72.)

In power electronics or grid-connected converters, the active and reactive power capabilities are generally limited by the internal voltage, temperature, and current limits. However, they are fast, customizable, and have many system protection features, including overcurrent control, islanding detection, and power quality management. With the right design, they can be considered the easiest and most reliable grid connection technology for microgrids, but in many instances, not the most cost-efficient. (Marnay et al. 2015, 41-43.)

3 COMBINED HEAT AND POWER

Combined heat and power, also known as cogeneration, is a form of energy production where electricity and heat are produced simultaneously in the same process. Cogeneration has higher overall efficiency compared to separate production, as the excess heat from electricity generation can be used in heating applications or various industrial processes.

This chapter studies the leading technologies for CHP applications focusing on 100 kW to 2 MW electrical power range with the delimitation of 5 MW. At first, the role of CHP is reviewed in the energy market. Secondly, the cogeneration technologies are examined with an emphasis on the operational characteristics, part-load performance, and controllability of the output power. To conclude, the different technologies are compared based on the collected data.

3.1 Role of cogeneration in the energy market

Secure, reliable, and affordable energy systems are a fundamental part of economic stability and development. The increasing energy needs of the world and continuing climate change pose significant challenges to the current energy production model, which has to be modified by adjusting the existing technologies to comply with the new environmental standards and support integrating emerging technologies and renewable energy sources. (IEA 2008, 5-9.)

CHP systems are advantageous in the current energy market because they can provide a variety of energy, environmental, and economic benefits. These benefits result mainly from avoiding wasted use of primary energy, reducing transmission and distribution losses, and increasing grid reliability. As a result, CHP systems provide increased energy efficiency, costs savings, lower emissions, enhanced electricity network stability, and guarantee resource adequacy. (Darrow et al. 2017, 13-21; European Commission 2008, 1-2; IEA 2008, 7.)

Large conventional power plants transform 35% to 60% of the energy in primary fuel to electricity based on the fuel source and plant characteristics. In a solely fossil-fueled power plant, the average efficiency is only 40%, and the remaining is lost as waste heat

to the environment in the form of exhaust gases and irreversible losses such as convection and radiation. In a CHP plant, the waste heat is recovered from the exhaust and cooling systems and further utilized to generate hot water and steam for buildings, industrial applications, and district heating. Depending on the fuel, plant design, and heat demand, a CHP unit can reach up to 90% total efficiency. Furthermore, the transmission and distribution losses from large power stations contribute to an average additional 5% of net generation, making CHP even more viable in terms of energy efficiency as it is located near the end-user. (European Commission 2013, 1-3; Spentzas 2009, 8-12; IEA 2008, 7-8.)

Cost savings from CHP applications are linked to reduced energy and operational costs as they provide useful energy services to facilities from a single process that requires less primary energy input compared to separate heat and power (SHP). In the larger perspective, decentralized CHP requires less transmission and distribution infrastructure, equalizes price volatility due to reduced grid congestion, and allows businesses to be more economically competitive on a global market by utilizing localized energy resources. It should also be noted that governments support most forms of modern CHP technologies as they are a viable near-term solution to reduce emissions. (Darrow et al. 2017, 13-14; IEA 2008, 7-9.)

The environmental aspect is the key motivator for the development of CHP technologies. By generating heat and power simultaneously, conventional fossil-fueled CHP can reduce carbon emissions by 20% to 30% compared to SHP. With renewable biomass and waste fuels in the energy mix, cogeneration can be carbon dioxide (CO_2) neutral, turning the technologies using RESs an even better contributor to the sufficiency of natural resources and climate change mitigation. In addition to reducing greenhouse gas emissions, CHP solutions can substantially lower the criteria air pollutants depending on the technology and fuel source. (Klimstra et al. 2017, 12-15.)

As cogeneration comprises of numerous different technologies and is not dependent on the primary fuel or power capacity, it can be effectively optimized for a specific function or application. The target can be a beneficial use of local or surplus energy resources, peak shaving, load following, or a less unpredictable way to integrate renewable energy

into the electricity grid. In addition, some CHP technologies operate with multiple fuels, providing much-needed flexibility at a time of growing fuel insecurity and dependence on imported fossil fuels. (Klimstra et al. 2017, 10-15.)

3.2 Cogeneration technologies

Cogeneration technologies can be divided into three categories by the size of the system: micro-CHP, small-scale CHP, and medium to large-scale CHP. Based on the European Parliament and of the Council directive on energy efficiency, micro-CHP units have maximum electrical power of 50 kW, and small-scale CHP systems are characterized to produce less than 1 MW. The larger systems are commonly referred without the specifying prefix. The categories are not defined based on thermal power output as it is closely related to the used technology. (2012/27/EU, Art 2.)

A typical CHP plant consists of a prime mover, electric generator, and equipment to recover and transfer the produced heat. Prime mover is a machine that converts the primary energy in fuel to mechanical energy, which is transformed into electricity with an electric generator. The heat produced from operating the prime mover is recovered and transferred to the application by utilizing heat exchangers. Conventional prime movers are combustion turbines, reciprocating engines, and steam turbines, while most newer technologies are their variations. This thesis first goes through the Brayton cycle processes, including microturbines, then reciprocating engine systems including gasification of biomass and Stirling engines, and finally through the traditional Rankine cycle and more innovative organic Rankine cycle (ORC). Other technologies like fuel cells and solar PV are not part of the research area. (Klimstra et al. 2017, 17; Takalo et al. 2013, 4-10; Kirjavainen et al. 2004, 8.)

Cogeneration technologies can operate with a variety of primary fuel sources. Gaseous fuels, light fuel oils, coal, biomass, and municipal waste are all used for CHP production. Depending on the technology, the cogeneration unit can utilize multiple fuels within the same process, but typically performance requirements of energy conversion components limit the usable fuel quality. Fuel composition is important as it is directly related to

emissions, but regardless of that, it also affects fuel combustion, maintenance needs, and fuel efficiency. (Sipilä et al. 2005, 11-12.)

Performance characteristics of the cogeneration technologies need to be estimated based on the application. For a long time, the market value of electrical energy has been considered higher than the same amount of thermal energy as electricity is more versatile than heat. It is also because electric power generation is more expensive than burning fuel in a boiler. Recently this generic view has altered because more RESs have been integrated into the electricity grid. In areas where most of the electricity is produced with solar panels and wind turbines, the market value of electric energy can be low or even negative during peak production times. The price volatility of the electrical energy means that the future cogeneration plants must be increasingly flexible, with adjustable power output, options for frequent shutdowns and start-ups, and load-following capabilities. (Klimstra et al. 2017, 17-18.)

In addition to the operational features, the emission limits are raising importance in determining a CHP unit's applicability. Best reference (BREF) and best available technology (BAT) of a typical technology are commonly used in defining limits for nitrogen oxides (NO_x), carbon monoxide (CO), sulfur oxides (SO_x), dust, and soot together with other pollutants like hydrocarbons (HC), aldehydes (R-HCO), and volatile organic compounds (VOC). (Klimstra et al. 2017, 17; Darrow et al. 2015, 22-24.)

The following sections go through biomass-, biogas-, and natural gas-fueled CHP technologies with combustion. Each section describes the functionality of the system and studies operational capabilities, part-load performance, and controllability of the produced electricity and heat. Besides, typical technical operating values and suppliers are presented. Thermal efficiency means the part of the fuel energy extracted to work, while total efficiency also considers the heat recovery. All efficiencies are given in the lower heating value (LHV) of the fuel unless otherwise stated.

3.2.1 **Combustion turbines**

Combustion turbines, also known as gas turbines, are the most extensively used prime movers for the large newly built cogeneration systems because they offer operational

flexibility, high power-density, and excellent reliability within a simple process. The system sizes are ranging from 500 kW to 300 MW for both power-only generation and CHP systems. For large utility-scale power plants, the most efficient technology is the gas turbine-steam turbine combined-cycle, whereas small-scale systems function primarily with simple-cycle gas turbines. This thesis does not cover combined-cycle power plants as their supplementary electricity generation process sequence from steam is intended for larger applications. From gas turbine models, this thesis focuses on the industrial version, as the aeroderivative systems are less common in continuous CHP applications. (Darrow et al. 2015, 54; DBEIS 2008, 30-33.)

Standard simple-cycle gas turbine operation is based on three consequent processes termed compression, combustion, and expansion. First, an axial or centrifugal compressor increases the pressure of intake air before the combustion stage. The combustion of fuel heats the medium, substantially increasing the volume of the initial airflow, which leads to a volumetric difference between upstream and downstream sections of the combustion chamber. As a result, the expansion turbine has enough mechanical energy to operate the air compressor and rotate the shaft of an electric generator at the same time. Figure 3.1 shows standard simple-cycle gas turbine process without a recuperator. (Klimstra et al. 2017, 18-19.)

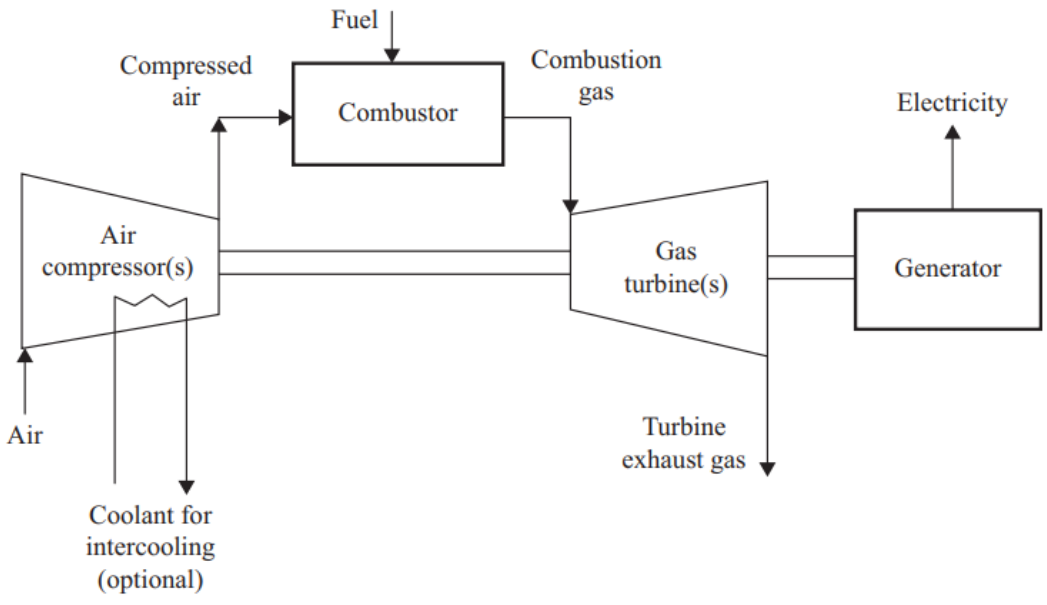

Figure 3.1: Standard simple-cycle combustion turbine process (Rosen et al. 2016, 59).

As seen from Figure 3.1, the turbine exhaust gas can be recovered from the expansion turbine, and the outlet temperature is in a range of 400-650 °C. Some designs include a recuperator that preheats the combustion air with the excess heat, increasing the electrical efficiency. However, it reduces the exhaust gas temperature and thus lowers the amount of thermal energy available. In theory, the exhaust temperature can be even higher than 650 °C by lowering the pressure ratio and increasing firing temperature, but for simplified process cycles, the pressure ratios are already low and cannot be decreased as it will negatively affect the thermal efficiency. The exhaust gas could be used to generate up to 80 bar steam. In this case, the ideal thermodynamic process is called the Brayton cycle, but these processes are not completely isentropic due to losses from flow friction, turbulence, and backflow at the blade tips. (Nadir et al. 2015, 811-825.)

Depending on the cogeneration application, it can be necessary to control the electrical output or the thermal output of a gas turbine. In smaller system sizes, the process configuration lacks bleed valves that blow-off some of the compressed air at lower loads and has no inlet guide vanes (IGV) that can adjust the air intake flow. Losses such as flow friction, mechanical friction, and backflow are not reducing in partial loads, which means that the operation with lower electrical output has a higher relative decreasing effect on the electrical efficiency. In simple-cycle designs, the electrical output is usually reduced by decreasing the turbine inlet temperature, leading to lower enthalpy and less energy extracted from the turbine. The relative efficiency will decrease around 15% to 25% at half load conditions. However, the exhaust energy does not decrease linearly with the power output due to reduced fuel efficiency on the part-load operation. Figures 3.2 and 3.3 show part-load performance data of combustion turbines featuring single-shaft, two-shaft, and single-shaft with IGVs designs. The first figure demonstrates the effect on power generation efficiency and usable heat energy, while the second figure contains exhaust gas temperature and exhaust flow statistics. (Klimstra et al. 2017, 21-23; Petchers 2003, 194-199.)

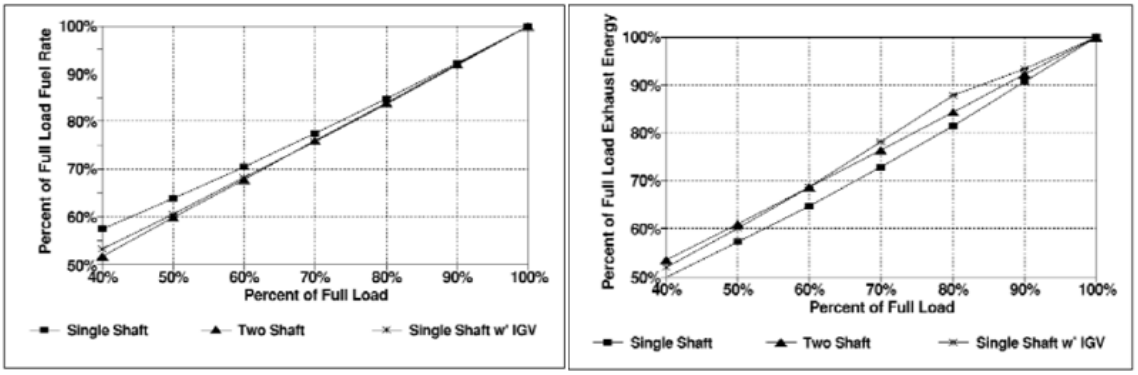

Figure 3.2: Effect of part-load operation on the fuel consumption and exhaust energy in different combustion turbine designs (Petchers 2003, 194).

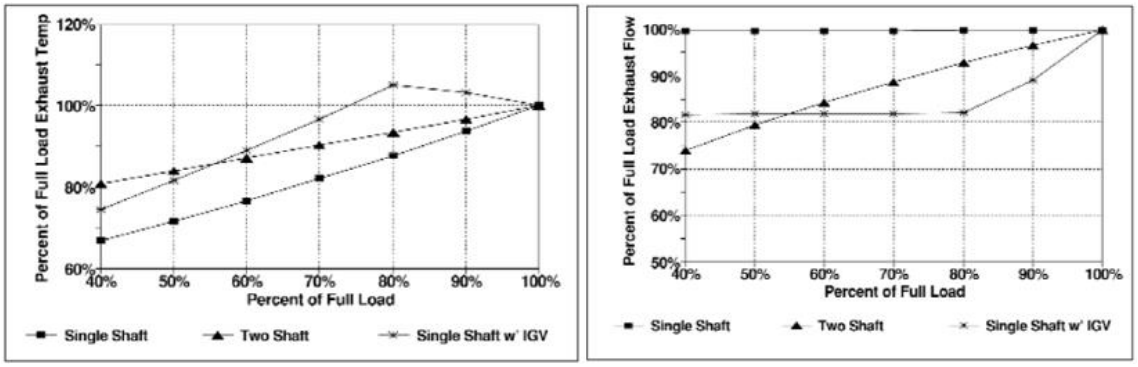

Figure 3.3: Effect of part-load operation on the exhaust temperature and exhaust steam flow in different combustion turbine designs (Petchers 2003, 199).

As seen from Figure 3.2, the single-shaft design has the lowest electrical efficiency on partial load because the fuel rate is the highest. Still, the exhaust energy graph proves that the relative amount of heat energy increases in partial load. For example, at 50% of full load, the percent of full load exhaust energy with the single-shaft design is 58%. Based on Figure 3.3, there is also a clear relationship between the exhaust temperature and the exhaust flow. As presented, the part-load operation reduces the exhaust temperature, especially with single-shaft turbines that maintain constant exhaust steam flow. (Petchers 2003, 193-199.)

Simple-cycle combustion turbines are considered flexible generation because the power output can be rapidly changed. Although the part-load efficiencies are considered low, it is viable to use gas turbines as load-following plants when high amounts of intermittent energy sources are available. The average ramping rate with small industrial combustion

turbines is 20% of full load per minute, which can be extended to around 35% in the modern turbine models. The simple design allows performing large instantaneous load steps while still maintaining power grid frequency and voltage limits, enabling the system to reach full output even 50% faster than using the linear ramping rate in the 20% to 35% range. The main disadvantage considering combustion turbines operational flexibility is the acceptable minimum load. Generally, the load should not be reduced under 30% to 40% to maintain a continuous combustion process, which drastically reduces the operational range. However, the average hot start-up time of 10 minutes is very good in contrast to other conventional power generation plants, creating a possibility to shut down the unit multiple times during the day. (Gonzalez-Salazar et al. 2018, 1498-1501; Welch 2016, 6-8.)

The most used primary fuel for gas turbine installations is natural gas, but other gaseous fuels such as biogas and landfill gas can be used if their calorific values and composition are consistent. Some gas turbines can use distillate oils and gas simultaneously, but residual oils are rarely used in CHP applications. The air and fuel supplied to the gas turbine have to comply with the severe operating conditions caused by momentary temperatures of up to 1600 °C and high rotational velocity. The intake needs to be free of particles that would erode the blades and contain minimal contaminants that would cause corrosion. (Nadir et al. 2015, 823-825; DBEIS 2008, 30-31.)

Combustion turbines in below 5 MW power range are primarily simplified versions of large industrial gas turbines. For CHP, these are used as on-site power generation in large commercial and institutional applications or process industries such as chemicals, refining, and pulp and paper. Electrical efficiencies start from around 20% for small 500 kW turbines, while large over 100 MW turbines can reach over 40% efficiency, especially in combined cycle processes. A combustion turbine’s electrical efficiency is a function of the pressure ratio, turbine inlet temperature, and component efficiency. Larger turbines are generally more efficient as they can accommodate more turbine stages, increasing the pressure ratio. After recovering the turbine exhaust gas in the form of high-temperature steam, the overall system efficiency is within a range of 70% to 90% depending on the system size. (Darrow et al. 2017, 58.)

Table 3.1 provides combustion turbine performance values from actual operative CHP units based on vendor supplier data compiled by technology consulting company ICF and shared by the United States Environmental Protection Agency (EPA). The supplier in this review is Solar Turbines that focuses on manufacturing small gas turbines. European Turbine Network (ETN) database lists other combustion turbine manufacturers, and with below 10 MW power output, the suppliers also include Siemens, Baker Hughes, and MAN Energy Solutions. Even though the Solar Turbines Taurus 70 is over the 5 MW_e research delimitation, it indicates how the turbine size corresponds to other operating values in a cogeneration system. By default, the surveyed unit operates at the nominal load prior to measurements. (ETN 2020; Darrow et al. 2017, 59-60.)

Table 3.1: Typical combustion turbine performance values in cogeneration (Darrow et al. 2017, 59-60).

		Solar Turbines Centaur 40	**Solar Turbines Taurus 70**
Electrical power output	[MW]	3.3	7.0
Electrical efficiency, HHV	[%]	24.0%	28.9%
Heat rate, HHV	[MJ/kWh]	15.0	12.5
Fuel input, HHV	[MW]	13.8	24.4
Exhaust mass flow	[kg/s]	18.8	26.7
Turbine exhaust temperature	[°C]	448	491
Recovery exhaust temperature	[°C]	169	151
Steam output	[MW]	5.7	10.1
Total CHP efficiency, HHV	[%]	65.7%	70.4%

As seen from Table 3.1, the electrical efficiency is usually lower with smaller units, but in return, the heat rate is higher. The increased heat rate means relatively more usable heat energy in cogeneration systems, balancing the total efficiencies between the turbine sizes.

3.2.2 **Microturbines**

Microturbines are small combustion turbines that are well suited for decentralized energy production. The output power is typically between 25 kW and 300 kW, limiting their functionality to micro or small-scale applications. Microturbines can utilize multiple fuel

sources, including natural gas, biogas, and liquid fuels like gasoline, diesel, and heating oil. (Badea et al. 2015, 66-70.)

A microturbine process is similar to a larger combustion turbine, but they typically always have a recuperator that preheats the combustion air to achieve higher electrical efficiency. The inlet air is first compressed, then heated due to combustion, and led to an expansion turbine that allows both the inlet compressor and a drive shaft capable of providing mechanical and electrical power. The main difference in comparison to the larger system is the high rotational speed of 90,000 to 120,000 rpm, which must be regulated to grid requirements, for example, to 50 Hz with power electronics or 3,000 rpm with an additional gearbox for a two-pole SG. Figure 3.4 shows a process diagram of a recuperative microturbine system with heat recovery. (Badea et al. 2015, 67.)

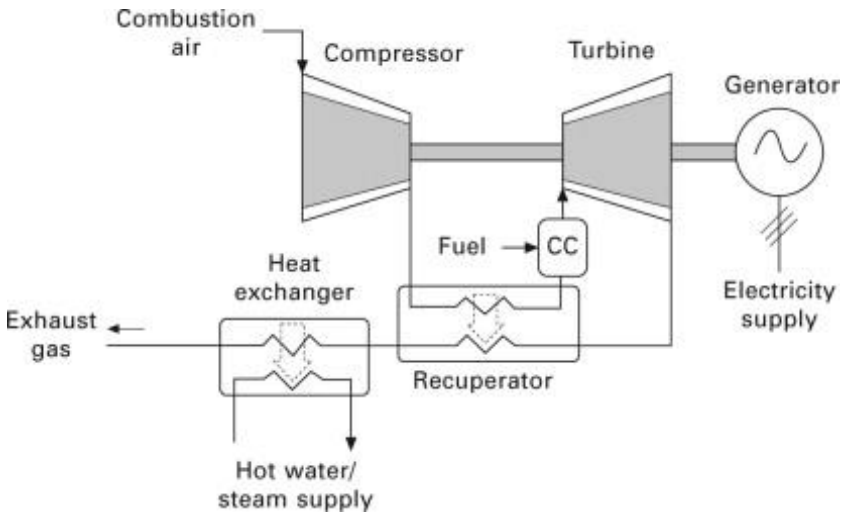

Figure 3.4: Process diagram of a gas-fired microturbine CHP system with recuperator (Beith et al. 2011, 373).

As shown in Figure 3.4, the exhaust heat goes through the recuperator before reaching the heat exchanger that provides hot water or steam to the user. In a nonrecuperative microturbine, the heat exchanger inlet temperature is between 540 °C to 600 °C, whereas with the recuperative version, the temperature has reduced to around 270 °C. The contrast in electrical efficiency is high since the nonrecuperative design generally has only 15% efficiency, while it ranges from 20% to 30% with a recuperator. In CHP applications, the typical total efficiency of the system is between 75% to 85%. (Badea et al. 2015, 67-70.)

The output power and heat production of a microturbine is controlled by adjusting the generator shaft's rotational speed. In practice, this is done by regulating the incoming mass flow. Because this results in increased exhaust temperature at the recuperator inlet, the turbine inlet temperature needs to be reduced to balance the change. In industrial simple-cycle gas turbines, the main parameter for power output control is the inlet temperature, whereas with microturbines, the main contributor is mass flow. The regulation method is the main reason why microturbines maintain power generation efficiencies better in off-design load levels. Figure 3.5 shows the relation between load and electric efficiency based on microturbine performance data provided by European Energy Agency (EEA). The performance parameters are given relative to the corresponding design values. (Beith et al. 2011, 169-171.)

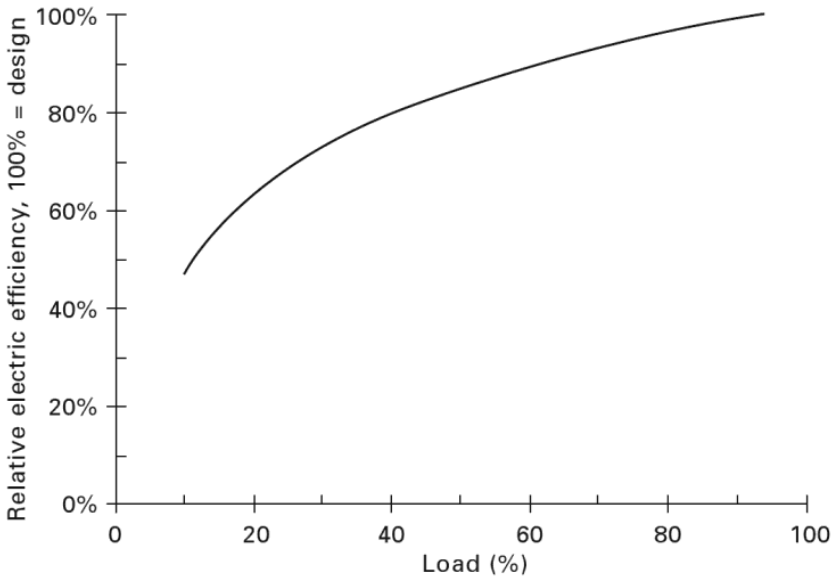

Figure 3.5: Effect of part-load operation on electric efficiency in microturbine installations based on EEA data (Beith et al. 2011, 171).

As shown in Figure 3.5, the decrease in electric efficiency at partial loads is not avoided with microturbines either. At the 20% load level, the relative electric efficiency decreased from 100% to around 60%. In larger combustion turbines, the lower electrical efficiency contributes to the heat output, while in microturbines, the reduced mass flow rate decreases the heat transfer rate. As a result, microturbine systems experience a reduction in total CHP efficiency as well. (Beith et al. 2011, 170.)

Microturbines are flexible in grid-independent and inconstant frequency applications because they can be operated in various ways. The cold start-up takes only 30 seconds for power delivery and less than two minutes to reach full output. The ramp-up rate in modern units is 50% per minute, and the minimum acceptable load is generally 10%. During operation, the speed can be lowered to an idle level where no electricity is generated, but still, the combustion occurs. This mode allows immediate power generation when needed. Microturbines can be connected parallel with the electric grid or as a stand-alone system, following either the electric or heat load demand. In installations where multiple units are used in parallel, the part-load operation or load following can be performed by sequentially turning down complete units, allowing higher efficiency and useful redundancy. (Beith et al. 2011, 172.)

Microturbines in CHP applications are primarily recuperative units that utilize the excess heat to produce hot water for process or space heating. Electrical efficiencies get higher with size but will not typically exceed 30%. After the heat recovery, the overall system efficiency is usually around 80%. Table 3.2 provides combustion turbine performance values from actual operative CHP units based on vendor supplier data compiled by technology consulting company ICF and shared by EPA. Capstone Turbine Corporation has inverter-based products Capstone C65 CARB and Capstone C1000-LE, and FlexEnergy has gearbox-based products FlexEnergy MT250 and FlexEnergy MT330. By default, the surveyed unit operates at the nominal load prior to measurements. (Darrow et al. 2017, 97-99.)

As shown in Table 3.2, the electrical efficiency typically increases in relation to the unit's electrical power output. However, the total CHP efficiency seems to decrease due to relatively weaker exhaust gas characteristics. Because microturbines have low power to heat ratios, large heat demand is required to get the highest benefit from CHP installation. (Badea et al. 2015, 67-70.)

Table 3.2: Typical microturbine performance values in cogeneration applications (Darrow et al. 2017, 98-99).

		Capstone C65 CARB	FlexEnergy MT250	FlexEnergy MT330	Capstone C1000-LE
Electrical power output	[kW]	61	240	320	950
Electrical efficiency, HHV	[%]	23.7%	26.0%	28.0%	26.6%
Heat rate, HHV	[MJ/kWh]	15.2	13.8	12.9	13.5
Fuel input, HHV	[kW]	257	920	1141	3562
Exhaust mass flow	[kg/s]	0.5	2.1	2.4	6.7
Turbine exhaust temperature	[°C]	311	256	267	279
Heat exchanger exhaust temperature	[°C]	88	88	88	93
Heat output	[kW]	120	376	450	1299
Total CHP efficiency, HHV	[%]	70.4%	66.9%	67.5%	63.1%

3.2.3 **Reciprocating engines**

Reciprocating engines, also known as internal combustion engines (ICE) or piston engines, are extensively used to generate mechanical power for a stationary generator or numerous transportation applications. The system configurations are generally divided into compression-ignition engines featuring diesel-cycle, and spark-ignition (SI) engines featuring Otto-cycle, with power capacities from less than 1 kW up to 100 MW. The compression-ignition engines are designed to operate on gas-oil, heavy fuel oil, or their mixture, whereas SI engines operate primarily on gaseous fuels. This thesis focuses on the SI technology because diesel engines have relatively high emissions, costly fuel, and they are increasingly restricted to only emergency standby applications. These systems may also be limited to 200 operational hours per year, turning their utilization in CHP impracticable. (Darrow et al. 2017, 31-33; Rosen et al. 2016, 73-74.)

In the SI engine, the process cycle starts when the piston moves from the top of the cylinder to the bottom, taking in a new combustible mixture through the intake valve. This action is called the intake stroke. When the piston reaches the bottom of the cylinder, the intake valve closes, and subsequently, the piston starts to move back to the top of the cylinder compressing the fuel mixture. This action is the compression stroke. When the piston reaches the top, the fuel mixture is compressed within a small area of the cylinder, referred to as the combustion chamber. A spark plug ignites the fuel in the following

expansion stroke, increasing pressure inside the cylinder substantially. As a result, the fuel's released energy moves the piston down, providing mechanical energy for the crankshaft, which further rotates the generator for electricity. Lastly, the exhaust valve is opened, resulting in released exhaust gases, while simultaneously the piston starts to move back and pushes out the remaining combustion end products from the cylinder. This action is the expulsion stroke. In total, four strokes within two revolutions of the flywheel are required to complete a full cycle. Figure 3.6 demonstrates the basic principle of a SI engine for cogeneration purposes. (Klimstra et al. 2017, 26-28; Petchers 2003, 139.)

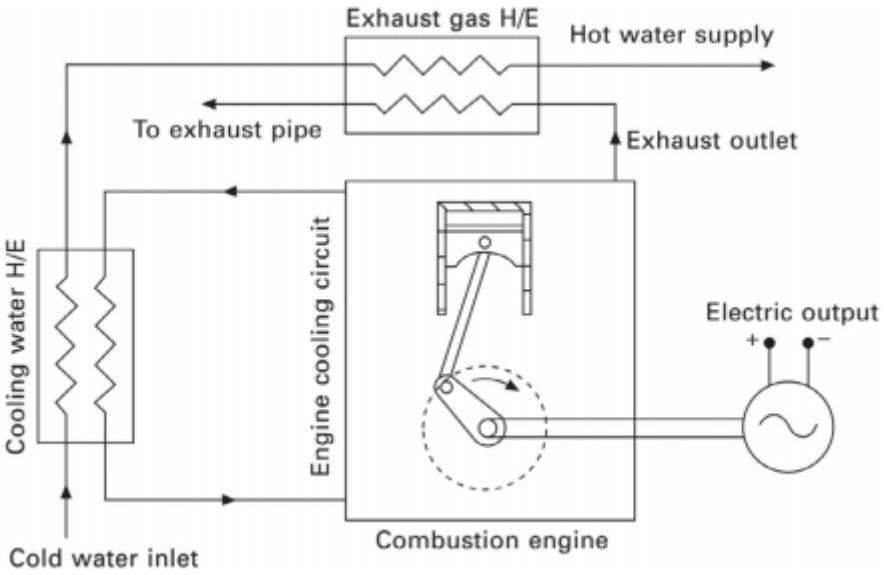

Figure 3.6: System configuration of ICE with heat recovery (Martinez et al. 2017, 267).

In reciprocating engine systems, the excess heat is separated into multiple energy streams, as shown in Figure 3.6. Most of the heat is available from the engine exhaust gas and jacket coolant water, but it can also be recovered from the lube oil cooler. Between 20% to 60% of the waste heat is contained in the coolant systems, but with a temperature of 80 °C to 100 °C, it is not suitable for steam generation. The rest of the waste heat is available from the engine exhaust gas, in a temperature range of 300 °C to 600 °C, which can generate steam at a maximum pressure of 26 bar. (Rosen et al. 2016, 73; Beith et al. 2011, 134-135.)

Modern reciprocating engines are equipped with one or more turbochargers to achieve higher power densities. This component works as an intake air compressor, providing

higher inlet air pressure in a ratio of 3:1 to 4:1. The increased air and fuel in the cylinder increase the power output of the engine. The turbocharger is connected to a turbine, powered by the exhaust gases leaving the combustion chamber. The intake air temperature to the cylinder must be relatively low, or it will affect the power capacity, fuel combustion, and released emissions negatively. The cooling is usually handled using heat exchangers, called aftercoolers or intercoolers, that discharge air from the turbocharger based on the specific temperature limit. For CHP applications, the turbocharger discharge air provides an additional heat energy stream, which should be recovered to reach higher total efficiency. (Petchers 2003, 140.)

SI engines are typically fueled with natural gas, but other gaseous fuels such as landfill gas can be utilized with a proper fuel system. Volatile liquid fuels are also usable, but they require changes to the engine pressure ratio and some tuning to the overall system design. Dual fuel engines that burn natural gas with a small percentage of diesel are also available. For CHP purposes, SI engines are mostly adjusted to operate with one exact fuel type to reduce maintenance and maintain high efficiency. (Darrow et al. 2017, 31-32.)

The part-load performance of a reciprocating engine is considerably better than with other prime movers. In CHP applications, the SI engine commonly runs at constant speed producing steady AC power by driving SG, while the heat exchangers recover the thermal energy from the exhaust gas and motor cooling system. If the load is reduced, the electrical efficiency decreases, and the relative heat rate increases. At 50% load from the nominal, the electrical efficiency is usually about 5% to 10% less when compared to the 100% load level. However, in most of the engines, the part-load efficiency decreases faster after the 50% load. (Klimstra et al. 2017, 32-34.)

The heat output of reciprocating engines is more complicated to evaluate than with combustion turbines because the energy balance consists of several significant heat sources. Figure 3.7 presents reciprocating engine energy balance in relation to the engine load by dividing the input energy into fractions of mechanical output, exhaust heat, cooling system heat, and non-recoverable losses. (Beith et al. 2011, 135-136.)

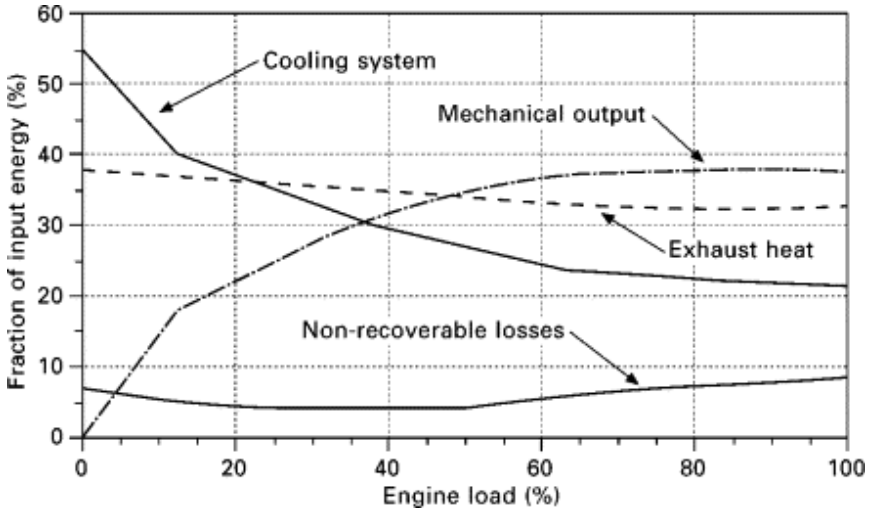

Figure 3.7: Typical energy balance of SI engine CHP system over the full load range (Beith et al. 2011, 136).

As shown in Figure 3.7, when idling, the fuel is used to keep the SI engine running, and most of the energy dissipates as heat caused by internal friction. When the load increases, the share of input energy transformed to mechanical output rises, and the fraction of energy lost to the exhaust and cooling systems reduce. The non-recoverable losses stay between 5% to 10% through the load range. At full load, the power generation efficiency is 37%, while the exhaust gas and cooling system contain 33% and 21% of the input energy, respectively. (Beith et al. 2011, 135-136.)

The power output of a reciprocating engine is a factor of engine speed, controlled through the fueling rate and torque. This equation makes the load adjustments fast but difficult in meeting highly efficient operational areas with constant speed. Figure 3.8 shows performance chart of SI engine with efficiencies in relation to torque as brake mean effective pressure (bmep) and engine speed. Superimposed on the figure are two curves indicating constant load, where Load 1 at 2500 rpm is the operating design point, and Load 2 demonstrates a 40% load reduction in comparison to Load 1. (Beith et al. 2011, 136-137.)

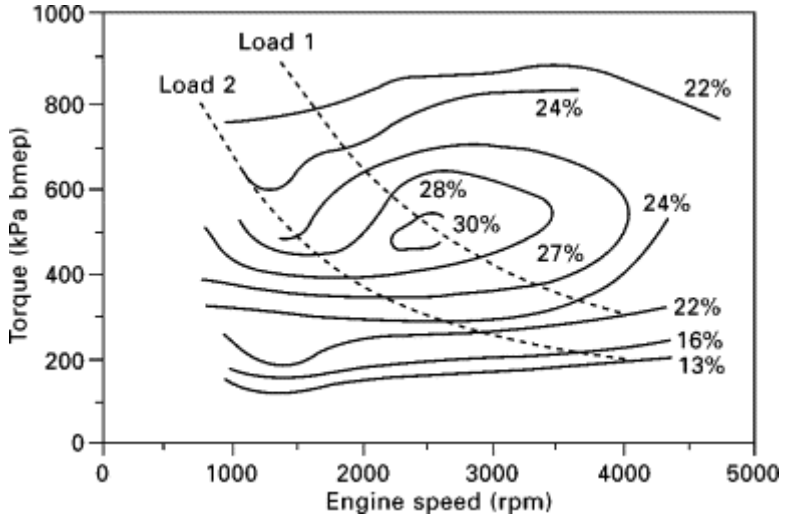

Figure 3.8: Example of SI engine performance chart with two constant load curves superimposed (Beith et al. 2011, 137).

As shown in Figure 3.8, the highest efficiency is usually achieved within a small specific operating area. The ability to vary both torque and engine speed increases the available load range and creates more optimization possibilities, but the electric machine may not be able to utilize the mechanical output power with all combinations. If constant engine speed is required, the system relies on altering torque, and as can be seen, it has the most undesirable result on efficiency. (Beith et al. 2011, 137.)

Modern SI engines have the capability to perform multiple starts and stops with fast ramp-up. Based on products offered by Wärtsilä, the preheated gas-fired ICEs can be synchronized to the grid in 60 seconds and ramp-up to full output in 5 minutes. From the hot start, lubrication takes 30 seconds, followed by 25 seconds of speed acceleration and 5 seconds synchronization to secure the output speed. In the remaining 4 minutes, the load is increased from 20% to 100% linearly with a ramp-up of 20% per minute. Once running at normal operating conditions, the load can be reduced and increased with a ramping rate of over 100% per minute in the newest gas engine models. Gas engines can also tolerate step loading as with combustion turbines. (Wärtsilä 2020, 24-30; Haga 2011, 5-11.)

Natural gas ICEs for power generation are primarily four-stroke engines with up to 18 MW power output. Electrical efficiencies start from 27% for small under 50 kW engines and reach up to 46% when the size goes over 3 MW. After recovering the waste heat in

the form of low-pressure steam and hot water, the overall system efficiency is usually around 80% regardless of the system size. (Darrow et al. 2017, 31.)

Table 3.3 provides SI engine performance values from actual operative CHP units based on vendor supplier data compiled by technology consulting company ICF and shared by EPA. The suppliers are Tecogen with product InVerde Ultra 100, and the rest belong to General Electric-Jenbacher. InVerde Ultra 100 functions through an inverter, while the other products produce the desired frequency through a gearbox. By default, the surveyed unit operates at the nominal load prior to measurements. (Darrow et al. 2017, 36-37.)

Table 3.3: SI engine performance values in cogeneration (Darrow et al. 2017, 36-37).

		InVerde Ultra 100	**GE JMS-312C65**	**GE JMS-416B85**	**GE JMS-620F01**
Electrical power output	[kW]	100	633	1121	3326
Electrical efficiency, HHV	[%]	27.0%	34.5%	36.8%	40.4%
Heat rate, HHV	[MJ/kWh]	13.3	10.4	9.8	8.9
Fuel Input, HHV	[kW]	369	1835	3042	8241
Exhaust mass flow	[kg/s]	0.15	0.99	1.72	5.06
Exhaust temperature	[°C]	649	505	425	383
Heat recovered from exhaust gas	[kW]	61	434	586	1474
Heat recovered from jacket cooler	[kW]	135	211	378	478
Heat recovered from lube oil cooler	[kW]	0	79	129	328
Heat recovered from intercooler	[kW]	0	91	173	847
Total CHP efficiency, HHV	[%]	80.0%	78.9%	78.4%	78.3%

According to Table 3.3 performance values, the electrical efficiency increases with the engine size. However, the total efficiencies of all engine models are close to each other, around 80%, due to the higher heat fraction with the lower electrical power output models. (Darrow et al. 2017, 36-37.)

3.2.4 **Gasification systems**

Gasification is one of the most promising modern technologies for micro and small-scale CHP systems. Even though the technical knowledge has been around for over a century, only the past decade has made it commercially feasible in smaller sizes due to the environmental and political pressure of mitigating energy-related CO_2 emissions.

Gasification systems in the 30 kW to 2 MW range are mostly using ICE as the prime mover, but other solutions are possible. (Beith et al. 2011, 98-100.)

In gasification systems, the main difference in comparison to conventional CHP is the gasification stage. After the synthetic gas, generally referred to as syngas, is produced, the system follows the main prime mover process, which on a small-scale is the spark-ignited ICE. Gasification is a thermochemical conversion process where solid biomass is converted to a gaseous energy carrier by partial oxidation at elevated temperatures. For under 1 MW_{th} thermal input, the most applicable technology is a downdraft gasifier, while in the 1-10 MW_{th} range, updraft gasifiers or fluidized beds are preferred. The partial oxidation is performed with air, oxygen, or steam as the gasification medium. Most designs utilize air gasification as it is cheap, but it results in the lowest calorific value of the gas. (Basu et al. 2013, 249-255.)

Figure 3.9 demonstrates the operation of a throatless downdraft gasifier with a temperature gradient in relation to the unit’s height. After the biomass is fed from the top, the reactor’s first zone is used to evaporate moisture from the solid fuel. When reaching above 350 °C, the second zone breaks the fuel into charcoal, noncondensable gases, and tar vapors through pyrolysis. The limited air supply from the middle of the reactor causes the pyrolysis to occur at a rich flame, thus called flaming pyrolysis. The third zone burns the remaining char and tar, creating the highest process temperature of 1350 °C and providing heat for the second zone by thermal conduction. The downflowing gas's temperature is still high, descending to the bed of hot char particles in the fourth zone, gasifying them. Finally, the produced syngas leaves from the lower section of the reactor through a bed of ash. (Basu et al. 2013, 255-257.)

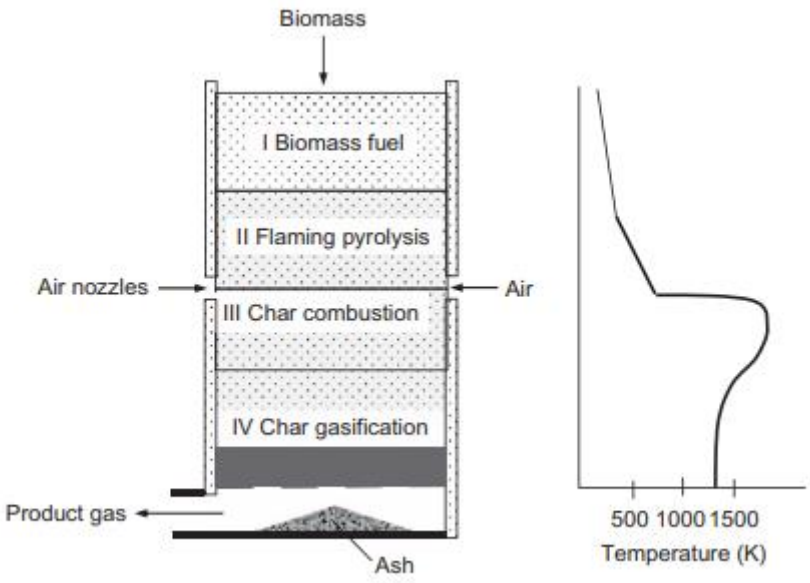

Figure 3.9: Operation of a throatless downdraft gasifier and temperature gradient in relation to the height (Basu et al. 2013, 255).

Compared to other gasifier types, a downdraft gasifier produces the cleanest gas and requires the shortest time of 20 to 30 minutes to ignite and bring the equipment to working temperature. According to Finnish supplier Volter which makes modular gasification and ICE CHP systems, the system hot start-up takes 10 minutes from standby mode and 45 minutes from the cold start-up. The disadvantage with all gasifier based CHP systems is the need for homogenous wood chips or biomass with relatively low moisture content to reach optimal parameters during the thermochemical conversion. Volter 40 kW_e and 100 kW_{th} system technical specifications state that 38 kg per hour fuel consumption requires under 15% moisture content and fuel particle size of P31S in standard EN-ISO 17225-4. (Volter 2020; Basu et al. 2013, 257.)

Although the small gasification systems include ICE, they are much less flexible in controlling the power due to the need for adjusting the syngas production. Fast load steps of over 10% are not possible, so the power increase needs to be made with steady ramping. Still, the ramping rate of 25% per minute is high, but an ESS is needed to ensure grid stability during high load deviations when islanded. However, the part-load performance is good with under 5% efficiency reduction when the load is 50% from the nominal, and with the 25% minimum load, 8% reduction is tolerable. (Volter 2020.)

Biomass gasification based cogeneration plants are generally small and modular units with up to 1 MW_e capacity, though larger systems exist. There are few suppliers in Finland, including Volter, Gasek, and Entimos, that provide gasification CHP systems with gas engines in predesigned container solutions. The electrical efficiencies are around 25%, with cogeneration efficiency of up to 90%. The gasification reactor's efficiency is typically around 75%, with additional losses in gas filtering, so the system cannot reach the same efficiencies as with fossil fuels. (Basu et al. 2013, 258; Takalo 2013, 12-16.)

3.2.5 **Stirling engines**

A Stirling engine is an external combustion engine generating movement on the generator shaft with a temperature imbalance. The technology does not need much process equipment, can be installed in any urban environment, and can utilize all fuel sources to maintain a higher temperature in the cylinder's other end. Since the design has separated continuous and controlled combustion, it results in very low emissions and high efficiency, also reducing the need for maintenance. The generally small electric power capacity of 1 kW to 100 kW creates various possibilities for the beneficial use of local energy sources, which is enhanced with high CHP efficiency of up to 90%. (Badea et al. 2015, 71-72.)

Stirling engine consists of a cylinder, regenerator, piston, and displacer. As the fixed volume of working gas, such as helium or hydrogen, is alternately heated and cooled, the expansion and contraction force the displacer to move the gas, consequently working the piston to derive power to a flywheel like in the reciprocating engines. The regenerator recovers heat with minor losses from the end of the cycle, and the process is repeated. Figure 3.10 presents a process diagram of a Stirling engine based CHP system featuring the main components. (Badea et al. 2015, 71-72.)

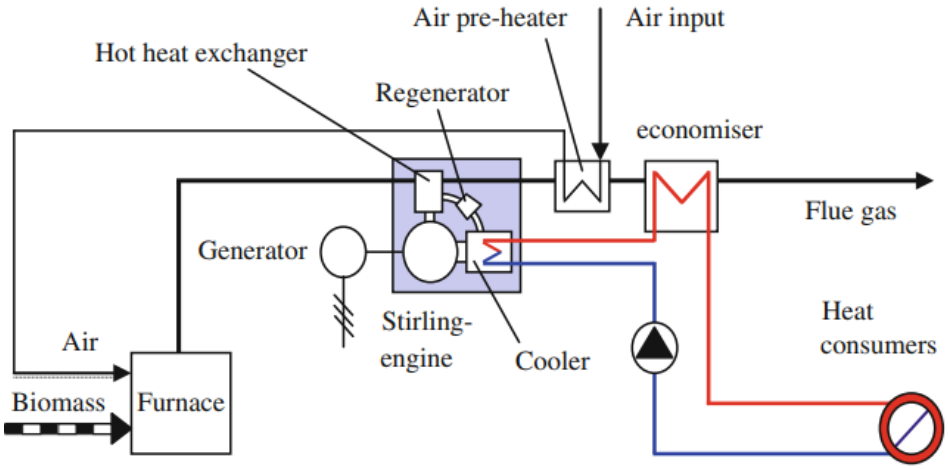

Figure 3.10: Process diagram of biomass-fired Stirling engine CHP system (Badea et al. 2015, 71).

As shown in Figure 3.10, the heat released from biomass combustion is used to maintain temperature difference in the regenerator, preheat the combustion air, and provide heat to the consumer. As the fuel type is not restricted, it creates many opportunities to customize the process. However, as the electric efficiency is considerably low, usually around 15% to 25%, the share of heat energy is substantial when considering the total efficiency. In the cold end, the cooling water circulates to keep the Stirling engine active and is also used as a medium to transfer the process heat to the user. (Beith et al. 2011, 180.)

The most significant difference between ICE and the Stirling engine is the operational flexibility. Combustion engines can do rapid power changes by directly controlling the fuel supply, but in Stirling engines, there is usually a large amount of thermal energy reserved in the hot end, which continues to transfer energy to the working gas for a long time even if the fuel supply is zero. Therefore, the Stirling engine systems are meant for stationary constant power applications. (Beith et al. 2011, 181.)

Stirling engines are still mostly in the development stage, trying to find their position in the market as the other forms of CHP are much more feasible. However, manufacturers like Microgen and Ökofen are already constructing early commercial micro-CHP units primarily meant for rural and remote areas. The concept is ecological and self-generated electricity from wood chips, pellets, and solar energy with 1-5 kW electric power output and up to 90% CHP efficiency. (Microgen 2020; Ökofen 2020.)

3.2.6 **Steam turbines**

Steam turbines are versatile prime movers and the most widely used CHP technology in terms of installed power capacity. The main difference in steam-based systems compared to the other conventional prime movers presented is that the steam turbine itself does not convert fuel to electric energy. Therefore, the incoming energy is always transferred from a separate process function that combusts the primary fuel, usually from a boiler. Consequently, steam turbines generate electricity as a byproduct of heat, whereas the other prime movers are considered to produce heat as a byproduct of electric power. (Petchers 2003, 215-216.)

The dichotomy between combustion of the primary fuel and power generation enables steam turbines to function with a variety of fuels, including all types of biomass like wood chips, residual wood, bark, pellets, and agricultural byproducts, with fossil fuels like coal, oil, and natural gas, or even with nuclear fuel. The fuels also include waste products, and in many instances, the boiler can burn a mixture of multiple fuels at the same time. Because the method for steam production is not limited, the steam turbine can be connected to other power generation, for example, combustion turbine, to provide additional electricity from the hot exhaust gases. This arrangement would upgrade the simple-cycle process to the already mentioned combined-cycle. (Breeze et al. 2014, 119-120.)

The design and complexity of a steam turbine plant are heavily dependent on the application, but generally, simplified designs are used when the output power is less than 5 MW. The smallest plants function with single-stage non-condensing, also known as back-pressure, or condensing steam turbines with an output power of 500 kW to 3 MW, and the mechanical efficiency positions between 30% to 60%. The multi-stage steam turbines are mostly used in larger over 3 MW plants but can be found in around 1 MW category. The technologies applied for multi-stage turbines are condensing, back-pressure, and extraction types together with their variations automatic-extraction, non-automatic-extraction, and admission techniques. Multi-stage turbines provide mechanical efficiencies between 50% and 80%. Steam turbines can be further classified according to their numerous fundamental operating principles, but this research only covers already

mentioned steam exhaust conditions as they are the most relevant when considering CHP. (Kirjavainen et al. 2004, 8-10; Petchers 2003, 215-220.)

Steam turbines operate on the Rankine cycle, which is the primary thermodynamic cycle of conventional power stations. The Rankine cycle can be reduced to four main processes. First, the boiler feedwater named condensate is pressurized and injected into a boiler or steam generator. The water is heated and evaporated in the boiler, resulting in the steam that can be yet superheated to increase its enthalpy and reduce moisture content. The steam is expanded in the turbine to a lower pressure, where a small fraction of total thermal energy is converted to kinetic energy that drives the generator shaft. The excess thermal energy is contained in the turbine exhaust steam, which can be utilized in multiple ways depending on the turbine type. Figure 3.11 shows the simplified steam-based cogeneration process with a back-pressure turbine. (Rosen et al. 2016, 70-73.)

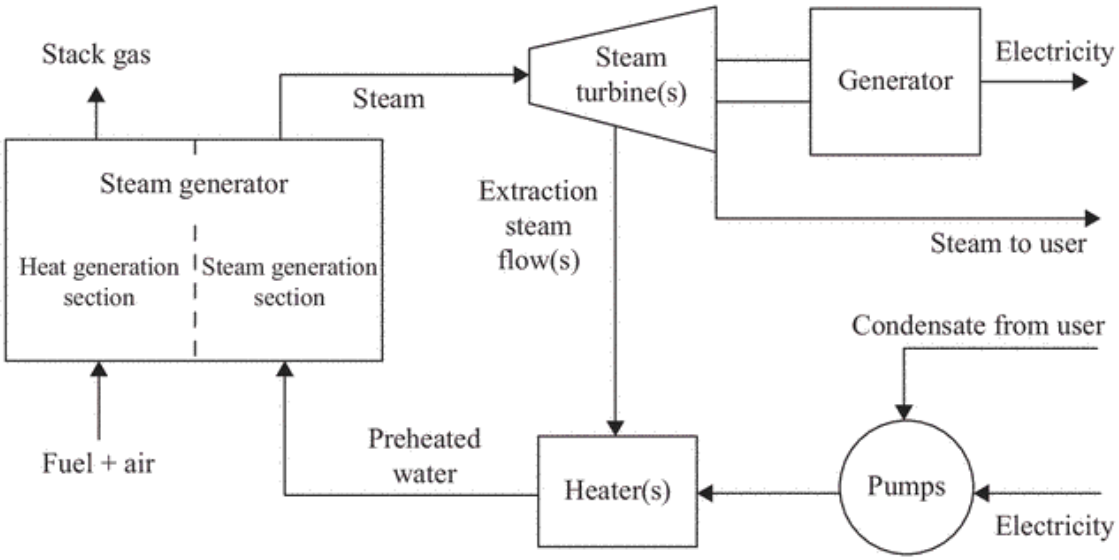

Figure 3.11: Simplified process diagram of a back-pressure steam turbine system (Rosen et al. 2016, 59).

As seen from Figure 3.11, the back-pressure turbine exhausts all or some of the total steam flow directly to the user or application. In CHP plants, this design's main advantage is the large amount of usable thermal energy, which can be discharged in chosen excess of atmospheric pressure. However, as the electrical efficiency is very low, the receiving application needs constant heat demand, which makes the technology best for industrial

processes. Figure 3.12 demonstrates the operating differences of the main three turbine types: condensing, back-pressure, and extraction turbines. (Breeze 2018, 42-49.)

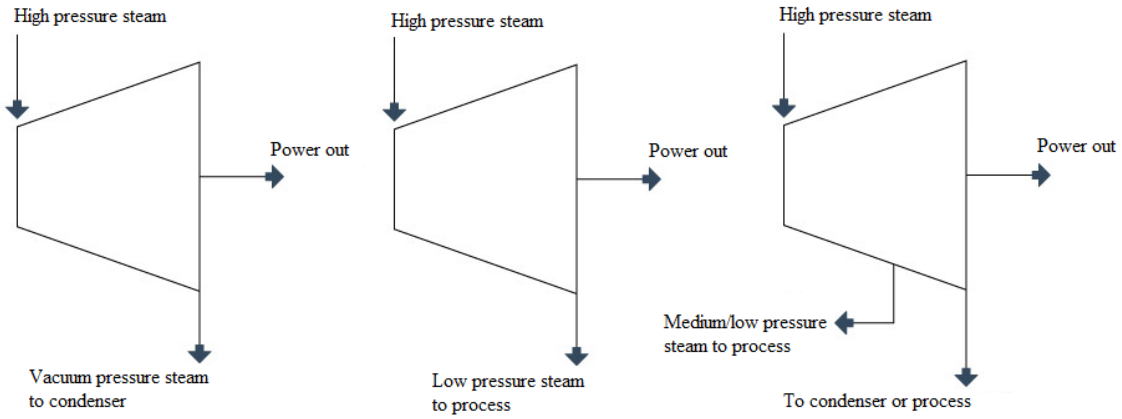

Figure 3.12: Condensing, back-pressure, and extraction steam turbines, respectively from left to right (Modified based on Breeze 2018, 43-48).

Condensing turbines operate with an exhaust pressure less than atmospheric, which is the vacuum pressure. As shown in Figure 3.12, the exhaust steam is directed to the condenser, not the user, and the same boiler feedwater circulates in the process. Because of the low exhaust pressure, the pressure drop through the turbine is more significant, and more energy is extracted from each unit of steam, resulting in the highest electrical efficiency between the turbine types. The condenser can be either air- or water-cooled, and in the water-cooled systems, the exiting water can sometimes be used for space or district heating. However, if the thermal energy is completely released into the atmosphere, the condensing turbine does not work for cogeneration purposes. (Petchers 2003, 217-218.)

Extraction turbines are multi-stage machines with the added design feature of having one or more outlets to extract steam between the inlet pressure and exhaust pressure. Otherwise, the process can follow either condensing or back-pressure turbine design by exhausting the remaining steam to either process or condensate. The number of steam outlets can be chosen, but smaller systems mostly use single-stage extraction. Extraction turbines are designed for applications that require discharged steam at different pressures or when there are varying low-pressure steam requirements. Compared to the back-pressure turbine, the extraction type is more flexible in changing the shaft power and can comply with varying process steam requirements. (Petchers 2003, 218-220.)

The steam generator, mostly boiler, shown in Figure 3.11, is another mandatory component for the steam-based process cycles. The main principle of all the boilers is to work as a heat exchanger that transfers the energy from the combustion of a fuel to a medium. Boilers are available in various designs, and generally, the larger size means more complex subprocesses with several stages of superheaters, evaporators, and economizers. Most of the boilers are for large industrial applications with over 50 MW_{th} thermal output, but simplified designs are used when less than 5 MW_e is needed from a steam turbine system. For solid biomass fuels, the small-scale CHP may use grate combustion technologies for steam production, while the more efficient and less pollutant fluidized bed combustion technologies are generally available in over 3 MW_e capacity plants. From these technologies, the bubbling fluidized beds (BFB) are more basic, whereas the circulating fluidized beds (CFB) are a better alternative for low-grade fuels and different wastes. (Kirjavainen 2004, 8-24.)

The rotational velocity of a turbine shaft depends on the driven load, incoming steam flow, and pressure through the turbine stages. If the load on the shaft increases while maintaining constant steam flow and pressure, the turbine speed decreases, and vice versa. Steam turbines can operate at speeds ranging from 1,800 rpm to over 14,000 rpm, but the optimal speed usually settles in the range of 3,600 to 5,600 rpm. Typically, the single-stage turbines can operate to 50% of the rated speed, but constant rotational speed is desired to produce steady AC power with SG. Mechanical energy output from a steam turbine is adjusted by governing steam flow and pressure, with the primary objective of maintaining steady speed irrespective of the load demand. (Petchers 2003, 224-226.)

Apart from turbine load and speed, it can be vital to control extraction and exhaust steam parameters in CHP applications. In a back-pressure turbine, the amount of exhaust heat available is interrelated to the steam flow. As a result, the whole process before the turbine needs to be adjusted. In an extraction turbine, the amount of steam exhausted from each outlet can be regulated with control valves. With an extraction-condensing turbine, for the most part, the process can be maintained even if the medium pressure steam extracted to the user needs to be reduced, as the rest is still guided to the condenser. (Petchers 2003, 225-227.)

The ramping rate of a biomass-fueled steam process is generally the slowest of all the technologies considered in this research. Even though the steam turbine can regulate the inlet and outlet steam flow, the combustor and all the subprocesses need to be tuned to comply with the increased power demand. When the fuel feed increases, it affects the fuel treatment, feed-in system, and combustion system before the feedwater can be heated. Before the boiler can combust all the additional fuel effectively, it also needs to be adjusted. The heat energy transfers to the process water progressively, and the steam flow is increased after a delay. In normal operating conditions where the biomass is solid, a steam system's ramping rate is between 4% to 10%, which can be slightly increased by using auxiliary fuels. Steam turbines can tolerate load steps because of large inertia, but too fast changes may damage the turbine blades, and output power cannot be increased rapidly. In small under 5 MW biomass plants, the grates or boilers can usually operate with 30% minimum load, while larger units can more easily adapt to lower load requirements. The standard hot start-up takes two to four hours, while cold start-up can take up to 16 hours, causing heat accumulators to be a mandatory investment if the unit needs to be stopped daily. (Guo et al. 2018, 5-8.)

Although the operational flexibility is low, steam turbine systems maintain good performance when operating at partial load. When above 70% from the nominal, the efficiency losses are usually less than 5% in comparison to the design level. At 40% load, the typical relative efficiency decrease is around 15%. Therefore, steam turbines are good in operating at reduced load, but the challenges are more related to slow ramping rate or issues in specific process components, for example, excessive formation of soot during the boiler combustion. (Petchers 2003, 237.)

Steam turbine operated CHP plants are mostly relatively large over 1 MW_e systems. Extraction turbines usually function with higher steam flows than back-pressure systems, as they discharge exhaust in multiple pressures or feature a condensing cycle. The large utility-scale steam plants using condensing turbines can achieve over 45% HHV power generation efficiencies, but it decreases to around 30% HHV in smaller system sizes. It is typical for back-pressure turbines to have low electrical efficiencies between 5-20% HHV as they focus on process heat production. As steam turbines are available in any size from 100 kW to 1300 MW, there is an immense amount of design choices throughout

the process. However, the total CHP efficiencies are high at around 80% HHV regardless of the plant size. (Breeze 2014, 119-121.)

Table 3.4 provides back-pressure turbine performance values from typical commercially available steam turbine generator systems that include a boiler. The systems examined are applied to heat universities and to provide steam for industrial use. The statistics are based on vendor supplier data compiled by technology consulting company ICF and shared by EPA. Although system three is over the 5 MW_e research delimitation, it indicates how the plant size corresponds to other operating values in a cogeneration system. By default, the surveyed system operates at the nominal load prior to measurements. (Darrow et al. 2017, 83.)

Table 3.4: Typical back-pressure turbine performance values in cogeneration (Darrow et al. 2017, 83-84).

		System 1	**System 2**	**System 3**
Electrical power output	[MW]	0.5	3.0	15.0
Boiler efficiency, HHV	[%]	80.0%	80.0%	80.0%
Turbine isentropic efficiency	[%]	52.5%	61.2%	78.0%
Generator and gearbox efficiency	[%]	94.0%	94.0%	96.0%
Electrical efficiency, HHV	[%]	6.3%	4.9%	7.3%
Fuel input, HHV	[MW]	8.0	61.0	205.2
Steam flow input	[kg/s]	2.5	19.2	62.3
Steam inlet conditions	[bar]/[°C]	34.5/289	41.4/302	48.3/343
Steam outlet conditions	[bar]/[°C]	3.4/148	10.3/189	10.3/193
Steam output	[MW]	5.8	45.6	148.5
Total CHP efficiency, HHV	[%]	79.6%	79.7%	79.7%

Based on Table 3.4 performance values, the larger turbines have generally higher isentropic efficiency, which measures the effectiveness of extracting work from the expansion process. As back-pressure turbines use only a portion of the incoming steam for power generation, the electrical efficiencies are below 10% HHV for all the systems. Still, the total CHP efficiencies are around 80% HHV when there is a demand for a large amount of produced steam. (Darrow et al. 2017, 82-84.)

3.2.7 **Organic Rankine cycle**

The Organic Rankine cycle is a Rankine process, where the working fluid is changed from water to an organic substance. Although water has excellent heat transfer properties, exceptional thermal stability, and various other advantages, selecting an organic fluid can be more beneficial if the heat source is low or medium temperature or if the plant's power capacity is low. The ORC plant's typical electric power range is from 150 kW to 2 MW, though even 1 kW micro-scale and 20 MW large-scale ORC plants are available. (Beith et al. 2011, 206.)

Most of the ORC plants are based on traditional steam turbine design and technology, including shaft seals, reduction gear, air-cooled electric generator, and a lubricating oil system. Thermal energy is transferred to the process directly or through an external thermal-oil circuit, while the selected organic fluid and other process stages are configured according to the heat source, application, and economic aspects. Even though most ORC plants are based on conventional steam turbine technology, also turbo-generator concepts have been proven viable. This design utilizes the process circulating medium to lubricate and cool the electrical generator, eliminating the need for external air cooling and oil lubrication systems. The completely hermetic design is possible by connecting a pump, an electrical generator, and a turbine on a single shaft. (Beith et al. 2011, 206-207.)

An ORC plant featuring boiler feed fluid preheating and its principle on temperature-entropy (T-s) thermodynamic diagram are presented in Figure 3.13. The numbering is done according to the process stage, with the following functions: turbine expansion (1-2), recuperator and condenser desuperheating (2-4), condensing (4-5), feed pump pressure rise (5-6), recuperator and evaporator preheating (6-8), evaporation (8, 9), and superheating (9-1). The T-s diagram visualizes the same process, where the additional plotted graph is unique for each substance, indicating the liquid, saturated, and superheated thermodynamic states of the fluid. (Uusitalo et al. 2014, 33-35.)

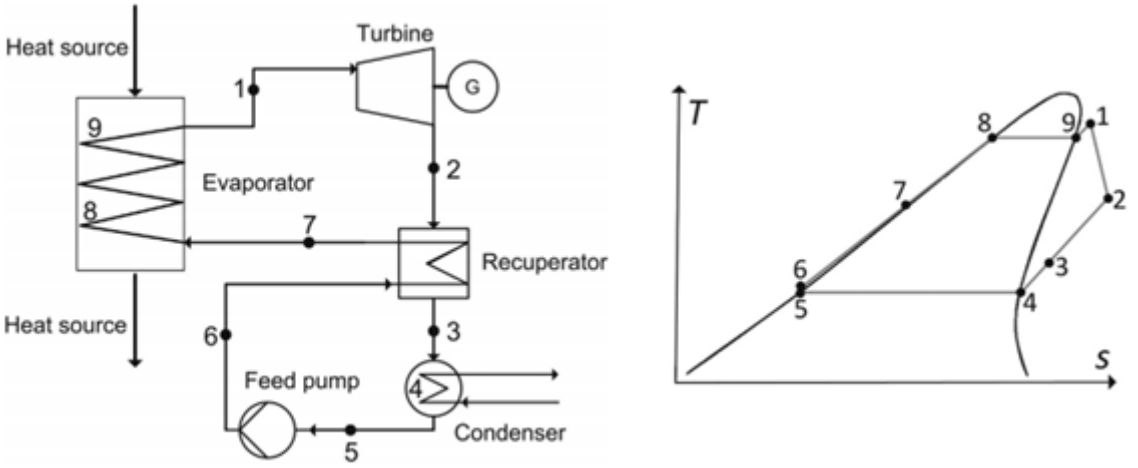

Figure 3.13: Example of recuperative ORC process and the corresponding T-s diagram (Uusitalo et al. 2014, 34).

One of the most significant advantages of the ORC process cycle is that the working fluid remains in the phase of superheated vapor through the complete expansion in the turbine, also seen from the T-s diagram of Figure 3.13. Compared to the traditional Rankine process, ORC avoids condensation problems in the low-pressure stages of the turbine, where the expansion with water would end to a saturated zone. Because the vapor is still in the superheated condition, a recuperator is typically used for desuperheating the vapor entering the condenser while simultaneously preheating the fluid fed to the boiler. In CHP applications, the condenser heat can be used to a district or process heating with a heat exchanger. (Beith et al. 2011, 207-208.)

The main idea in the present ORC plants is to produce electric power from low-temperature heat sources, waste heat, or with fuels that are not easy to utilize in other processes. As conventional Rankine process does not allow efficient utilization of under 370 °C heat sources, and it is challenging to construct large steam processes with limited capacity fuels such as biomass, landfill gas, biogas, or heat from solar collectors, the proper selection of the fluid may lead to comparatively higher efficiency, and solve design problems of the steam expansion. Generally, the suitable inlet temperature for ORC is 100-600 °C, creating numerous synergizing possibilities with other forms of CHP or industrial waste heat producers. For example, one of the ORC suppliers called Rank states to take advantage of 90 °C heat sources while also complementing the electrical generation with 50 °C water for space heating. (Rank 2020; Beith et al. 2011, 207-211.)

The organic fluid of the ORC process is dependent on the cycle temperature. At a temperature of less than 200 °C, it can be pentane, whereas, at less than 280 °C and 350 °C, it can be silicone oil or toluene, respectively. At higher temperatures, ORC process is often connected to a separate thermal-oil circuit that transfers heat to other parts of the process. The selection of the working fluid, the ORC process parameters, and cycle configuration will have the highest factor on the cycle efficiency and determine the temperature and pressure of evaporation and condensation stages. (Uusitalo et al. 2014, 37-38.)

The part-load performance of an ORC plant is better than with steam turbines. Studies done for micro-CHP units conclude that when the net power is reduced to 50% from the nominal, the efficiency reduces relatively around 10% from the nominal level depending on the cycle temperature and the working organic fluid. This decrease results in the same range as with the Rankine cycle. However, with over 50 kW_e capacity, ORC part-load performance decreases more slowly at the medium load range, whereas the efficiency of a simple steam turbine is reduced almost linearly. Here even under 5% efficiency reductions are possible in the half nominal conditions. The minimum allowed load is better than with steam turbines, being mostly around 10% to 20%. The hot start-up time of 15 to 30 minutes is still relatively high but more tolerable than with the conventional alternative. If the ORC plant is based on combustible fuel, the ramping rate is good at 15% to 30% per minute, while waste heat like geothermal energy leads to a lower ramping rate of 2% to 5% per minute. Still, the varying load causes the same issues as with steam turbines due to the system design. The organic fluid allows faster adjustability than using water, but the biomass boiler cannot increase heat transfer to the medium instantly. (Pini et al. 2019, 35-38; Lecompte et al. 2017, 6-8; Ibarra et al. 2014, 149-158.)

ORC technology is already commercially feasible and has numerous suppliers. According to research by the Polytechnic University of Milan, the largest suppliers are Ormat and Turboden, with 1701 MW and 363 MW of installed ORC capacity, respectively. In total, these two suppliers have installed 1370 operative units. In the small-ORC category, the largest supplier is Triogen that manufactures 50-170 kW_e container solutions with a biomass boiler or gas engine. In most cases, the electrical efficiency is between 15% to 25%, but the sites are not directly comparable because of different organic fluids, cycle

temperatures, heat sources, and process designs. The primary energy resources for ORC plants are waste heat, geothermal energy, biomass, and low-grade gaseous fuels, while the cogeneration efficiency may reach up to 90%. (Tartiere & Astolfi 2017, 3-9.)

3.3 Comparative analysis of cogeneration technologies

The previous sections studied cogeneration technologies with below 5 MW electric power output. In small-scale, internal combustion is still the most prominent technology, but external combustion is penetrating the market with promising ORC and Stirling engine CHP systems. For biomass, the gasification and ICE system provides decent operational flexibility and good electrical efficiency, which should be a great option for decentralized microgrids when the price reduces. This thesis did not consider technologies without combustion, but solar thermal PV and fuel cell micro-CHP are likely to receive lots of installed capacity in the residential and transportation market during the following decade. For industry, commercial, and district heating purposes, the trend is probably favoring combustion processes before fuel cells can reach higher power capacity and overcome the safety concerns.

In small-scale, the conventional combustion turbine and steam turbine systems can be considered less efficient and inflexible compared to their progressive solutions microturbines and ORC. They are generally optimized for centralized power generation in the design load level and prone to high minimum load requirements, slower ramping, increased start-up time, and more reduced part-load efficiency. However, they start to outperform advanced solutions as the capacity increases, and already in over the 2 MW_e range, their low cost and high reliability can be favorable in many applications. On the other hand, conventional reciprocating engines are still the best solution for CHP in terms of part-load performance, controllability, applicable load steps, electrical efficiency, and start-up time. Still, the fact is that uncontrollable internal combustion creates the highest emissions, which creates opportunities for more environmentally friendly systems like gasification of biomass and Stirling engine.

The flexibility of technologies utilizing biomass is more dependent on the adjustability of the external combustion and durability of process components. The separation

generates challenges in complying with rapid load fluctuations and is the main reason why biomass is hard to utilize in decentralized microgrids. The ramping curve needs to be steady, where already over 10% load steps need to be supported with ESS. Another disadvantage with external combustion is the long start-up time, requiring forecasting the daily energy pattern and preheating for the unit to start and shut down daily.

The satisfactory operational flexibility of biomass CHP is, however, countered with generally good part-load performance. Although reciprocating engines have great part-load efficiencies, especially ORC outperforms combustion turbine systems noticeably well. In general, combustion turbines are more viable in peaking power generation, while combustion engines can also perform load following with high efficiency. In turn, biomass systems provide proper efficiency in load following if their adjustability can be increased.

Apart from flexibility and efficiency, the emission portfolio is a significant factor in future installations. In comparison to conventional SHP, all the technologies reduce CO_2 emissions and primary air pollutants. As biomass is a nonintermittent renewable energy source with a net-zero effect on the climate, and the external combustion produces lower amounts of NO_x, CO, and HCs per power generated, it enables the highest emission savings. However, if the gas-fired units are used to support the integration of renewables, their total emission portfolio needs to be evaluated in a larger perspective.

Results of the comparison are presented on the next pages. Table 3.5 compares the reviewed CHP technologies' main characteristics with the maximum power capacity of 5 MWe for units without a specific upper limit. Figure 3.14 shows indicative evaluation of the technologies based on Table 3.5 statistics, scaling each characteristic on a 1-10 imaginary scale, and Figure 3.15 visualizes interpolated part-load efficiency curves of CHP technologies based on supplier data.

Table 3.5: Comparison of CHP technologies characteristics in below 5 MW_e power range (*).

		Simple-cycle gas turbine	**Microturbine**	**Spark-ignition engine**	**Gasifier and ICE**	**Stirling engine**	**Steam turbine**	**Organic Rankine cycle**
Power capacity	[kW_e]	>500	25-350	>50	30-2000	1-100	>500	>1
Electrical efficiency, LHV	[%]	22-28%	20-30%	35-45%	25%	15-25%	5-15% (6)	15-25%
Total CHP efficiency, LHV	[%]	65-80%	65-80%	75-85%	75-90%	80-90%	80-90%	75-90%
Minimum load	[%]	30-40%	10%	10%	25%	10%	20-30%	10-20%
Start-up time, preheated		5-15 min	30-60 s	10-30 s	10-20 min	20 min	2-5 h	15-30 min
Ramping rate (1)	[%/min]	20-35%	20-50%	20-140%	25%	n/a (5)	4-10%	15-30% (7)
Part-load performance		poor	moderate	very good	good	good	moderate	good
Operational flexibility (2)		good	very good	very good	moderate	n/a (5)	poor	good
Power to heat ratio		0.5-1.1	0.4-0.7	0.5-1.2	0.3-0.5	0.1-0.35	0.07-0.3	0.15-0.35
CHP installed costs (3)	[EUR/kW_e]	700-2800	1000-3700	800-2500	3000-5000	1000-3000	250-1000	1500-5000
Energy sources		natural gas, biogas, landfill gas, propane, fuel oils	natural gas, biogas, sour gas, liquid fuels	natural gas, biogas, sour gas, industrial waste gas, propane	homogenous biomass < 20% moisture content	biomass, solar energy, gaseous and liquid fuels	all primary fuels	biomass, waste heat, gaseous fuels, geothermal and solar energy
Uses for thermal output		LP-HP steam, hot water, space heating	hot water, space heating	LP steam, hot water, space heating	LP steam, hot water, space heating	hot water, space heating	LP-HP steam, hot water, district heating, space heating	hot water, district heating, space heating
Primary emissions without post-combustion control (4)	[kg/MWh]	NO_x 0.24-0.59, CO 0.24-0.73, VOC 0.02-0.04, CO_2 660-840	NO_x 0.06-0.22, CO 0.06-0.82, VOC 0.02-0.10 CO_2 610-920	NO_x 0.80-1.12, CO 1.90-3.68, VOC 0.44-0.63 CO_2 400-620	NO_x 0.5-1.1, CO 0.3-1.5, PM 0.15-0.25, CO_2 net zero	NO_x 0.15-0.50, CO 0.08-0.60, CO_2 net zero	NO_x 0.34-0.76, CO 0.09-0.92, PM 0.15-0.25, SO_2 0.50-1.00, CO_2 net zero	biomass ≈ steam turbine, possibility for fluid leakages

(*) (Microgen 2020; Volter 2020; Wärtsilä 2020; Pini et al. 2019; Guo et al. 2018; Gonzalez-Salazar et al. 2018; Klimstra et al. 2017; Tartiere & Astolfi 2017; Lecompte et al. 2017; Rosen et al. 2016; Welch 2016; Badea et al. 2015; Darrow et al. 2015; Nadir et al. 2015; Breeze et al. 2014; Ibarra et al. 2014; Uusitalo et al. 2014; Wideskog & Wägar 2014; Basu et al. 2013; Takalo 2013. Beith et al. 2011; Haga 2011; DBEIS 2008; Kirjavainen et al. 2004; Petchers 2003.)

(1) Ramping rates are typically at the high end when the unit has reached normal operating conditions. Also, system-specific.
(2) Evaluation of overall operating flexibility by considering the ramping rate, start-up time, minimum load, and acceptable load steps together with general effects on process and combustion parameters.
(3) CHP installed costs include the power generation equipment, heat recovery system, and installation.
(4) Assuming natural gas or biomass fuels without after-treatment equipment. CO_2 from power generation based on fuel content and efficiency, others on system characteristics. Review only indicative and highly process- and system-related.
(5) Stirling engine has inconsistent ramping rate and overall operational flexibility, thus no reliable values.
(6) Dependent on the turbine type. Considers back-pressure and extraction types in under 5 MW_e range. Condensing turbines have higher electrical efficiencies than presented.
(7) If using combustible fuels. Ramping rate of 2% to 5% when using waste heat or geothermal energy.

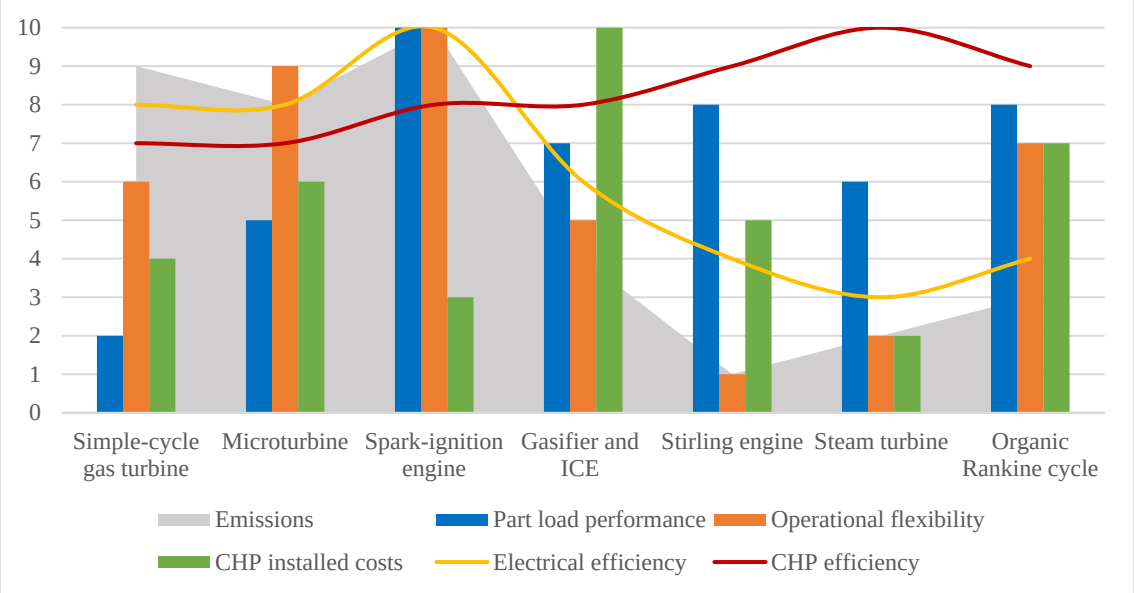

Figure 3.14: Comparative evaluation of below 5 MW_e CHP technologies key features by rating each category on a 1-10 scale.

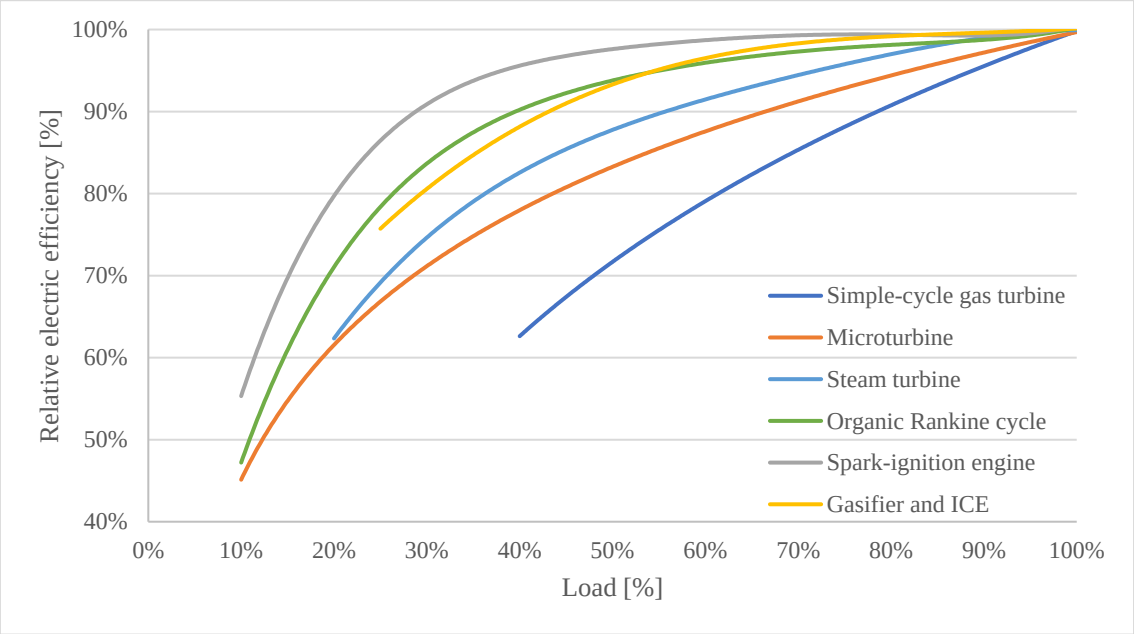

Figure 3.15: Comparison of CHP technologies part-load performance in below 5 MW_e power range. Relative electric efficiency curves in proportion to load interpolated based on supplier data. (Volter 2020; Pini et al. 2019, 36-38; Welch 2016, 4-6; Wideskog & Wägar 2014, 7-8; Beith et al. 2011, 171.)

4 UNINTERRUPTIBLE POWER SYSTEMS

Uninterruptible power systems protect electrical distribution network from problems that would otherwise damage the critical loads, equipment, and grid-connected energy resources. Even though their primary function is securing power quality and reliability, modern bi-directional technology has enabled various secondary applications that utilize the system's reserved energy more efficiently.

This chapter briefly presents Eaton as a company, then goes through double-conversion UPSs primary operation, and lastly focuses on the secondary grid support applications with Eaton EnergyAware technology.

4.1 Eaton as a company

Eaton Corporation is a multinational power management company doing business in more than 175 countries. It was founded in the United States to serve the automotive industry and expanded to various other business segments, including Electrical, Hydraulics, Aerospace, and eMobility, with over 97,000 employees. The year 2019 sales were total 21.4 billion USD. (Eaton 2020a.)

The Electrical business segment concludes around half of the sales to which the Power Quality division belongs. The Finnish business unit, Eaton Power Quality Oy, is part of this and provides a wide range of electrical products and design, commissioning, and maintenance services. The primary purpose is to offer high standard expertise primarily to Europe, the Middle East, and Africa (EMEA) market. (Eaton 2020b.)

Factory located in Espoo manufactures high-end customized uninterruptible power systems and energy storage solutions for information technology, healthcare, marine offshore, and renewable energy applications. At present, the power capacity of a single unit ranges from around 8 kVA up to 1.2 MVA, while the runtime is dependent on the energy storage. Eaton highly promotes innovation and product development with progressive releases annually, including new product models and software upgrades. (Eaton 2020c.)

4.2 Double-conversion UPS

Double-conversion topology is the basis for UPSs designed for continuous power protection. In this arrangement, the output power is completely regenerated with two power conversion stages that ensure a consistent power quality regardless of disturbances in the incoming mains. This type of electronic power systems can be used with any electrical loads as there are no transients when shifting from normal double-conversion to stored energy mode. Figure 4.1 shows the simplified operating principle of double-conversion topology in normal, stored energy, and bypass modes. (IEC 62040-3 2011.)

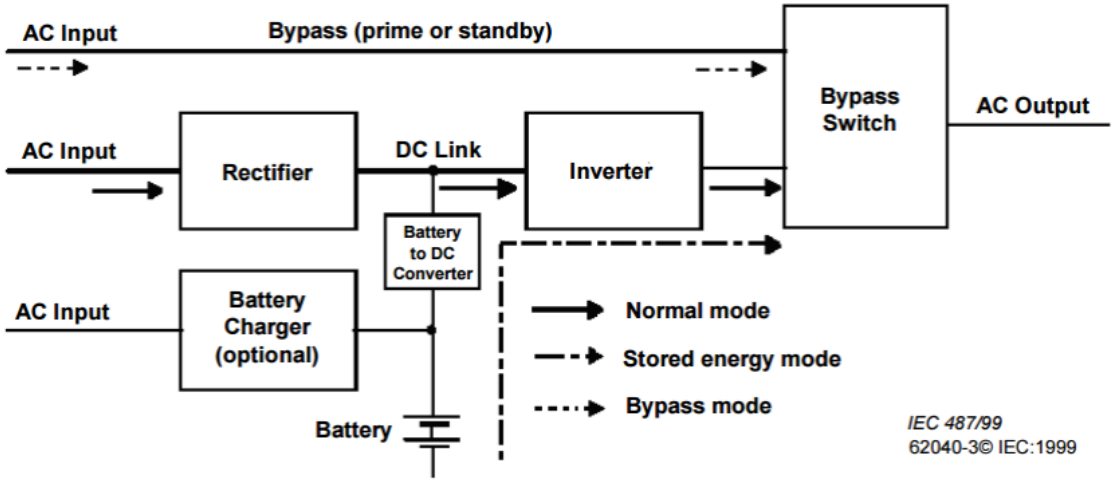

Figure 4.1: Illustrative operation diagram of double-conversion UPS (IEC 62040-3 1999).

As seen from Figure 4.1, in the normal mode, AC input is converted to DC with a rectifier followed by DC to AC conversion with an inverter. UPS goes automatically to stored energy mode if the mains experience a power outage or the input power quality is outside the allowed limits. In this mode, UPS draws current from external battery cabinets or integrated battery blocks. Also, other forms of energy storage possible, including supercapacitors or flywheels. The bypass mode is a circuit bypassing the converters and used in case of a failure, overload, overtemperature, or other anomalies. It also provides extra fault clearing capability for the downstream short circuits, enhancing reliability. (IEC 62040-3 2011.)

The critical or protected load may consist of one or multiple pieces of equipment that the user has determined to be provided with power that has better continuity and quality than

normally available. The load is predominantly some form of data processing equipment, instrumentation, pumps, control software, or communications apparatus. The stored energy to support the load is mostly valve-regulated lead-acid (VRLA) battery, but installations with lithium-ion batteries (LIB) are increasing because they have become cheaper and are more appropriate for the UPS secondary applications. The long-term back-up solutions are commonly diesel generators, but UPSs are still needed to filter the produced AC power. (Eaton 2012, 28-29; IEC 62040-3 2011.)

The power reliability is stated as the percentage of time for which the power is available. If the reliability percentage is 99.9 percent or 8.8 hours non-availability per year, it causes hardware and software damage, data corruption, communication breakdowns, and process outages, leading to security issues and huge replacement losses. Therefore, most information technology providers require more than five-nines of reliability, translating to a maximum of 3.2 seconds of non-availability per year. (Eaton 2012, 30; IEC 62040-3 2011.)

A variety of UPSs has been developed to meet the power system requirements for different types of loads in a wide range of operating environments. The single unit's power output goes from a few hundred watts to several megawatts, and large data centers may need around fifty units to achieve 70 MW of protected loads. In turn, for example, the marine environment demands extreme durability to tolerate moisture, dust, and vibration during operation. (IEC 62040-3 2011.) Figure 4.2 shows the main components and connection section of a medium-sized data center unit from the Eaton 9395P product family with two uninterruptible power modules (UPM), creating 600 kVA of power. The mechanical dimensions of this unit are 189 x 88 x 188 cm. Other values and additional details can be found from Power Xpert 9395P 500-600 kVA UPS technical specifications attached to Appendix 1.

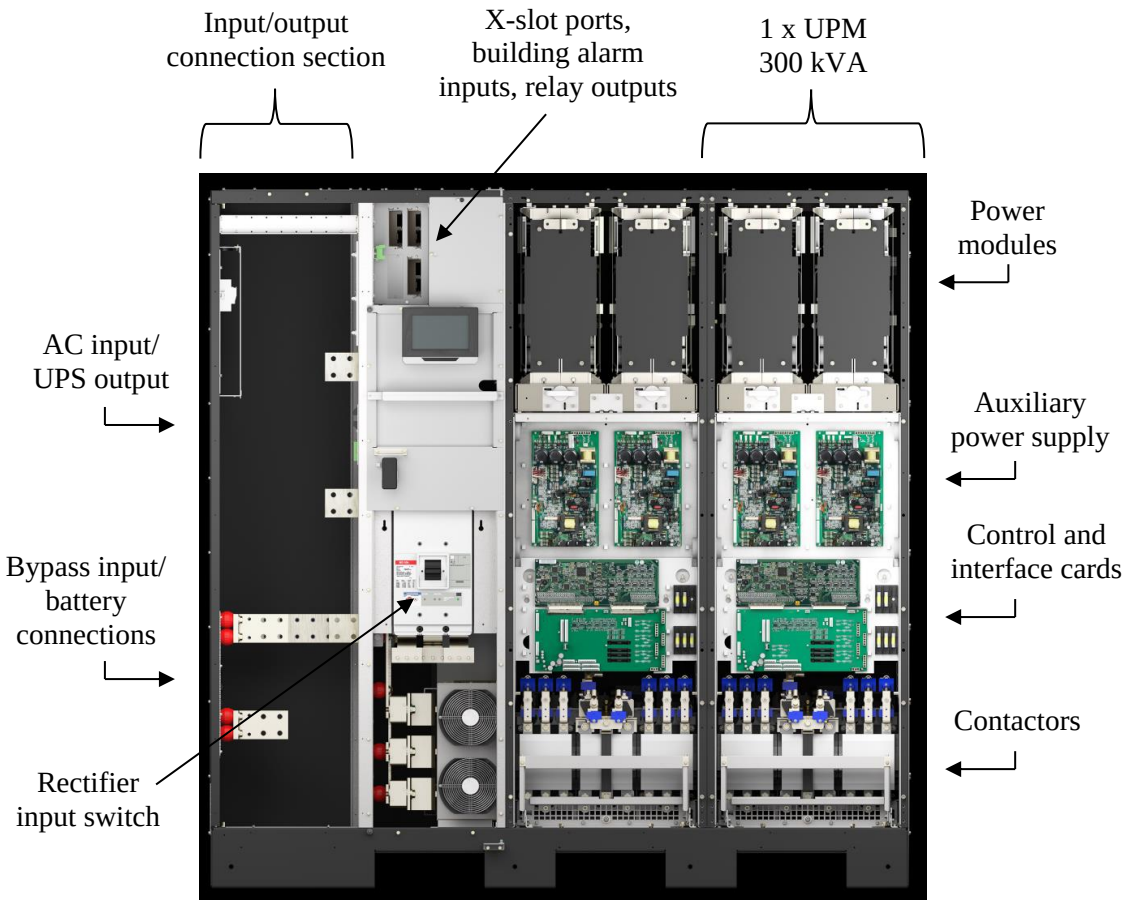

Figure 4.2: Eaton 9395P 600 kVA UPS primary components.

The 9395P units are implemented modularly, where the required amount of UPM sections with independent control and monitoring circuit boards are added next to the input/output connection section. The control and interface cards are responsible for controlling all UPM internal actions, including rectifier and inverter operation, contactor regulation, speed of cooling fans, and DC-link charging. To discharge energy bi-directionally back to the utility and not only to protected loads, one of the key components of is insulated gate bipolar transistor (IGBT) rectifier that has replaced thyristors in all modern UPS designs. An electronic power system like this is primarily intended for solving all the nine common power protection problems described in Table 4.1.

Table 4.1: The nine common power protection problems (Eaton 2012, 9).

Problem	Definition
1) Power failure	A total loss of utility power
2) Power sag	Short-term low voltage
3) Power surge	Short-term high voltage above 110% of nominal
4) Undervoltage	Reduced line voltage for periods ranging from a few minutes to a few days
5) Overvoltage	Increased line voltage for periods ranging from a few minutes to a few days
6) Electrical line noise	High-frequency waveform caused by electromagnetic interference
7) Frequency variation	A change in frequency stability
8) Switching transient	Instantaneous under-voltage
9) Harmonic distortion	Distortion of the normal line waveform, transmitted by nonlinear loads

Despite the UPS's primary function in securing power quality and reliability, it has numerous secondary applications that have been already researched comprehensively by Eaton. For microgrids containing CHP, the best support services may be frequency regulation, load following, and energy time-shifting. The solution that allows UPS systems to participate in grid support is called EnergyAware.

4.3 Grid support with EnergyAware technology

Eaton's EnergyAware solution enables UPS and its energy storage to participate in grid support by taking advantage of the modern bi-directional operation capabilities. In general, the stored energy in UPS systems is only partially needed to guarantee primary functions, which allows the technology to regulate demand via up and downstream discharging without compromising the load protection. The system's dynamic power response is immediate, balancing power fluctuations in a microgrid or providing additional capacity for the frequency containment reserve (FCR) market. (Alaperä et al. 2018, 69-70.)

For microgrid regulation purposes, the solution can balance normal instabilities of electricity generation and consumption, respond to a sudden loss of generation, and reserve energy during outages to maintain grid frequency. In load following purposes, it can reduce shutdowns and part-load operation of generators, improving operational efficiency and emission characteristics. Some applications may also benefit from energy

time-shifting, where cheap or excess energy can be stored and discharged back to the grid in profitable or essential periods of the day. (Alaperä et al. 2018, 69-70.)

For FCR purposes, the technology can provide rapid frequency response but only for a limited time without oversizing the energy storage. As a result, it works best as a primary reserve in FCR for normal operation (FCR-N), FCR for disturbances (FCR-D), fast frequency response (FFR), enhanced frequency response (EFR), and frequency control ancillary services (FCAS) markets. The UPS system owner can participate in the FCR market directly with the transmission system operator (TSO) if the available capacity is large enough, usually over 1 MW. The more common practice is to offer the capacity to an electricity aggregator that combines smaller energy resources to a virtual power plant and handles the energy transfer with TSO. In the Nordics, Eaton EnergyAware has been functioning as part of the Fortum Spring virtual power plant. (Alaperä et al. 2018, 70-72.)

In practice, the frequency is regulated through controller area network (CAN) protocol, dry contact activation, or autonomously with UPS internal parameters. In the FCR event, the aggregator or TSO will request UPS for grid support via CAN, or a UPS internal parameter will activate the function when a preset frequency is reached. Before the response activates, UPS system logic determines if there are sufficient power and battery capacity to fulfill the request. In microgrids, UPS can also be set to droop control UPS input power based on grid frequency to support the operation of grid-connected DG. (Paakkunainen 2020, 5-9.)

Participating in the FCR market provides both financial and environmental benefits. As the compensation is based on availability and not usage, the typical revenue return is up to 50,000 EUR per MW of power allocated to grid support per year. In turn, the stored energy capacity provides more grid reserves for allocating new flexible generation, like RESs, to the electricity grid. As mentioned, the technology can also reduce the need for generators to operate at unfavorable load levels, leading to increased fuel efficiency, as noted in the CHP comparative analysis. (Eaton 2020d.)

The response speed and reliability have been proved with Swedish TSO Svenska Kraftnät and in Eaton’s test laboratory. Within one cycle from the command, the system fed energy

to the grid, and full stabilization took two to three cycles. Eaton EnergyAware was also the fastest reserve to activate when the frequency in the Nordic system reached the FFR trigger level due to the trip of a Finnish nuclear power plant Olkiluoto 2. Figure 4.3 shows oscilloscope capture from one of the reaction tests in Eaton's test laboratory. The response was triggered via CAN pulse for a 200 kW 93PM UPS unit. Oscilloscope recorded voltage and current waveforms for the UPS input and output together with battery current. (Alaperä et al. 2018, 73-75; Statnett 2018, 8.)

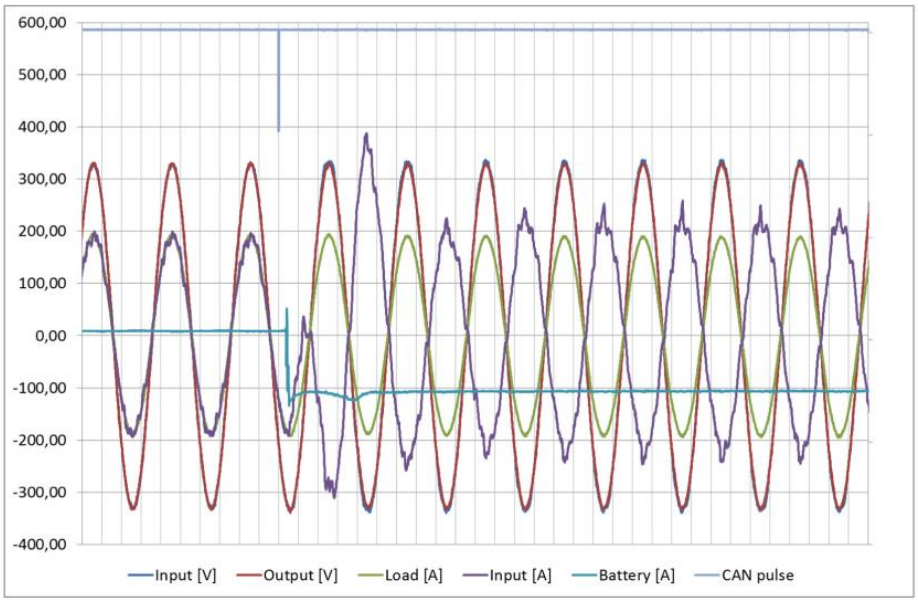

Figure 4.3: Oscilloscope recording of a reaction test with Eaton EnergyAware UPS (Alaperä et al. 2018, 75).

As seen from Figure 4.3, output current and voltage waveforms remain unchanged, proving that the operation has no impact on protecting critical loads. After the CAN pulse activates, the UPS draws energy from the batteries within five milliseconds, seen as an increase in the battery current. Instead of drawing 100 kW from the grid to the loads, the UPS draws 200 kW from the batteries, feeding the excess 100 kW back to the grid. The event can be seen from the 180-degree phase shift in the input current and unchanged output current. Based on the results, the reaction speed of the EnergyAware functionality is very high and can easily meet the reserve market and grid requirements. (Alaperä et al. 2018, 73-77.)

5 DYNAMICS OF CHP AND UPS PARALLEL SYSTEM

According to previous chapters, decentralized cogeneration systems have significant potential in reducing primary energy consumption, greenhouse gas emissions, and the need for energy transmission infrastructure. In microgrids, they also provide an additional layer of reliability through fuel independence and securing electricity and heat demand even without the utility grid. Still, especially biomass-fueled CHP plants have weak operational flexibility and cannot change the output power quickly.

In the current situation, the slow response of power generation makes diesel generators mandatory in ensuring long-term grid stability when islanded. Despite the operational reliability and easy synchronization, the high emissions restrict them to emergency applications, leading to expensive investment in relation to runtime and unused assets. Alternative solutions may include oversizing the generation capacity leading to operation at partial loads or installation of parallel redundant units, but neither can be considered optimal.

As a better solution, in this chapter, UPS is connected in parallel with the CHP unit, while the EnergyAware technology ensures grid stability during islanded operation. The purpose is to analyze the dynamics and durability of cogeneration systems to rapid load deviations and find regulation parameters for the EnergyAware UPS. The simulation model is constructed to Matlab Simulink based on transfer function analysis. As previous research has already simulated engine-generator systems, this thesis focuses on turbine-generator dynamics.

5.1 Previous research

The operation of EnergyAware technology for grid frequency stabilization has been proved with a diesel generator in research conducted by Karjalainen (2020). The standard EnergyAware control loop measures the grid frequency in 100 ms periods, but in low inertia networks, the regulation can be set to a lower value, for example, 5 ms, to counter even faster deviations. Based on simulations, even lower regulation times are theoretically possible by considering the ROCOF value in the secondary control loop,

allowing the UPS to issue power command after the deviation also with the frequency gradient. (Karjalainen 2020.)

The validation has been done with a 200 kW diesel generator and EnergyAware UPS in the Eaton test laboratory at Espoo. In summary, if the generator is not running prior to the load step and is the only source of inertia in the grid, the 100 ms measurement period is too slow to counter extremely high ROCOF values. However, the faster droop control with 5 ms regulation time has been proven to function reliably even during the largest power imbalances. As UPS can issue power command after the deviation with close to zero delay after receiving the input signal, the grid frequency does not fall under the specified level even in the low inertia networks. (Karjalainen 2020.)

The simulation model consists of ICE operated SG, electrical loads, load step function, and rectifier circuit of an EnergyAware UPS. As the dynamics of engine-based CHP systems can be simulated with this model, it is not replicated nor studied in this thesis. The simulation and tests prove that EnergyAware UPS can be used to counter frequency nadirs and ROCOF values of small networks effectively.

5.2 Examination of the operational framework

A typical microgrid consists of an array of redundant UPSs feeding the critical loads, with a large enough energy reserve to start-up diesel generators in case of a utility failure or other anomaly. The heating can be arranged through district heating, electric heating, or with an on-site boiler, where some electricity is needed to function pumps and other transmission components in the heating subsystem.

Considering the optimal integration of CHP to this microgrid structure, the unit should not only serve heating loads and produce electricity, but more importantly, be able to make back-up generators useless. In the grid-connected mode of operation, the utility allows maintaining the power balance between the grid elements regardless of the CHP unit’s operational flexibility. Therefore, the key aspect is to evaluate the functionality of the system when islanded.

Figure 5.1 presents a microgrid schematic with a CHP unit, EnergyAware UPS, and intermittent solar PV generation. As shown, the mains can be disconnected via PCC, resulting in an islanded microgrid where critical loads are fed primarily through the double-conversion topology. The CHP unit generates AC power to the grid and transfers the produced heat energy to a circulating water medium using heat exchangers. The back-up boiler can be used to balance heat loads if the CHP output power is reduced, for example, if lots of intermittent renewables are available, or during peak heat demand periods, for example, during winter in the Northern hemisphere. Generally, UPSs are redundant, but only one UPS and its battery management system (BMS) are presented. Similarly, the CHP units can be multiplied.

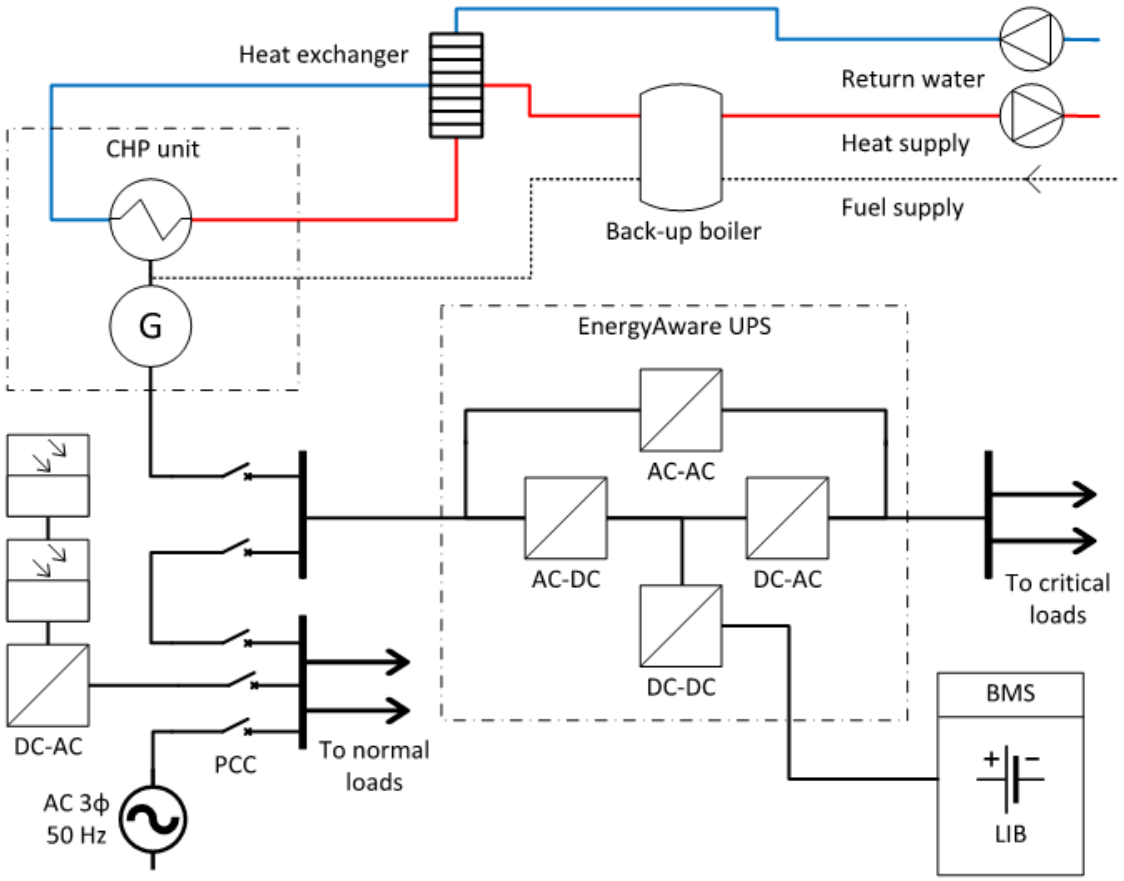

Figure 5.1: Schematic of a microgrid with CHP and UPS parallel system.

Today, the CHP unit is replaced with diesel generators in almost all the systems. When mains are lost, the UPS system is sized to maintain all critical loads for a specific period, for example, two minutes, before the generators are fully synchronized with the islanded

grid from idle. However, with the CHP and UPS parallel system, the primary purpose is not to function as a back-up reserve but continuous operation regardless of the utility connection.

5.3 Technical requirements for distributed generation

Most grid-connected power generation is designed for a stable operating environment with strict frequency, voltage, and ROCOF limits, and exceeding the thresholds may cause disconnection or damage to the equipment. This thesis uses system technical requirements for power plants by Fingrid as the limits for system functionality. The guidelines apply to the Finnish electricity system with a rated power of at least 0.8 kW. The requirements are divided into type categories according to the power plant's design power and the voltage level at the connection point gathered in Table 5.1. (Fingrid 2018, 9.)

Table 5.1: Type classification of power plants based on the connection point voltage and rated power (Fingrid 2018, 9).

Type class	Connection voltage	Rated power
Type A	< 110 kV	0.8 kW ≤ P_{max} < 1 MW
Type B	< 110 kV	1 MW ≤ P_{max} < 10 MW
Type C	< 110 kV	10 MW ≤ P_{max} < 30 MW
Type D	≥ 110 kV	≥ P_{max} 30 MW

The rated power of the synchronous power plant shall be classified according to the equipment's size and shall include all parts of the power plant that normally run together inseparably, such as separate alternators for a single combinate system operated by separate gas and steam turbines. A plant that includes several of such combined units should be assessed based on the size of one combined unit and not on the plant's total capacity. (Fingrid 2018, 9.)

The rated power of a rectifier-connected power plant must be classified based on the power plant's total capacity. Such a power plant comprises one or more rectifier-connected production units grouped into a single economic unit and having a single connection point. (Fingrid 2018, 9-10.)

The requirements do not apply to stand-alone back-up power plants if connected to the electrical system for less than five minutes per calendar month when the electrical system is in normal mode. In the case of energy storage, these requirements only apply to pumped storage power plants. Other types of energy storage are excluded, such as battery storage. (Fingrid 2018, 10.)

CHP plants connected to the grid shall only meet the requirements for active power and frequency control if the main purpose of the plants is to generate heat for the production processes of the industrial plant, and the production of electricity and heat are inextricably linked. In other words, a change in heat production inevitably leads to a change in the production of active power and vice versa. (Fingrid 2018, 10.)

In this thesis, DG is classified as either type A or B. In both instances, the unit must operate continuously and normally when the frequency of the electrical system is between 49.0-51.0 Hz, and 30 minutes when the frequency of the electrical system is 51.0-51.5 Hz or 49.0-47.5 Hz. Regarding voltage control, the unit must operate continuously and normally when the voltage of the electrical system is between 90% to 105% from the connection point nominal, and 60 minutes at overvoltage of up to 110%. The unit must sustain and continue to operate normally when ROCOF values are less than 2.0 Hz/s. (Fingrid 2018, 33-43.)

When islanded, the power plant can be automatically connected to the electrical system when the following conditions are met: 1) the frequency of the electrical system is between 49.0–51.0 Hz; 2) the voltage at the connection point is within the normal range; 3) the maximum permitted rate of change of the actual power is maximum 100% of the rated power per minute; 4) TSO permits installation and automatic switching of the automatic reconnection system with 1-10 minutes time interval after the failure. (Fingrid 2018, 33-35.)

5.4 System dynamics in the islanded mode

The islanded mode of operation isolates the microgrid from the utility, turning the power system to rely on the remaining internal energy sources. Chapter 3 presented the different

cogeneration technologies, while Chapter 2 indicated that their grid connections could be made with SG, IG, or inverter. As IGs are considered to have protection and power quality issues when islanded, this thesis focuses on synchronous connection and assumes that CHP systems with an asynchronous generator, including microturbines and high-speed ORC, are grid-connected via inverter interface.

By not considering voltage control, the grid stability can be assumed to depend on the power system inertia and frequency response of connected DG. In the event of a power imbalance, the rotating masses of the grid-connected generation absorb or release kinetic energy reserved to the turbine and generator systems and transfer it with the microgrid in the form of electric power. The power balance can be written as: (Björnstedt 2012, 23.)

$$J\omega_{\mathrm{nom}}\frac{d\omega}{dt} = P_{\mathrm{m}} - P_{\mathrm{e}} \tag{5.1}$$

where J [kgm^2] is the total inertia of the rotating masses, ω [rad/s] is the angular velocity, P_{m} [W] is the mechanical power, and P_{e} [W] is the electrical power.

If the power generation system suddenly encounters a change in the load demand, the mismatch between P_{m} and P_{e} causes the rotational speed to increase or decrease, causing an alteration in the microgrid frequency. During the first seconds after a load step, the frequency response is determined by the inertia, interrelated to the amount of reserved kinetic energy in the generation system. In the case of a single SG, the total inertia can be replaced by inertia constant and generator rated power, forming the equation: (Björnstedt 2012, 24-25.)

$$\frac{2S_{\mathrm{n}}H}{\omega_{\mathrm{nom}}}\frac{d\omega}{dt} = P_{\mathrm{m}} - P_{\mathrm{e}} \tag{5.2}$$

where H [s] is the inertia constant, and S_{n} [W] is the generator rated power.

Inertia constant measures the time that a rotating generator can provide rated power without additional power input from the prime mover. In thermal plants, this is typically between three to seven seconds. Furthermore, it is conventional to express the inertia of

the power system in megawatt seconds as the inertia constant of a small rated unit has less effect on the network. This relation can be written as: (Kuivaniemi et al. 2013, 8-9.)

$$E_{\mathrm{k,sys}} = S_{\mathrm{n,sys}} H_{\mathrm{sys}} = \sum_{i=1}^{N} S_{\mathrm{n},i} H_i \tag{5.3}$$

where $E_{\mathrm{k,sys}}$ [Ws] is the kinetic energy stored in rotating masses of the system, $S_{\mathrm{n,sys}}$ [W] and H_{sys} [s] are system rated power and inertia constant respectively, and $S_{\mathrm{n},i}$ [W] and H_i [s] are rated power and inertia constants of the individual turbine-generators respectively.

Cogeneration technologies with SG connection can be combustion turbines, steam turbines, ICEs, and ORC. If the technology has a turbine, the total inertia in the system can be higher compared to reciprocating engines where the internal combustion rotates the electric generator. Still, the turbine governor cannot increase the input power instantaneously, meaning that the system inertia has to provide enough time for the rest of the system to increase input to the turbine so the generator can restore the grid frequency. With ICEs, the inertial response can be lower as they do not include a turbine, but the power can be controlled much faster by adjusting the fuel intake. However, the gasification process is an exception and cannot regulate the fuel intake of the engine rapidly.

If the frequency falls below the critical level, DG may be automatically disconnected from the grid, causing a blackout if the utility cannot be restored before the energy storage runs out of charge. Based on power plant technical requirements, the critical under frequency level in this thesis is 47.5 Hz, and the maximum speed of the change is limited to 2.0 Hz/s ROCOF, although some of the power generation can still tolerate momentarily larger deviations. However, according to the previous research, it has been proved that the EnergyAware technology can support the grid effectively during the frequency event, reducing the change in frequency nadir. Figure 5.2 shows an example of frequency response to a power system imbalance and the typical performance indicators in frequency regulation.

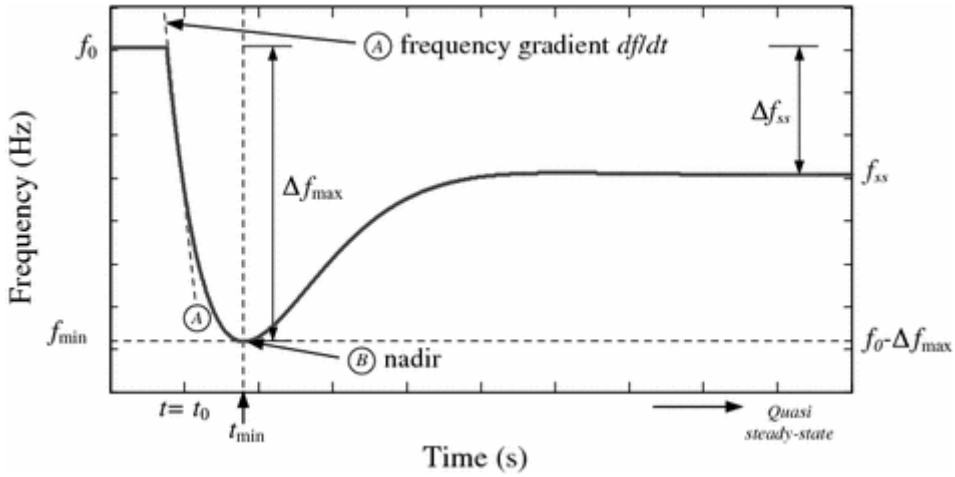

Figure 5.2: System frequency control graph showing the main performance indicators after frequency event (Hossain et al. 2014, 203).

Figure 5.2 shows that the maximum frequency gradient, drawn as line A, is based on the instantaneous inertial response after the frequency deviation. The point B (t_{min}, f_{min}) measures the minimum frequency nadir after the event, creating deviation (Δf_{max}) in relation to the nominal conditions (t_0, f_0). The steady-state deviation (Δf_{ss}) is governed by the amplitude of the disturbance and the network DG characteristics, leaving the system to steady-state frequency (f_{ss}). After the frequency event, the system will not be able to return to the nominal frequency without additional secondary control, called load frequency control (LFC). LFC compensates the remaining frequency error after the fast primary response has acted, regulating the system back to the nominal frequency. (Hossain et al. 2014, 201-203.)

Considering CHP systems stability, the crucial factors are the minimum frequency nadir after power imbalance and the maximum frequency gradient. As can be deduced from Equations 5.1 and 5.2, the inertia is in the numerator, which has a reducing effect on the change of the turbine-generators rotational speed. The supportive result means that both frequency nadir and ROCOF are highly dependent on the system inertia. If the microgrid consists of several generators, Equation 5.3 indicates that the unit with the highest rated power provides more kinetic energy to the grid with the same inertia constants. Based on this, one large and stable unit can support integrating more volatile generation sources to the microgrid without a large effect on the overall frequency characteristics.

Apart from system inertia, the control of the power generation unit also affects the frequency response. As discussed in Chapter 3, for example, governing tries to keep the rotation of the turbine constant. When the load changes, the control system tries to stabilize the change, but with slow time constants, the system-critical limitations may not be met. With turbomachinery, losing the load can be easily regulated with automatic overspeed valves, but high increases in the load can lead to too fast deacceleration of the machine, which can instantly damage, for example, the turbine blades. With reciprocating engines, the control system is usually faster, but as the controller senses the speed change and gives an input signal for the fuel injector, the pace of the strokes is important to match as incorrectly fed and combusted gaseous fuel may damage the equipment.

5.5 Transfer function analysis

Simulation of prime mover and generator system dynamics is highly equipment specific because of changing mechanical characteristics, process configurations, and generator and power grid capabilities. As dynamics of reciprocating engines are already simulated by Eaton, this section focuses on turbine prime movers. Since gas turbines are not the most competitive technology in small-scale applications and high-speed technologies are already commonly connected with power electronics, the modeling is limited to steam turbines and standard ORC with biomass fuels.

Transfer functions are an indicative presentation of the input-output relation of the system and can be used to model dynamics of any power generation unit to a certain accuracy. In this thesis, the simulation model is intended to show the system response to a large load deviation when the microgrid is islanded. Thus, the most critical factor is the initial frequency response to analyze how EnergyAware UPS is required to operate to mitigate all the damaging effects.

Transfer function analysis for turbines can be found from numerous scientific articles which mostly utilize IEEE validated models to construct simulation model that suits their needs. The same approach is used in this section of the study. The following sections create a dynamic model of the isolated system and simulate frequency responses.

5.5.1 **Modeling of turbine-generator dynamics**

In an interconnected power system, LFC and automatic voltage regulators (AVR) are used to control active and reactive power to keep the system in the steady-state. The system's frequency is mainly affected by changes in the real power, while voltage magnitude is mostly dependent on the reactive power. Because the time constant of the excitation system is much smaller than the prime mover time constant, its transient decays much faster, and it does not affect LFC dynamics, the active and reactive power control can be analyzed independently. (Saadat et al. 2003, 527-528.) Figure 5.3 shows a block diagram of a power system control framework with automatic generation control (AGC) signal (Maasoumy et al. 2014, 2228).

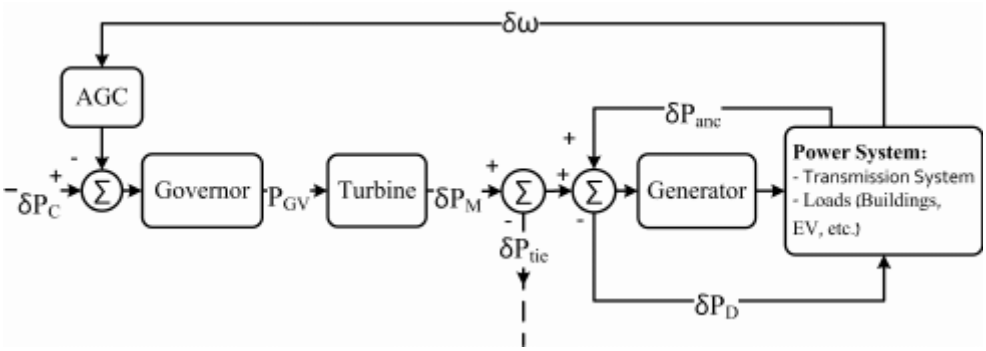

Figure 5.3: Block diagram of governor, turbine, and generator connected to a power system (Maasoumy et al. 2014, 2228).

As shown in Figure 5.3, AGC senses speed or frequency deviation in the grid (δω), giving input to the speed governor of the system trying to restore the frequency back to the nominal value. Thus, it can be referred to as the secondary LFC discussed in the previous section. However, the steady-state frequency deviation, demonstrated in Figure 5.2, results from the primary speed control action, dependent on governor droop characteristics, frequency sensitivity of the load, and system inertia. Therefore, to simulate the frequency response after a load deviation, the primary control loop modeling is necessary, whereas AGC may work as a secondary control loop. As the governor senses power control input (δP_C) from the primary control loop or AGC, the speed controller adjusts the power-change for the turbine (δP_{GV}). The turbine transforms the input energy to mechanical power deviation (δP_M), which is noted as tie-line power flow (δP_{tie}), and

the generator block transfers mechanical power to electric power. Also, the power system side may create power demand deviation (δP_D) and possible ancillary power (δP_{anc}). (Maasoumy et al. 2014, 2228-2230.)

The governor type can be mechanical-hydraulic or electro-hydraulic, where a general model can be demonstrated with three time constants. The input-output transfer function can be presented as: (Maasoumy et al. 2014, 2228.)

$$F_{gv}(s) = \frac{(1 + t_2 s)}{(1 + t_1 s)(1 + t_3 s)} \tag{5.4}$$

where F_{gv} [s] is the governor transfer function, and t_1, t_2 and t_3 [s] are the time constants.

Thermal power plants mostly use mechanical-hydraulic governors with typical time constants of $t_1 \in [0.2, 0.3]$, $t_2 = 0$, and $t_3 = 0.1$. For electro-hydraulic governors without steam feedback typical values are $t_1 = t_2 = 0$ and $t_3 \in [0.025, 0.1]$. (Maasoumy et al. 2014, 2229.) Depending on the prime mover, the speed regulation may be faster, for example, with reciprocating engines, or slower, for example, with steam turbines that have maximum gate opening limits for the steam flow. Numerous turbine and governor systems are demonstrated from actual prime mover models in a catalog by Neplan (2015) including steam, hydraulic and gas turbines, and reciprocating engines. If only the speed regulation that leads to steady-state is modeled, the AGC feedback loop can be neglected. The speed regulation loops typically have 5% to 6% speed regulation from zero to full load in thermal power plants, which gives a command to the hydraulic amplifier to change the governor valve position. (Saadat et al. 2003, 533-534.)

In order to transform the governor change into mechanical power via a turbine, the operation of different prime movers needs to be considered. As discussed in Chapter 3, with steam turbines, the shaft power is dependent on the steam flow, pressure, and temperature. In ORC, the process and design are similar if not considering the hermetic design. With simple-cycle gas turbines, the mass flow is constant, so the change is done by inlet temperature, whereas with microturbines also the mass flow changes. If reciprocating engines were modeled, the speed controller would adjust the fueling rate to the combustion chamber. Because the enthalpy can be considered slower to adjust, the

initial governor control can be limited to change the steam or gas flow to the turbine while other parameters are assumed to stay constant.

Steam turbines may have multiple turbine sections, including high pressure (HP), intermediate pressure (IP), and low pressure (LP). As the governor increases steam intake to the turbine, the energy is divided into these sections, and each produces part of the total mechanical torque to the generator shaft. Figure 5.4 shows a model of a tandem compound single reheat turbine. The mechanical torque (T_{m}) per maximum torque (T_{max}) is divided into fractions F_{HP}, F_{IP}, and F_{LP} of power generated by HP, IP, and LP turbine sections. Therefore, by considering the valve position (Y) in a range of $0 \leq Y \leq 1$ as input and time constants for steam chest and the inlet piping (T_{CH}), reheater (T_{RH}), and the crossover piping (T_{CO}), the output is the mechanical torque available for the shaft that rotates the electric generator. (Krishna 2014, 117-118.)

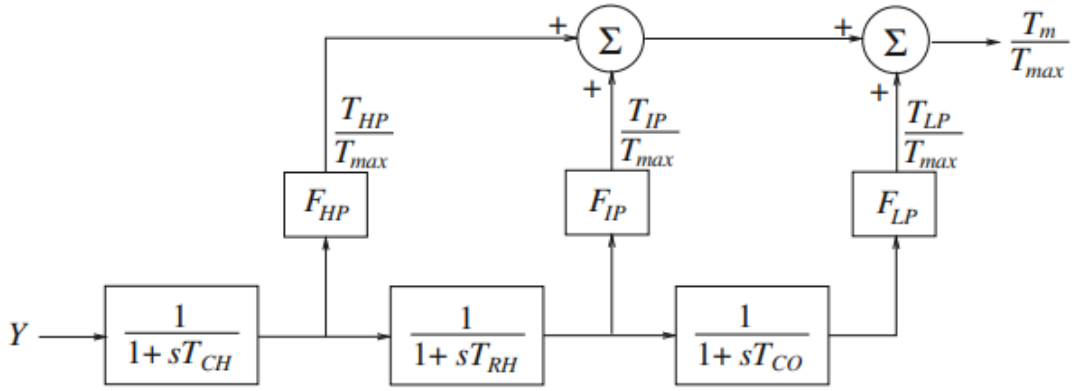

Figure 5.4: Model of a tandem compound single reheat turbine (Krishna 2014, 117).

As each turbine section creates independent torsional dynamics to the generator shaft, it is easier to model the system performance by concentrating all mass on the generator rotor (Krishna 2014, 118). Thermal power plant transfer functions and time constants are found in numerous research papers. For example, Vahidi et al. (2007) have made comprehensive turbine parameter calculations using IEEE models and heat balance data. Steam turbine or ORC thermal plant without reheater can be considered with a single turbine time constant in a range of 0.2 to 2.0 seconds, and the transfer function can be written as: (Vahidi et al. 2007, 1548-1551.)

$$F_{\mathrm{t}}(s) = \frac{1}{1 + t_{\mathrm{t}}s} \tag{5.5}$$

where F_{t} [s] is the turbine transfer function, and t_{t} [s] is the turbine time constant.

The transfer function of the generator block can be calculated based on the swing equation and has been calculated as its entirety, for example, in Saadat et al. (2003). The final equation in the Laplace domain for SG can be written as: (Saadat et al. 2003, 529-530.)

$$\delta f(s) = \frac{1}{2H_{\mathrm{tg}}s}[\delta P_{\mathrm{m}}(s) - \delta P_{\mathrm{e}}(s)] \tag{5.6}$$

where $\delta f(s)$ is the frequency deviation [s], H_{tg} [s] is the combined inertia constant of the turbine-generator when all mass is concentrated to the generator rotor, $\delta P_{\mathrm{m}}(s)$ is the mechanical power deviation transferred from the turbine to generator shaft, $\delta P_{\mathrm{e}}(s)$ is the electric power deviation in the power system.

The power system consists of a variety of electrical loads with different speed-load characteristics. For resistive loads, the electrical power is independent of frequency, but motor loads are sensitive to these changes. Composite load sensitivity to speed can be expressed as: (Saadat et al. 2003, 530.)

$$\delta P_{\mathrm{e}} = \delta P_{\mathrm{L}} + D\delta\omega \tag{5.7}$$

where δP_{L} is the non-frequency-sensitive load change, D [%] is the relative change in load per change in frequency. For example, if load changes by 2% for a 1% change in frequency, D = 2.0.

Equations 5.6 and 5.7 can be combined to a single transfer function, where the output frequency deviation $\delta f(s)$ is dependent on mechanical power $\delta P_{\mathrm{m}}(s)$ and load deviation δP_{L}(s). The combination can be written as: (Saadat et al. 2003, 531.)

$$F_{\mathrm{g}}(s) = \frac{1}{2H_{\mathrm{tg}}s + D} \tag{5.8}$$

where F_g [s] is the transfer function of the generator block including composite load sensitivity to speed changes.

Figure 5.5 shows the block diagram of the turbine-generator model in an isolated power system with Equations 5.4-5.8. During islanded operation, loads connected to the power system create load deviation (δP_L) as the input for the model. The generator senses the load change as a difference between mechanical and electrical power, leading to acceleration or deceleration of the generator shaft. The output frequency change occurs due to the change in angular speed. Speed regulation tries to equalize the change and gives a command for the governor block to change the turbine intake valve position. The rest of the values, for example, supply pressure, are assumed to stay constant. As a result, the turbine generates more mechanical power for the generator, eventually reaching the steady-state.

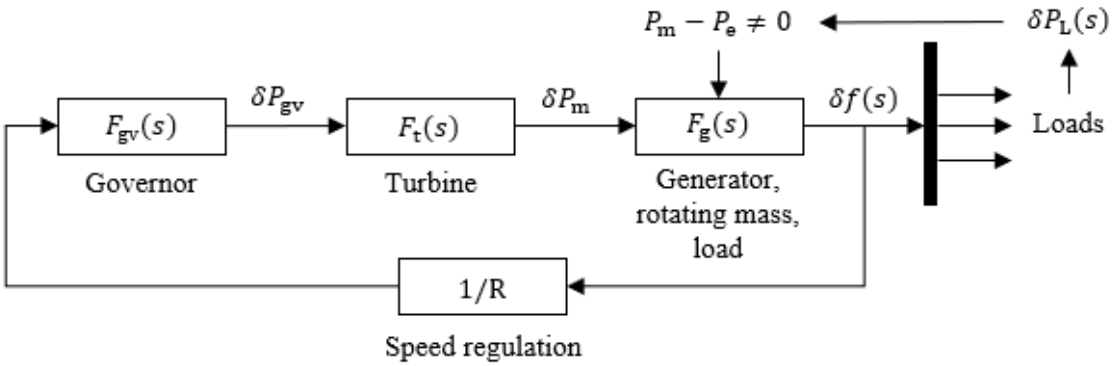

Figure 5.5: Block diagram of the turbine-generator model in an isolated power system.

Figure 5.6 shows the same system model in Matlab Simulink. Equations 5.4-5.8 are used to model the dynamics of the governor, turbine, generator, and load. The speed regulation loop is set to 1/R, where typical R is 0.05-0.06 (Saadat et al. 2003, 533). The load step function is used to set a sudden load change to the system (δP_L) in a range of 0% to 100% from the nominal power. The magnitude of the load step affects the frequency deviation (δf), and by deriving it in relation to time, it gives the corresponding ROCOF values. This model can be assumed to give results of the initial frequency response for steam turbine and ORC units with only one turbine section. If the time constants are changed, it can be assumed to give indicative results of other configurations also.

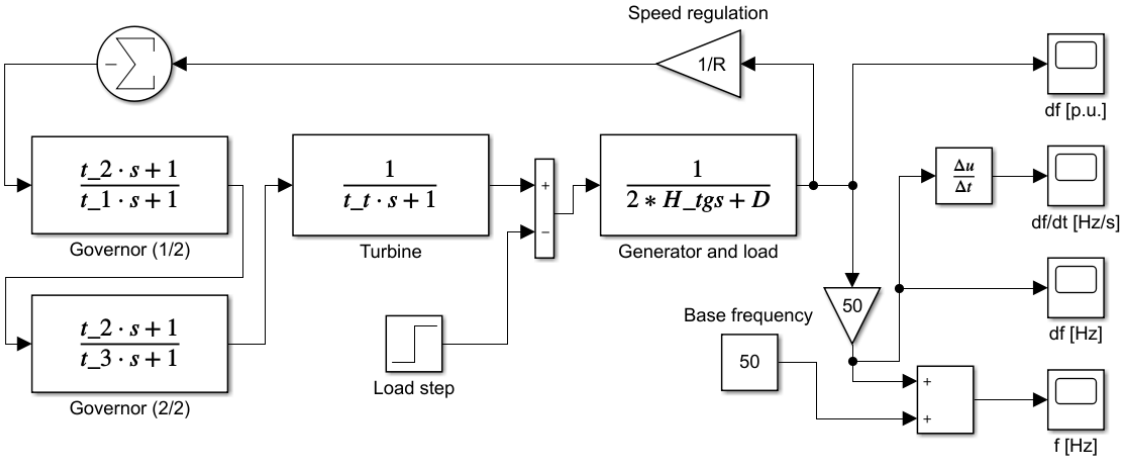

Figure 5.6: Isolated power system model in Matlab Simulink with transfer functions representing dynamics of ORC or steam turbine connected to a generator.

5.5.2 Frequency response simulation

The frequency response of ORC and steam turbine to load steps is simulated with the created model shown in Figure 5.6. In the beginning, the system is running at 50 Hz, and it encounters an immediate load step in a range of 0% to 100%, resulting in frequency transient.

The simulation is divided into three sections. At first, the effect of different load steps is simulated by keeping the other values constant. Secondly, the turbine-generator combined inertia constant is changed to see the effect of system inertia on the nadir and ROCOF values. In the third simulation, the turbine and governor time constants are changed. Table 5.2 presents base values for the simulations.

Table 5.2: Base values for frequency response simulations.

Description			**Value**
Governor time constant 1	t_1	[s]	0.2
Governor time constant 2	t_2	[s]	0
Governor time constant 3	t_3	[s]	0.1
Speed regulation	R	[p.u.]	0.05
Turbine time constant	t_t	[s]	0.5
Frequency sensitivity of the load	D	[%]	0.9
Inertia constant of the turbine-generator	H_tg	[s]	5.0
Load step	δP_L	[%]	20%

Figure 5.7 shows the frequency response graphs with three different load steps, and Table 5.3 gathers the simulation results.

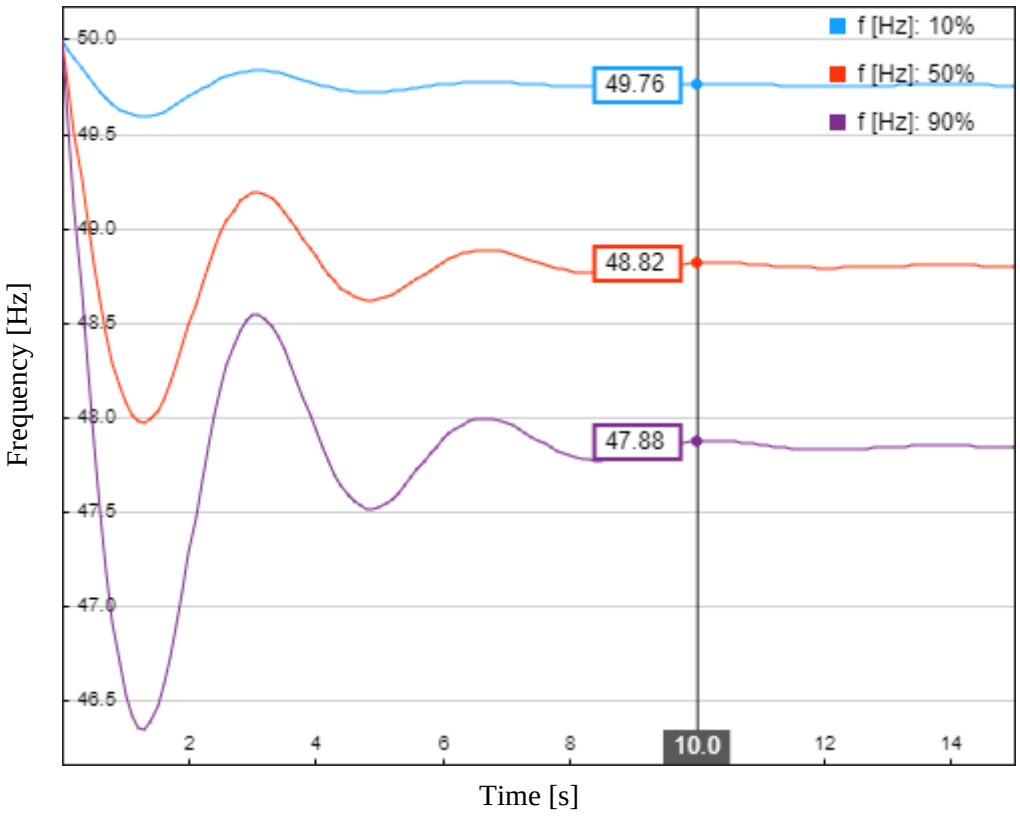

Figure 5.7: Frequency response graphs when the system is exposed to sudden load steps of 10%, 50%, and 90% from nominal level. Measurement line indicating frequency at t = 10s.

Table 5.3: Results of frequency response simulation with different load steps.

Load step from nominal [%]	**Maximum ROCOF** [Hz/s]	**Frequency nadir** [Hz]	**Frequency overshoot** [Hz]	**Steady-state frequency** [Hz]
10%	0.50	49.59	49.84	49.76
20%	0.99	49.19	49.68	49.52
30%	1.49	48.78	49.51	49.28
40%	1.98	48.38	49.35	49.04
50%	2.49	47.97	49.19	48.80
60%	2.97	47.57	49.03	48.56
70%	3.48	47.16	48.87	48.33
80%	3.98	46.76	48.71	48.09
90%	4.49	46.35	48.54	47.85
100%	4.98	45.95	48.38	47.61

Figure 5.8 shows the frequency response graphs with three different turbine-generator inertia constants, and Table 5.4 gathers the simulation results.

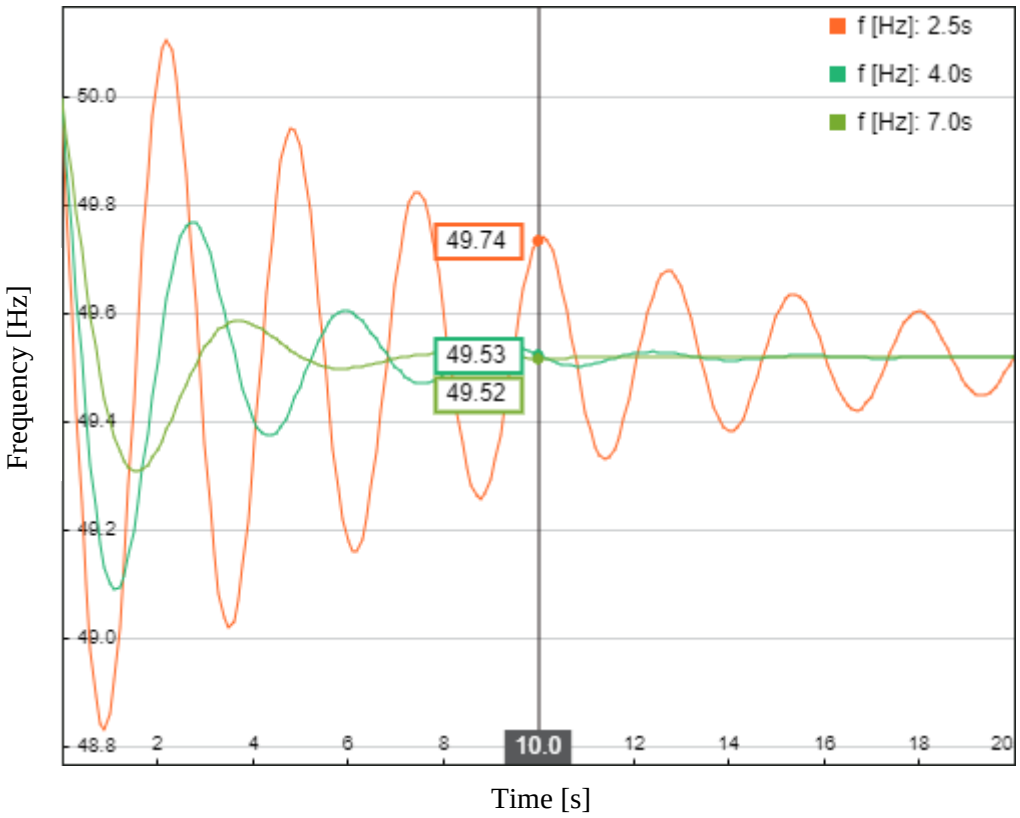

Figure 5.8: Frequency response graphs with different turbine-generator inertia constants when the system is exposed to a 20% load step. Measurement line indicating frequency at t = 10s.

Table 5.4: Results of frequency response simulation with different turbine-generator inertia constants and 20% load step.

Turbine-generator inertia constant [s]	**Maximum ROCOF** [Hz/s]	**Frequency nadir** [Hz]	**Frequency overshoot** [Hz]	**Steady-state frequency** [Hz]
2.5	1.98	48.83	50.11	49.52
3.0	1.65	48.95	49.95	
4.0	1.24	49.09	49.77	
5.0	0.99	49.19	49.68	
6.0	0.83	49.26	49.62	
7.0	0.71	49.31	49.59	

Figure 5.9 shows the frequency response graphs with higher turbine time constant t_t = 1, and then with electro-hydraulic governor $t_1 = t_2$ = 0 and t_3 = 0.05. Graph with base values is for comparison.

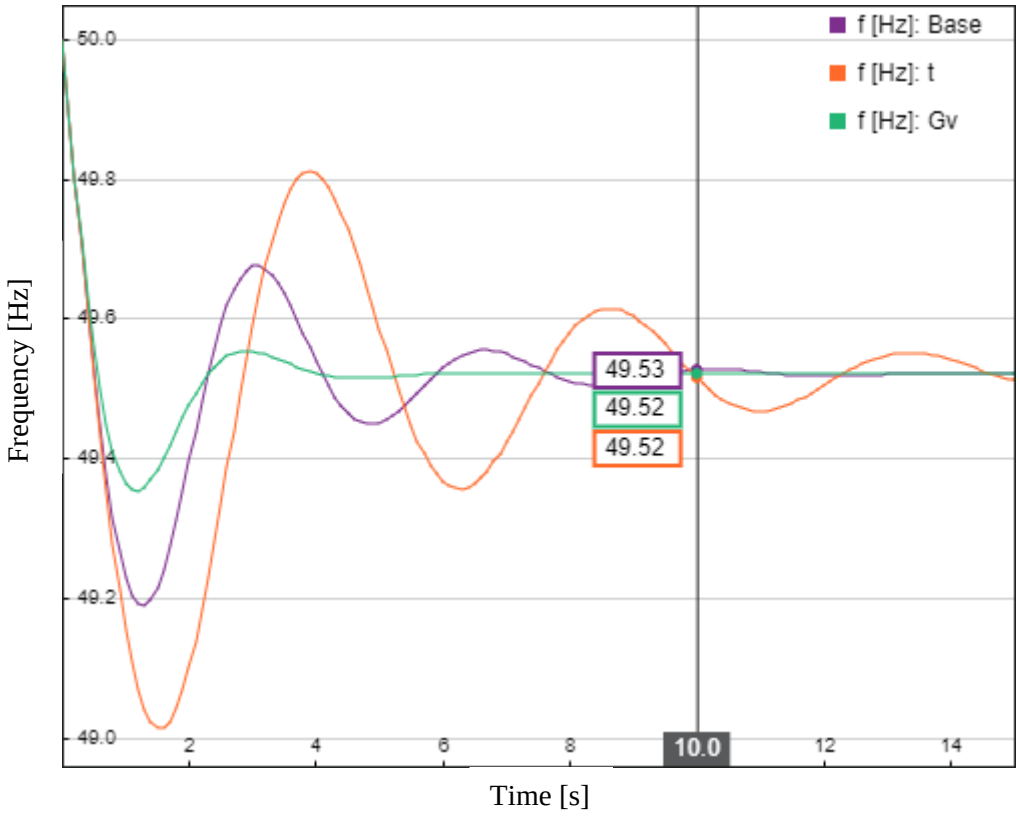

Figure 5.9: Frequency response graphs with higher turbine time constant and with the faster electro-hydraulic governor. Measurement line indicating frequency at t = 10s.

Table 5.5: Results of frequency response simulation with higher turbine time constant and with the faster electro-hydraulic governor.

Changes compared to the base values	**Maximum ROCOF** [Hz/s]	**Frequency nadir** [Hz]	**Frequency overshoot** [Hz]	**Steady-state frequency** [Hz]
t_t = 1s	0.99	49.01	49.81	49.52
$t_1 = t_2$ = 0s and t_3 = 0.05s	0.99	49.35	49.55	

Based on the first simulation, increasing the load deviation will cause higher ROCOF, lower frequency nadir, and lower steady-state frequency. With the base values, over 40%

load step creates too high maximum ROCOF of over 2.0 Hz/s, and over 60% load step may trip the unit when the frequency nadir falls under 47.5 Hz.

Based on the second simulation, decreasing the turbine-generator inertia constant creates high ROCOF even with small load steps and decreases the frequency nadir. It also creates instability to the system with higher frequency overshoots and longer time to reach the steady-state. In turn, increasing the turbine-generator inertia constant protects the system from too high ROCOF and too low frequency nadirs.

Based on the third simulation, changing the time constants of the turbine and governor ends up to the same maximum ROCOF value as with base values. The increased turbine time constant creates more delay to the system, lowering the frequency nadir and reducing system stability. In turn, the faster governor time constants stabilize the system more rapidly after the frequency event. Still, it notable that the turbine-generator inertia and magnitude of the possible load deviations must be evaluated when connecting the system to a microgrid as faster adjustability does not protect the system during the first seconds of the frequency event.

6 PROFITABILITY ASSESSMENT

The economic viability of an energy investment depends on multiple factors, but the reasoning has shifted to follow closely environmental politics. Domestically, regulation of the energy sector is based on legislation including fuel taxes, feed-in tariffs, and subsidies, which have turned decentralized solutions profitable even if the conventional generation has higher process efficiency. At the European Union level, the Emission Trading Directive has placed emission reduction obligations for all the members where non-compliance leads to fees and sanctions (2003/87/EC).

This chapter does investment calculations for the CHP and UPS parallel systems and compares the costs and payback times to a typical diesel generator back-up system. The objective is to get an idea of the initial investment and operating costs between the solutions and in what circumstances they are financially profitable. All calculations comply with the Finnish legislation and results may differ in other countries.

6.1 Calculation of investment costs

The most optimal combustion-based CHP technologies for microgrids in the 100 kW to 2 MW power range are microturbines, SI engines, gasification and ICE systems, and ORC. This section calculates the fixed and variable costs of these technologies combined with UPSs when installed on a site instead of a diesel generator.

6.1.1 **Fixed costs**

In the parallel system, the initial investment cost is dependent on CHP installed costs and UPS system costs, where the battery capacity needs to be evaluated based on the ramping rate and start-up time of the prime mover. If the time before the ramping starts after the frequency event is completely supported via batteries, and UPS supports the load for the full duration of the ramp-up by gradually decreasing the power output, the energy requirement can be approximated with equation:

$$E_{\mathrm{BAT}} = t_{\mathrm{LFC}}(P_1 - P_0) + \int_0^{\frac{(P_1 - P_0)}{r}} [P_1 - (rt + P_0)]\, dt \qquad (6.1)$$

where E_{BAT} [Wh] is the energy drawn from the batteries, P_1 [W] is the power level at the end, P_0 is the power level at the beginning, and t_{LFC} [h] is the time when the ramping r [W/h] starts.

Assuming 1 MW rated capacity for each CHP technology, values from Table 3.5, and t_{LFC} of 5s for natural gas-fueled prime movers and t_{LFC} of 20s for biomass-fueled prime movers, the energy needed for different load steps from 30% initial conditions can be approximated by equation 6.1. The initial values and results are presented in Table 6.1.

Table 6.1: Energy required from batteries with different CHP technologies and load steps.

			Micro-turbine	**SI engine**	**Gasifier and ICE**	**ORC**
Load level at start	P_0	[kW]	300	300	300	300
Delay time	t_{LFC}	[s]	5	5	20	20
Avg. ramping rate		[%/min]	35%	80%	25%	23%
Ramping rate	r	[kW/s]	5.8	13.3	4.2	3.8
40% load level	E_{BAT}	[kWh]	0.4	0.2	0.9	0.9
50% load level	E_{BAT}	[kWh]	1.2	0.7	2.4	2.6
60% load level	E_{BAT}	[kWh]	2.6	1.4	4.6	5.0
70% load level	E_{BAT}	[kWh]	4.4	2.2	7.5	8.1
80% load level	E_{BAT}	[kWh]	6.7	3.3	11.0	11.9
90% load level	E_{BAT}	[kWh]	9.5	4.6	15.2	16.5
100% load level	E_{BAT}	[kWh]	12.7	6.1	20.1	21.8

The overhead costs of power electronics need to be evaluated against the power requirement. In normal conditions, UPS capacity can be sized in relation to critical load power consumption if not considering redundancy, and normal loads are left unprotected. However, if the connected CHP unit has higher rated power than the critical loads, the parallel UPS should be sized according to operational characteristics of the CHP technology to support the system during the full load range. In turn, the UPS capacity needed for the series system would be the total power requirement behind the UPSs.

Assuming that a 1 MW power generation unit is installed to microgrid with 300 kW of critical loads, the capital expenditure of different design options can be approximated. To simplify the comparison, the parallel system is considered to have UPS capacity relative to the rated power of the CHP plant, normal loads are assumed to survive prolonged

periods without power, and diesel generator meets the power quality requirements of the islanded microgrid without the EnergyAware feature. The battery costs are calculated with the Eaton battery runtime calculator using market average costs for LIBs with CHP technologies and VRLA batteries with a diesel generator. The runtime requirement for diesel generators is set to five minutes, and the average hot start-up time with extra five minutes and three full 70% load step cycles for CHP units. UPS costs can be estimated to be 30 k€ for a 300 kW standard unit and 140 k€ for the 1 MW unit with EnergyAware. The typical cost of a diesel generator is 500 €/kW, and other values are found in Section 3.3, Table 3.5. New CHP plants that primarily utilize biomass fuels and have rated power of less than 5 MW can apply for energy subsidies from several sources. In this thesis, a 20% subsidy from Business Finland is assumed (Business Finland, 2020). The initial values and indicative investment costs of different technologies are shown in Table 6.2.

Table 6.2: Fixed costs of CHP and UPS parallel system designs compared to a diesel generator.

		Micro-turbine	**SI-engine**	**Gasifier and ICE**	**ORC**	**Diesel generator**
Avg. installed costs	[k€]	2350	1650	4000	3250	500
UPS costs	[k€]			140		30
Avg. hot start-up time	[min]	0.7	0.3	15	23	0.2
Runtime requirement	[min]	7	6	18	26	5
Battery costs	[k€]	30	25	90	120	12
Subtotal	[k€]	2520	1820	4230	3510	540
Subsidies	[k€]	-	-	800	650	-
Total	[k€]	2520	1820	3430	2860	540

6.1.2 **Variable costs**

Variable costs are linked to the activity level of the generation unit and can be limited to consists of operation and maintenance (O&M), fuel costs, and taxes. In Finland, energy taxes, including energy content tax, carbon dioxide tax, the security of supply charge, and VAT, are levied on electricity, coal, natural gas, peat, oil, and liquid fuels. Fuel used for electricity and heat production needs to be divided because of different taxation policies. Excise duty, which includes energy content tax and carbon dioxide tax, is paid on fuels used for heat production but not for electricity generation. Also, wood biomass is excluded from excise duty. (Sikiö 2019, 48-49.)

In CHP plants, the energy content tax will be reduced by 100%, meaning that the fuel price in heat production consists of fuel price in electricity production, carbon dioxide tax, and other parafiscal charges. Table 6.3 presents O&M costs and total fuel costs allocated per energy produced based on 2019 power plant fuel prices in Finland excluding VAT. (Sikiö 2019, 48-52.) The fuels are assumed to be natural gas for combustion turbines and SI engines, light fuel oil for the diesel generator, and wood chips for the rest of the technologies. Although diesel generator is used only for electricity generation, other values are presented for comparability. O&M costs are higher for CHP units due to additional process equipment.

Table 6.3: O&M costs, fuel costs, and taxes in SHP and CHP production (Sikiö 2019, 51-52; Darrow et al. 2017, 18; Badea et al. 2015, 74-75).

		Micro-turbine	**SI engine**	**Gasifier and ICE**	**ORC**	**Diesel generator**
O&M costs	[€/MWh$_e$]	12	17	25	20	5
Fuel costs, electricity	[€/MWh]	31		21		48
Taxes	[€/MWh]	20		0		26
Fuel costs, heat	[€/MWh]	51		21		74
Fuel costs, CHP heat	[€/MWh]	43		21		65

Considering on average ten-year service life for the CHP systems, the UPS and energy storage variable costs need to include spare parts and new equipment for the whole duration. Generally, LIBs payback the higher initial investment cost in the long run with lower maintenance and energy costs and a long replacement period of up to 15 years compared to around five years with VRLA batteries. For LIBs, 5% annual maintenance and energy costs can be approximated, and 10% for VRLA. The typical replacement period for the UPS system is ten years, so dividing the price as annual cost indicates the O&M costs needed. (Eaton 2020e, 4-14.)

Table 6.4: UPS and batteries O&M and replacement costs for a ten-year operating period.

		Micro-turbine	**SI engine**	**Gasifier and ICE**	**ORC**	**Diesel generator**
UPS O&M costs	[k€/a]			14		3
Batteries O&M costs	[k€/a]	1.5	1.3	4.5	6.0	1.2
Batteries replacement costs	[k€/a]			-		2.4

The cost characteristics can now be presented as a function of operating time. By dividing the total energy required to electricity and heat proportions with the system efficiencies, and considering Table 6.3 and 6.4 statistics, the total variable costs can be presented as equation:

$$C_{\mathrm{V,tot}} = t_{\mathrm{a}} \left[E_{\mathrm{F}} \left(\frac{\eta_{\mathrm{e}}}{\eta_{\mathrm{e}} + \eta_{\mathrm{th}}} C_{\mathrm{F,e}} + \frac{\eta_{\mathrm{th}}}{\eta_{\mathrm{e}} + \eta_{\mathrm{th}}} C_{\mathrm{F,th}} \right) + P_{\mathrm{e}} C_{\mathrm{OM}} \right] + C_{\mathrm{BAT}} + C_{\mathrm{UPS}} \qquad (6.2)$$

where $C_{\mathrm{V,tot}}$ [€] is the variable cost, t_{a} [h] is the operating time, E_{F} [MWh] is the input fuel energy, $C_{\mathrm{F,e}}$ and $C_{\mathrm{F,th}}$ [€/MWh] are the total fuel costs for electricity generation and heat production respectively, C_{OM} [€/MWh] is O&M cost of power generation, and C_{BAT} and C_{UPS} [€] are O&M and replacement costs of batteries and UPSs in the duration.

6.2 Profitability of the investment

Energy investment is a long-term expense that is expected to generate revenue over several years. The investment payback calculation methods aim to determine the rationality and profitability of the used capital. In this instance, the savings come from on-site CHP generation and not buying the equivalent electricity and heat from conventional operators. The exclusion of diesel generators from the site reduces the initial investment, but still, CHP energy production incurs operating and maintenance costs and fuel costs, which need to be considered when calculating the net savings.

All investment payback methods can be said to be based on a comparison of investment income and expenditure, and when assessing profitability, it is practical to look at the issue through the cash flows generated by the investment. From an accounting perspective, investment is often seen as a revenue and payment sheet with monthly and annual transactions. In addition, the time value of money should be considered in calculations with an interest rate. Modern investment theory divides investment calculation methods into two parts; advanced methods it recommends and traditional methods. The net present value (NPV) and the internal rate of return (IRR) methods are considered more advanced methods, while traditional investment accounting methods

include the payback period method (PP) and the return on investment (ROI). (Ranta 2019, 19-22.)

NPV method discounts income and expenses to the present time with an interest rate. An investment is profitable if the net income of the future is higher than the initial investment. NPV with residual value (RV) can be calculated by equation: (Ranta 2019, 38.)

$$NPV = \sum_{t=1}^{n} \frac{S_{\text{net}}}{(1+i)^t} - \left(I - \frac{RV}{(1+i)^n}\right) \tag{6.3}$$

where I [€] is the initial investment, S_{net} [€] is the total net savings per period t [a], i [%] is the interest rate, n is the number of periods, and RV [€] is the residual value.

IRR method calculates the interest rate, which sets the present value of the net savings on investment equal to the initial investment. The higher the outcome, the more profitable the investment is. IRR can be calculated by equation: (Ranta 2019, 46.)

$$IRR = i \;\Leftrightarrow I - S_{\text{net}} \frac{(1+i)^n - 1}{i(1+i)^n} = 0 \tag{6.4}$$

PP method indicates in years the time when the initial investment cost is repaid. The shorter the time, the more profitable the investment is. By considering the interest rate, PP can be calculated by equation: (Ranta 2019, 49.)

$$PP = \frac{-\ln\left(\frac{1}{i} - \frac{I}{S_{\text{net}}}\right) - \ln(i)}{\ln(1+i)} \tag{6.5}$$

Before the investment payback methods can be used, the savings and annual costs need to be calculated. Assuming 95% annual availability and average electricity and heat prices for business consumers (Sikiö 2019, 50.), the net savings can be solved based on the previous chapter and Table 3.5 in Section 3.3. The initial values and results are presented in Table 6.5.

Table 6.5: Calculation of annual net savings by considering the average system efficiency and 95% availability (Sikiö 2019, 50).

			Micro-turbine	SI engine	Gasifier and ICE	ORC
Avg. electric efficiency	η_e	[%]	25%	40%	25%	20%
Avg. thermal efficiency	η_{th}	[%]	48%	40%	58%	63%
Power capacity, electric	P_e	[MW_e]	1.0	1.0	1.0	1.0
Thermal capacity, heat	P_{th}	[MW_{th}]	1.9	1.0	2.3	3.2
Intake fuel energy	E_F	[MWh]	4	2.5	4	5
Peak operating time	t_a	[h/a]	8320			
Electricity produced		[MWh/a]	8320			
Heat energy produced		[MWh/a]	15810	8320	19140	26620
Variable costs, fuel			1294	770	699	874
Variable costs, other			115	157	227	186
Variable costs, total	$C_{V,tot}$	[k€/a]	1410	926	925	1060
Price of electricity		[€/MWh]	100			
Electricity savings		[k€/a]	832			
Price of thermal energy		[€/MWh]	40			
Heat savings		[k€/a]	632	333	766	1065
Net savings	S_{net}	[k€/a]	54	239	673	837

The profitability of the investment is calculated assuming a ten-year service lifetime, zero residual value after the period, and a 6% interest rate. The calculation replaces a diesel generator with a CHP unit, so the CHP fixed costs are reduced with diesel generators fixed costs. The initial values and the results of the investment calculation are presented in Table 6.6. NPV, IRR, and PP are calculated using equations 6.3-6.5 with the net savings shown in Table 6.5.

Table 6.6: Investment calculation results with NPV, IRR, and PP methods.

			Micro-turbine	SI engine	Gasifier and ICE	ORC
Investment	I	[k€]	1980	1280	2890	2320
Interest rate	i	[%]	6%			
Service lifetime	n	[a]	10			
Net savings	S_{net}	[k€/a]	54	239	673	837
Net present value	NPV	[k€]	-1582	479	2063	3840
Internal rate of return	IRR	[%]	-	13.3%	19.3%	34.2%
Payback period	PP	[a]	-	6.7	5.1	3.1

6.3 Investment sensitivity analysis

The sensitivity analysis examines the effect of changing factors in the investment assessment on the overall profitability. When assessing risk, especially the most negatively affecting risk factors should be found to make more accurate predictions of the future state. In this section, the analysis is performed by changing one default value while the other values remain constant. Consequently, the change's effect can be determined by comparing the outcome to Table 6.6 investment calculation results.

The analysis variables are chosen to be a decrease in heat demand, increase in variable costs, increase in the initial investment, and decrease in the peak operating time. The first two options will directly affect the annual cash flow, while the additional investment cost may cause problems in paying the capital during the service life. In turn, the peak operating time will affect both variable costs and revenue.

Table 6.7 shows the investment sensitivity calculation results with decreased heat demand. The net savings are calculated with 70% and 50% heat demands from the values presented in Table 6.5.

Table 6.7: Investment sensitivity calculation with decreased heat demand.

			Micro-turbine	**SI engine**	**Gasifier and ICE**	**ORC**
Investment	I	[k€]	1980	1280	2890	2320
Interest rate	i	[%]			6%	
Service lifetime	n	[a]			10	
Heat savings (70% heat)		[k€/a]	442	233	536	746
Net savings	S_{net}	[k€/a]	-135	139	443	518
Net present value	NPV	[k€]	-2974	-257	371	1493
Internal rate of return	IRR	[%]	-	1.5%	8.6%	18.1%
Payback period	PP	[a]	-	13.8 > n	8.5	5.4
Heat savings (50% heat)		[k€/a]	316	167	383	533
Net savings	S_{net}	[k€/a]	-262	73	290	305
Net present value	NPV	[k€]	-3908	-743	-756	-75
Internal rate of return	IRR	[%]	-	-	-	0.1%
Payback period	PP	[a]	-	-	-	10.5 > n

Table 6.8 shows the investment sensitivity calculation results with increased variable costs. The change will mostly result from changes to fuel costs, such as increased taxation, as O&M costs are a relatively small share of the total variable costs. The difference can be seen by comparing other variable costs to fuel variable costs in Table 6.5. In the calculation, +10% and +20% increases to the total variable costs are used.

Table 6.8: Investment sensitivity calculation with increased variable costs.

			Micro-turbine	**SI engine**	**Gasifier and ICE**	**ORC**
Investment	I	[k€]	1980	1280	2890	2320
Interest rate	i	[%]		6%		
Service lifetime	n	[a]		10		
Variable costs (+10%)	$C_{\mathrm{V,tot}}$	[k€/a]	1551	1019	1018	1166
Net savings	S_{net}	[k€/a]	-87	146	581	731
Net present value	NPV	[k€]	-178	-205	1386	3060
Internal rate of return	IRR	[%]	-	2.5%	15.2%	29.0%
Payback period	PP	[a]	-	12.8 > n	6.1	3.6
Variable costs (+20%)	$C_{\mathrm{V,tot}}$	[k€/a]	1692	1111	1110	1272
Net savings	S_{net}	[k€/a]	-228	54	488	625
Net present value	NPV	[k€]	-3658	-883	702	2280
Internal rate of return	IRR	[%]	-	-	10.9%	23.7%
Payback period	PP	[a]	-	-	7.5	4.3

Table 6.9 shows the investment sensitivity calculation results with increased initial investment costs. The increase can be caused by higher equipment costs, lower diesel generator costs, extra battery and UPS costs, or a lower amount of subsidies for biomass-fueled CHP than expected. In the calculation, +10% and +20% increases to the total investment are used.

Table 6.10 shows the investment sensitivity calculation results with decreased peak operating time. This change will decrease the variable costs based on equation 6.2 and lower the beneficial electricity and heat savings. In the calculation, -30% and -60% decreases to the peak operating time are used, corresponding to 5850 and 3350 hours per year, respectively.

Table 6.9: Investment sensitivity calculation with increased initial investment costs.

			Micro-turbine	SI engine	Gasifier and ICE	ORC
Interest rate	i	[%]	6%			
Service lifetime	n	[a]	10			
Net savings	S_{net}	[k€/a]	54	239	673	837
Investment (+10%)	I	[k€]	2178	1408	3179	2552
Net present value	NPV	[k€]	-1781	351	1774	3608
Internal rate of return	IRR	[%]	-	11.0%	16.6%	30.5%
Payback period	PP	[a]	-	7.5	5.7	3.5
Investment (+20%)	I	[k€]	2376	1536	3468	2784
Net present value	NPV	[k€]	-1979	223	1485	3376
Internal rate of return	IRR	[%]	-	8.9%	14.3%	27.4%
Payback period	PP	[a]	-	8.4	6.3	3.8

Table 6.10: Investment sensitivity calculation with decreased peak operating time.

			Micro-turbine	SI engine	Gasifier and ICE	ORC
Investment	I	[k€]	1980	1280	2890	2320
Interest rate	i	[%]	6%			
Service lifetime	n	[a]	10			
Peak operating time (-30%)	t_{a}	[h/a]	5850			
Net savings	S_{net}	[k€/a]	38	167	471	586
Net present value	NPV	[k€]	-1700	-51	577	1993
Internal rate of return	IRR	[%]	-	5.2%	10.0%	21.7%
Payback period	PP	[a]	-	10.6 > n	7.8	4.7
Peak operating time (-60%)	t_{a}	[h/a]	3350			
Net savings	S_{net}	[k€/a]	22	96	269	335
Net present value	NPV	[k€]	-1818	-573	-910	146
Internal rate of return	IRR	[%]	-	-	-	7.3%
Payback period	PP	[a]	-	-	-	9.2

The investment calculations reveal that the biomass-fueled CHP technologies are the most profitable if the heat energy can be utilized efficiently. Although the initial investment costs are higher compared to fossil-fueled technologies, they payback the capital faster with lower variable costs due to cheapness and favorable taxation policies of wood chips. As microturbines have high fuel costs and still relatively low electrical efficiency, they seem to be unfavorable with all indicators. If the peak operating time is

very low, the gas-fired SI engine outperforms both ORC and gasification because of low initial investment and high electrical efficiency. Still, it should be noted that all CHP technologies are unprofitable with low peak operating times.

According to the sensitivity analysis, the ORC plant performs the best in changing circumstances and can tolerate decreased heat demand, increased variable costs, higher investment costs, and lower peak operating time. The increase to the initial investment seems to have the least effect on the profitability with all technologies. If the SI engine faces a 10% increase in variable costs, the payback goes over the expected service life. The reduction of 30% to heat demand also makes the SI engine investment negative. Still, the percentual reduction is not always the best indicator since, for example, ORC produces over three times more heat than the SI engine, making the efficient utilization of all the thermal energy more difficult.

Consequently, to benefit optimally from CHP technologies, the peak operating time and heat demand needs to be high. If the heat demand is not much higher than electricity demand, the microgrid supply may be preferred to build with a combination of conventional reciprocating engines and biomass-based technologies. This arrangement would also lower the need for batteries and enhance flexibility. The remaining excess heat can also be utilized to generate additional electricity, space cooling, and dry the biomass to reach a higher calorific value of the fuel. The most optimal design from an environmental, operational, and financial standpoint would probably consist of gasification or ORC, sized to fulfill the system’s heating and cooling needs, with additional gas-fueled, more flexible power generation capacity to meet the remaining electricity needs.

7 RESULTS AND DISCUSSION

This chapter reviews the findings of this thesis and analyzes their meaning. First, the research questions are answered, and then suggestions for future research are made.

(1) What are the challenges of CHP in islanded microgrids?

Islanded microgrids are prone to stability, protection, and power quality problems because of low inertia and intermittent RESs. The smaller share of active and reactive power control reserves creates difficulties in balancing power generation and load, leading to system instabilities, especially with slowly adjustable CHP technologies. Too high voltage and frequency deviations may trip the generation from the grid, leading to a possible system blackout. The rapidness of these deviations is a critical issue since high ROCOF values can damage turbomachinery components and create combustion phasing problems for reciprocating engines. The fault current in microgrids can be higher than in a standard distribution network, creating issues for the power generation safety and protection devices. Also, starting additional generation during islanded may affect the grid's frequency and voltage due to sudden intake of current, possibly tripping CHP units in the initial phase of the start-up.

The ability to balance generation and load without auxiliary equipment is dependent on the CHP technology. Combustion turbines are capable of step loading and can perform load following even during higher load deviations of 20% to 40% from nominal. Steam turbines and ORC have inertia to tolerate the changes, but already 20% load imbalances may damage the process components and the ramping should be steady. SI engines have the highest ramping rate and can tolerate the same step loading as gas turbines, but possible combustion phasing problems must be assessed in the design. Gasifier and ICE systems need steady ramping because of slowly adjustable syngas production and have less inertia than turbine prime movers, causing a need for ESS already with small 5% to 10% load steps.

Cogeneration systems are mainly dedicated to continuous operation at the design load level. The changes in electric power output relate to heat production, which may cause problems in meeting heat loads during islanded. If the intermittent generation is high and

CHP unit's output power is reduced, the fraction of fuel energy converted to heat increases, but the total heat energy may reduce excessively to fulfill the heat demand. Thus, the system may need thermal energy storage or a back-up boiler for heat, or extra battery storage for electricity, leading to efficiency losses and additional investments. If the CHP plant is used primarily for load following, it will affect the system efficiency, which can be seen from Figure 3.15. Consequently, one challenge of integrating CHP to microgrids is sizing the unit to meet the electric and heat loads without compromising the fuel efficiency.

(2) How should EnergyAware UPS be configured to mitigate the emerged operational and dynamical problems?

CHP units with under 5 MW_e power capacity can operate normally for 30 minutes when the frequency of the electrical system is 51.0-51.5 Hz or 49.0-47.5 Hz, and ROCOF stays under 2.0 Hz/s. Regarding voltage, the unit must operate continuously and normally when the voltage of the electrical system is between 90% to 105% from the connection point nominal, and 60 minutes at overvoltage of up to 110%.

The frequency response simulation proved that the system inertia and the magnitude of the load deviation have the highest effect on ROCOF and frequency nadir. With ORC and steam turbines, the typical inertia constant of three to seven seconds provides enough inertia to stay above 47.5 Hz after under 50% load step, but ROCOF of over 2.0 Hz/s can be exceeded already at 20% load increase. If the prime mover is ICE, the dynamical analysis should be read from research done by Karjalainen (2020) as it was delimited from this study. However, as ICE based CHP does not have a turbine, the inertia constant can be smaller and create higher ROCOF values as the initial response is so heavily dependent on the kinetic energy reserved in the rotating masses. Still, the frequency nadir can be higher because of faster regulation time, which was noticed in the third simulation with an electro-hydraulic governor with smaller time constants than the standard mechanical-hydraulic.

As a result, EnergyAware UPS needs to be configured to mitigate over 2.0 Hz/s ROCOF and limit the change in the speed of the CHP system while also maintaining frequency over 47.5 Hz/s. In practice, the frequency regulation threshold, the point where UPS starts

to feed active power to the grid, needs to be set according to the CHP technology. Gasifier and ICE system will need more continuous support because of slow fuel adjustment and small inertia, while turbine prime movers can tolerate around 20% load steps without UPS depending on the system characteristics. The parallel system designs will need UPM capacity in relation to the system's adjustability range, while the amount of batteries depends on the start-up time and ramping rate. The large number of batteries reserved for hot start-up also brings synergy benefits with intermittent generation as CHP unit may not need to perform load following, increasing fuel efficiency, and can focus on filling the heat demand.

(3) In which circumstances different CHP and UPS systems are feasible compared to the alternative solutions?

The feasibility of the CHP and UPS parallel system was compared against the standard diesel generator back-up system. From technical and operational viewpoints, gas turbines are inefficient technology in under two-megawatt power range, steam turbines have too long start-up time leading to oversizing the batteries, and Stirling engines are difficult to control precisely. Therefore, only ORC, gasifier and ICE, microturbines, and SI engines were analyzed in the profitability section.

SI engines and microturbines are simpler to control, have higher ramping rates, and faster start-up times compared to ORC and gasification. These aspects reduce the need for batteries and relying on UPS during islanded. However, the profitability assessment proved that the biomass-fueled technologies have higher return expectations if most heat energy can be utilized efficiently. This is because gas-fired technologies have higher fuel taxation policies. Investment calculation with 8320 hours peak operating time and 70% heat utilization rate lead to 5.4 years payback period with ORC, while gasifier and ICE rank second with 8.5 years. Microturbines are not profitable with any indicator, but SI engines sustain the higher variable costs because of high electric efficiency. If the peak operating time is reduced, the gas-fired technologies start to get relatively more profitable compared to biomass due to lower initial investment costs.

The investment sensitivity analysis proved that the ORC plant performs the best in changing circumstances and can tolerate decreased heat demand, increased variable costs,

higher investment costs, and lower peak operating time. The highest negative effect for biomass technologies was caused by decreased peak operating time because otherwise, low fuel variable costs cannot be exploited efficiently. With gas-fired technologies, the highest negative effect is caused by increased variable costs. For SI engine, already 10% increase to variable costs makes the investment unprofitable during the design lifetime. The change is remarkable since in the normal conditions investment payback time is 6.7 years. The lowest effect was by increasing the initial investment, making biomass-fueled technologies safer option in the long-term regardless of the higher equipment costs.

By considering technical, operational, and financial aspects, ORC, gasification and ICE, and SI engine based CHP can be connected with UPSs and be feasible compared to a diesel generator. Biomass systems are better if the peak operating time and heat demand are high, while SI engines tolerate relatively better the lower peak operating times and have higher power to heat ratio. By considering the environmental aspect, biomass technologies are CO_2 neutral and produce fewer air pollutants such as NO_x, CO, and VOCs compared to SI engines, enhancing their feasibility.

The feasibility of the CHP and UPS series system is only thought in this part of the thesis. As this arrangement isolates prime mover and generator from the microgrid, it counters the above-mentioned operational and dynamical problems of CHP. The double-conversion energy storage balances the load, corrects the power factor, and filters ideal power to the grid. Therefore, the generator can be driven at the chosen speed regardless of the mains frequency, enhancing fuel efficiency at partial loads and creating adjustability benefits.

The negative aspects of this solution are converter losses and the need for an increased amount of power electronics as all the loads are behind UPS. According to the Power Xpert 9395P 500-600 kVA UPS technical specification, shown in Appendix 1, the double-conversion efficiency at rated linear load is between 95.6% to 96.3% at different load levels. Based on this, around 4% efficiency reduction is typical in regular operation.

Because the continuous efficiency losses from double-conversion affect the annual profitability, it is clear to say that the parallel system design is better in microgrids where the generating unit is driven most of the time at the nominal load level. However, if the

generating unit is operating most of the time at partial loads, whether due to high amount RESs or oversized capacity, the part-load performance with chosen generator speed can be higher than demonstrated in Figure 3.15, where the shaft speed is regulated to stay constant at grid frequency. An example of this is shown in Figure 3.8, where a 40% load reduction would decrease the electric efficiency of the SI engine by six percentage points if the constant speed is maintained, and by altering the speed, the same load can be met with only two percentage point reduction. Scientific references for other prime movers were not found during the literature review.

In the end, the series system is not probably the most efficient solution in cogeneration applications, where the primary intention is high peak operating time per year. Still, it ensures easy, secure, and reliable operation. The applications where efficiency advantages from the variable-speed operation are higher than converter losses are probably limited to microgrids where the operation focuses on supporting intermittent renewables at off-design load levels.

Eaton has now researched the dynamics, operation, and feasibility of biomass- and gas-fired CHP in this thesis and the dynamics of ICE and generator systems in the study by Karjalainen (2020). Future research should take the background research to the real environment and design how intermittent generation, CHP, and UPSs should be sized to meet the site’s electric and heat loads optimally, minimize operation at partial loads, and benefit the most from UPS energy reserves. The work could include patterning the energy consumption and islanding needs to create load following and energy time-shifting strategies for different months. The energy consumption patterns would also indicate if the microgrid should have a combination of fossil-fueled reciprocating engines and biomass-based generation.

Another research suggestion is to extend this study to find better utilization methods for generated heat, such as in the data center, medical or commercial applications. Here the target would be transferring surplus heat energy of CHP and the site to cooling or additional electricity. For example, the waste heat from UPSs in the data center space could be tried to utilize as one of the heat streams in these systems.

8 CONCLUSIONS

The global energy sector requires innovative ideas to meet the sustainability goals of the future. Modern microgrid structures create an excellent platform for integrating more RESs and decentralized CHP to the power system, but the islanded operating mode poses the generation units to power quality, safety, and operational challenges. This thesis utilized double-conversion UPSs with grid regulation capabilities to accelerate the energy transition towards decentralization.

The research aimed to utilize UPS technology to overcome the challenges of CHP in the microgrids operational framework. The thesis studied what are the challenges of CHP in islanded microgrids, found configuration parameters for UPS to ensure system reliability, and analyzed the overall feasibility of different CHP and UPS system combinations compared to the alternative solutions.

The research consisted of theoretical and assignment phases. The theoretical part studied microgrids, CHP, and UPSs based on literature review and supplier interviews, creating the basis for the modeling and simulation and profitability assessment of the assignment part. During the literature review, CHP technologies were studied from technical, operational, and economic perspectives, and the findings were compared. The dynamic response of CHP to load steps was modeled and simulated to find parameters for the UPS system. The profitability of different design options was assessed by using investment calculation methods. Lastly, the feasibility was evaluated against a diesel generator back-up system and oversized power generation capacity.

Islanded microgrids are prone to stability, protection, and power quality problems because of low inertia and intermittent RESs. CHP's primary issues are slow adjustability, leading to difficulties in balancing power generation and load, and the low toleration of rapid changes in the grid frequency, damaging turbomachinery and causing combustion phasing problems for reciprocating engines. The ability to operate in islanded microgrids without support from UPS is dependent on the used CHP technology. In general, natural gas-fired technologies can tolerate higher load deviations because of better adjustability, but biomass-based systems are slow and need steady ramping, causing a need for ESS with smaller load steps.

CHP units with under 5 MW power capacity can operate normally for 30 minutes when the frequency of the electrical system is 51.0-51.5 Hz or 49.0-47.5 Hz, and ROCOF stays under 2.0 Hz/s. The over-frequency can be controlled easily with fast, automatic speed control, but the main issues are related to keeping ROCOF under 2.0 Hz/s and frequency nadirs over 47.5 Hz after a load deviation. In general, turbine prime movers have enough inertia to stay over 47.5 Hz after under 50% load step, but ROCOF of over 2.0 Hz/s can be exceeded already at 20% load increase. If the prime mover is a reciprocating engine, the inertia constant can be smaller and create higher ROCOF values as the initial response is so heavily dependent on the kinetic energy reserved in the rotating masses. Still, the frequency nadir can be higher because of lower time constants.

In conclusion, UPS can support CHP units to maintain stable operation, but the frequency regulation threshold needs to be set according to the CHP technology. Gasifier and ICE system will need more continuous support because of slow fuel adjustment and small inertia, while turbine prime movers can tolerate around 20% load steps without UPS depending on the system characteristics. If the prime mover is a gas-fired reciprocating engine, the dynamical analysis should be read from research done by Karjalainen (2020).

The feasibility of the CHP and UPS parallel system was compared against the standard diesel generator back-up system. CHP comparative analysis limited the suitable technologies to ORC, gasifier and ICE, microturbines, and SI engines. The profitability assessment proved that the biomass-fueled technologies have higher return expectations if most heat energy can be utilized efficiently because gas-fired technologies have higher fuel taxation policies. Microturbines are not profitable for the application at any investment calculation indicator, but the other selected technologies were proven viable.

Biomass systems are better if the peak operating time and heat demand are high, while SI engines tolerate relatively better lower peak operating times and have higher power to heat ratio. By considering the environmental aspect, biomass technologies are CO_2 neutral and produce fewer air pollutants such as NO_x, CO, and VOCs compared to SI engines, enhancing their feasibility.

The feasibility of the CHP and UPS series system was considered based on the research results. As the arrangement isolates prime mover and generator from the microgrid, it

counters the issues of CHP during islanded. The double-conversion energy storage balances the load, corrects the power factor, and filters ideal power to the grid. Therefore, the generator can be driven at the chosen speed regardless of the mains frequency, enhancing fuel efficiency at partial loads and creating adjustability benefits.

The negative aspect of the solution was a 4% efficiency reduction in typical operation, affecting annual profitability. However, based on the research, at least with SI engines, the efficiency benefits from the ability to vary both torque and engine speed may overcome the converter losses. Consequently, connecting the UPS in series with the power generation unit may be advantageous in microgrids where the operation focuses on supporting intermittent renewables at off-design load levels. In this framework, the benefit is not only the profitability but the reliability and security the power electronics provide.

REFERENCES

2003/87/EC. 2003. Directive of the European Parliament and of the Council on Establishing a Scheme for Greenhouse Gas Emission Allowance Trading Within the Community and Amending Council Directive. [online document]. [referred 1.12.2020]. Available: https://eur-lex.europa.eu/legal-content/EN/TXT/?uri=CELEX%3A32003L0087

2012/27/EU. 2012. Directive of the European Parliament and of the Council on Energy Efficiency. [online document]. [referred 6.9.2020]. Available: https://eur-lex.europa.eu/legal-content/EN/TXT/?uri=CELEX:02012L0027-20200101

Alaperä et al. 2018. Data Centers as a Source of Dynamic Flexibility in Smart Girds. In: Applied Energy Journal. Vol. 229. Pp. 69–79. Publisher: Elsevier. ISSN: 0306-2619.

Badea et al. 2015. Design for Micro-Combined Cooling, Heating and Power Systems. Pp. 396. Publisher: Springer. ISSN: 1865-3529.

Basu P. 2013. Biomass Gasification, Pyrolysis and Torrefaction - Practical Design and Theory. Pp. 548. Publisher: Elsevier. ISBN: 978-0-12-396488-5.

Beith et al. 2011. Small and Micro Combined Heat and Power (CHP) Systems: Advanced Design, Performance, Materials and Applications. Pp. 560. Publisher: Woodhead Publishing. ISBN: 978-1-84569-795-2.

Björnstedt J. 2012. Integration of Non-synchronous Generation - Frequency Dynamics. Doctoral Dissertation by Lund University. Pp. 127. Publisher: Lund University. ISBN: 978-91-88934-56-7.

Bordons et al. 2020. Model Predictive Control of Microgrids. Pp. 280. Publisher: Springer. ISBN: 978-3-030-24569-6.

Breeze P. 2014. Power Generation Technologies (2nd Edition). Pp. 409. Publisher: Elsevier. ISBN: 978-0-08-098330-1.

Breeze P. 2018. Combined Heat and Power. Pp. 102. Publisher: Elsevier. ISBN: 978-0-12-812908-1.

Business Finland. 2020. Energiatuki. [website]. [referred 31.11.2020]. Available: https://www.businessfinland.fi/suomalaisille-asiakkaille/palvelut/rahoitus/energiatuki

Darrow et al. 2017. Catalog of CHP Technologies. Research Report by ICF International, U.S. Environmental Protection Agency & U.S. Department of Energy. Pp. 150.

DBEIS (Department for Business, Energy & Industrial Strategy). 2008. Combined Heat and Power Technology. [online document]. [referred 14.9.2020]. Available: https://www.gov.uk/government/collections/combined-heat-and-power-chp-developers-guides

Eaton. 2012. UPS Handbook. [online document]. [referred 10.10.2020]. Available: https://powerquality.eaton.com/EMEA/Technology-Applications/UPS-Handbook-Download.asp

Eaton. 2020a. About Us. [website]. [referred 8.10.2020]. Available: https://www.eaton.com/us/en-us/company/about-us.html

Eaton. 2020b. Our Businesses. [website]. [referred 8.10.2020]. Available: https://www.eaton.com/us/en-us/company/investor-relations/our-businesses.html

Eaton. 2020c. Backup Power UPS. [website]. [referred 8.10.2020]. Available: http://powerquality.eaton.com/Products-services/Backup-Power-UPS/

Eaton. 2020d. Eaton EnergyAware UPS. [website]. [referred 11.10.2020]. Available: https://www.eaton.com/gb/en-gb/products/backup-power-ups-surge-it-power-distribution/backup-power-ups/backup-power-solutions/eaton-upsaar.html

Eaton. 2020e. The Large UPS Battery Handbook. [online document]. [referred 3.12.2020]. Available: https://www.eaton.com/content/dam/eaton/products/backup-power-ups-surge-it-power-distribution/backup-power-ups/services-resources/Eaton-Battery-Handbook-BAT11LTA.pdf

European Commission. 2008. Combined Heat and Power Generation (CHP). [online document]. [referred 21.8.2020]. Available: https://ec.europa.eu/commission/presscorner/detail/en/MEMO_08_695

European Commission. 2013. Cogeneration, or Combined Heat and Power (CHP). Technology Information Sheet. [online document]. [referred 22.8.2020]. Available: https://setis.ec.europa.eu/system/files/Technology_Information_Sheet_Cogeneration.pdf

European Turbine Network (ETN). 2020. [website]. [referred 15.9.2020]. Available: https://etn.global/about-etn/gas-turbine-technology/gas-turbine-products/

Fingrid. 2018. Voimalaitosten järjestelmätekniset vaatimukset VJV2018. [online document]. [referred 16.11.2020]. Available: https://www.fingrid.fi/globalassets/dokumentit/fi/palvelut/kayttovarma-sahkonsiirto/vjv2018.pdf

Frigo et al. 2014. Small-Scale Wood-Fueled CHP Plants: A Comparative Evaluation of the Available Technologies. In: Chemical Engineering Transactions Journal. Vol. 37. Pp. 847-852. Publisher: Aidic. ISBN: 978-88-95608-28-0.

Gonzalez-Salazar et al. 2018. Review of the Operational Flexibility and Emissions of Gas- and Coal-Fired Power Plants in a Future with Growing Renewables. In: Renewable and Sustainable Energy Reviews Journal. Vol. 82. Pp. 1497-1513. Publisher: Elsevier. ISSN: 1364-0321.

Guo et al. 2018. Flexibility and Ramping Requirements. Research Report by Technical University of Denmark. Pp. 22.

Haga N. 2011. Combustion Engine Power Plants. [online document]. [referred 21.10.2020]. Available: https://www.wartsila.com/docs/default-source/power-plants-documents/downloads/white-papers/general/wartsila-bwp-combustion-engine-power-plants.pdf

Hossain et al. 2014. Large Scale Renewable Power Generation: Advances in Technologies for Generation, Transmission and Storage. Pp. 462. Publisher: Springer. ISBN: 978-981-4585-30-9.

Ibarra et al. 2014. Performance of a 5 kWe Organic Rankine Cycle at Part-Load Operation. In: Applied Energy Journal. Vol. 120. Pp. 147-158. Publisher: Elsevier. ISSN: 0306-2619.

IEC 62040-3. 1999. Uninterruptible Power Systems (UPS) – Part 3: Method of specifying the performance and test requirements. Internal Standard by International Electrotechnical Commission.

IEC 62040-3. 2011. Uninterruptible Power Systems (UPS) – Part 3: Method of specifying the performance and test requirements. Internal Standard by International Electrotechnical Commission.

International Energy Agency (IEA). 2008. Combined Heat and Power: Evaluating the Benefits of Greater Global Investment. Research Report by International Energy Agency. Pp. 39. Publisher: IEA Publications.

International Energy Agency (IEA). 2020. Global Energy Review 2020. Research Report by International Energy Agency. Pp. 55. Publisher: IEA Publications.

Jenkins et al. 2010. Distributed Generation. Pp. 294. Publisher: The Institution of Engineering and Technology. ISBN: 978-0-86341-958-4.

Karjalainen A. 2020. Power System Regulation with UPS Rectifier. Master’s Thesis by Tampere University.

Kirjavainen et al. 2004. Small-Scale Biomass CHP Technologies: Situation in Finland, Denmark and Sweden. OPET Report 12 by VTT Processes & Finnish District Heating Association. Pp. 76.

Klimstra et al. 2017. Cogeneration: Technologies, Optimization and Implementation. Pp. 361. Publisher: The Institution of Engineering and Technology. ISBN: 1-5231-1155-0.

Krishna S. 2014. An Introduction to Modelling of Power System Components. Pp. 134. Publisher: Springer. ISBN: 978-81-322-1846-3.

Kuivaniemi et al. 2013. Future System Inertia. [online document]. [referred 14.11.2020]. Available: https://eepublicdownloads.entsoe.eu/clean-documents/Publications/SOC/Nordic/Nordic_report_Future_System_Inertia.pdf

Lecompte et al. 2017. Case Study of an Organic Rankine Cycle (ORC) for Waste Heat Recovery from an Electric Arc Furnace (EAF). In: Energies Journal. Vol. 10. Pp. 1-16. ISSN: 1996-1073.

Liu et al. 2011. A Hybrid AC/DC Microgrid and Its Coordination Control. In: IEEE Transactions on Smart Grid. Vol. 2. Pp. 278–286.

Maasoumy et al. 2014. Model Predictive Control of Regulation Services from Commercial Buildings to the Smart Grid. In: American Control Conference (ACC) Proceedings. Pp. 2226-2233. Publisher: IEEE. ISSN: 0743-1619.

Majumder R. 2014. A Hybrid Microgrid With DC Connection at Back to Back Converters. In: IEEE Transactions on Smart Grid. Vol. 5. Pp. 251-259.

Marnay et al. 2015. Microgrids – Engineering, Economics, & Experience. Research Report by CIGRE. Pp. 144. Publisher: CIGRE. ISBN: 978-2-85873-338-5.

Microgen. 2020. Engines. [website]. [referred 28.10.2020]. Available: https://www.microgen-engine.com/engines/

Nadir et al. 2015. Thermo-Economic Optimization of Heat Recovery Steam Generator for a Range of Gas Turbine Exhaust Temperatures. In: Applied Thermal Engineering Journal. Vol. 106. Pp. 811-826. Publisher: Elsevier. ISSN: 1359-4311.

Neplan. 2015. Turbine-Governor models: Standard Dynamic Turbine-Governor Systems in NEPLAN Power System Analysis Tool. [online document]. [referred 25.11.2020]. Available: https://www.neplan.ch/wp-content/uploads/2015/08/Nep_TURBINES_GOV.pdf

Petchers N. 2003. Combined Heating, Cooling & Power Handbook: Technologies & Applications – An Integrated Approach to Energy Resource Optimization. Pp. 875. Publisher: The Fairmont Press. ISBN: 0-88173-349-0.

Pini et al. 2019. Technology and Case Studies Factsheets. Research Report by European Institute for Energy Research. Pp. 83.

Rank. 2020. ORC Products. [website]. [referred 25.10.2020]. Available: https://www.rank-orc.com/products/

Ranta T. 2019. Investointilaskentamenetelmät. [lecture material]. [referred 31.11.2020]. Energiatalouden johdantokurssi, Lappeenranta-Lahti University of Technology LUT.

Ray et al. 2020. Microgrid: Operation, Control, Monitoring and Protection. Vol. 625. Pp. 347. Publisher: Springer. ISBN: 978-981-15-1780-8.

Saadat et al. 2003. Power System Control. Pp. 720. Publisher: McGraw-Hill. ISBN: 0-07-561634-3.

Sikiö P. 2019. Polttoaineiden hinnat. [lecture material]. [referred 31.11.2020]. Energiatalouden johdantokurssi, Lappeenranta-Lahti University of Technology LUT.

Sipilä et al. 2005. Small-Scale Biomass CHP Plant and District Heating. Research Report by VTT Processes. Pp. 140. Publisher: Valopaino. ISBN: 951-38-6722-6.

Spentzas, S. 2009. Benefits and Applications of Small-scale and Micro-CHP Systems. In: Distributed Generation & Alternative Energy Journal. Vol. 23. Pp. 6-36. Publisher: River Publishers. ISSN: 2156-6550.

Statnett. 2018. Fast Frequency Reserves 2018 - pilot for raske frekvensreserver. [online document]. [referred 11.10.2020]. Available: https://www.statnett.no/globalassets/for-aktorer-i-kraftsystemet/utvikling-av-kraftsystemet/nordisk-frekvensstabilitet/fast-frequency-reserves-pilot-2018.pdf

Sulla F. 2009. Island Operation with Induction Generators: Fault Analysis and Protection. Licentiate Thesis by Lund University. Pp. 150. Publisher: Lund University. ISBN: 978-91-88934-51-2.

Takalo H. 2013. Mikro- ja pien-CHP: teknologia- ja laitekantaselvitys sekä kannattavuuden tarkastelu tapausesimerkin avulla. Research Report by Micropolis. Pp. 32.

Tamrakar et al. 2017. Virtual Inertia: Current Trends and Future Directions. In: Applied Sciences Journal. Vol. 7. Pp. 1-30. Publisher: Multidisciplinary Digital Publishing Institute. ISSN: 2076-3417.

Tartiere T. & Astolfi M. 2017. A World Overview of the Organic Rankine Cycle Market. In: Energy Procedia Journal. Vol. 129. Pp. 2-9. Publisher: Elsevier. ISSN: 1876-6102.

Tielens P. & Van Hertem D. 2016. The Relevance of Inertia in Power Systems. In: Renewable & Sustainable Energy Reviews Journal. Vol. 55. Pp. 999–1009. Publisher: Elsevier. ISSN: 1364-0321.

Vahidi et al. 2007. Determining Parameters of Turbine's Model Using Heat Balance Data of Steam Power Unit for Educational Purposes. In: Power Systems IEEE Transactions. Vol. 22. Pp. 1547-1553. Publisher: IEEE.

Volter. 2020. Haapakoski, J. CEO, Sales. [phone and email interviews]. [20.10.2020-10.11.2020].

Wärtsilä. 2020. Power Plant Solutions Catalogue. [online document]. [referred 21.10.2020]. Available: https://www.wartsila.com/docs/default-source/power-plants-documents/pps-catalogue.pdf

Ökofen. 2020. MyEnergy365 - Pellets, Solar and Stirling Engine Generator. [website]. [referred 28.10.2020]. Available: https://www.oekofen.com/en-gb/myenergy365/

Power Xpert 9395P 500-600 kVA UPS Technical Specification

Manufacturer's declaration in accordance with IEC 62040-3

Appendix I,1

IEC 62040-3 Subclause	MODEL RATING	500 kVA / 500 kW	600 kVA / 550 kW	600 kVA / 600 kW
	Model catalogue reference	9395P-500(600)	9395P-600(600)	9395P-600(600)-PF1
	Number of UPM's (Uninterruptible Power Modules)	2 UPM's	2 UPM's	2 UPM's
	UPS options:	External battery cabinets, UPM status LED lights, System Bypass Module (SBM), separate battery input, separate rectifier feed		
	Upgradeability	up to 600 kVA	-	-
	External paralleling	Up to 5 units with distributed bypass Up to 7 units with centralized bypass		
5.1.1	UPS topology	Double conversion, 3-level IGBT converters		
5.3.4	UPS performance classification	VFI-SS-111		
MECHANICAL				
	UPS dimensions (width x depth x height)	1890 x 880 x 1880 mm		
	Shipping weight	1505 kg	1505 kg	1505 kg
	Installed weight	1450 kg	1450 kg	1450 kg
	UPS Cable entry	Top / bottom entry		
	UPS Degree of protection	IP20		
	UPS color	Black, RAL 9005		
ENVIRONMENTAL				
6.5.5	Acoustic noise at 1 m in 25 °C ambient temperature	< 81dBA in double conversion, full load < 74dBA in double conversion, <60% load		
4.1.4	Ambient UPS storage temperature range	-25 °C to +60 °C in the protective package		
4.2.1.1 and 5.4.2.2 h	Ambient operating temperature range UPS	0 to +40 °C		0 to +35 °C
		The maximum rate of temperature change shall be limited to 1.67 °C over 5 minutes (20 °C/hour), based on the ASHRAE standard 90.1-2013		
	External battery	+ 20 °C to + 25 °C recommended for optimized battery lifetime		
4.2.1.1	Relative humidity range	5 to 95%, no condensation allowed. There shall be at least a 1.0 °C difference between the dry bulb temperature and the wet bulb temperature, at all times, to maintain a non-condensing environment.		
4.2.1.2	Operating altitude	1000 m above sea level at rated maximum ambient temperature Maximum 2000 m with 1% de-rating per each additional 100m above 1000m		
	RoHS/WEEE compliancy	Yes		

Manufacturer's declaration in accordance with IEC 62040-3

Appendix I,2

	MODEL RATING	500 kVA / 500 kW	600 kVA / 550 kW	600 kVA / 600 kW
EFFICIENCY				
5.3.2 r and 6.4.1.6	Efficiency in double-conversion, rated linear load			
	100% load	95,8 %	95,6 %	95,5 %
	75% load	96,1 %	96,0 %	95,8 %
	50% load	96,2 %	96,3 %	96,3 %
	25% load	95,1 %	95,6 %	95,7 %
	Heat dissipation in double conversion			
	100% load	22,1 kW	25,3 kW	28,3 kW
	75% load	15,2 kW	17,2 kW	19,7 kW
	50% load	9,9 kW	10,6 kW	11,5 kW
	25% load	6,4 kW	6,3 kW	6,7 kW
	No load	4,3 kW	4,3 kW	4,3 kW
	Efficiency in ESS, rated linear load			
	100% load	99,3 %	99,3 %	99,3 %
	75% load	99,3 %	99,3 %	99,3 %
	50% load	99,2 %	99,2 %	99,2 %
	25% load	98,7 %	99,0 %	99,0 %

ELECTRICAL CHARACTERISTICS

INPUT				
5.2.1.a and 5.2.1 b	Rated input voltage	220/380 V; 230/400 V; 240/415 V		
	Voltage tolerance Rectifier input	rated voltage -15% / +15%		rated voltage -9% / +15%
	Bypass input	rated voltage -10% / +10%		
5.2.1 c and 5.2.1 d	Rated input frequency	50 or 60 Hz		
	Frequency tolerance	45 to 65 Hz		
5.2.2 a and 5.2.2 b	Number of input phases			
	Rectifier input	3 phases + PE		
	Bypass input	3 phases + neutral + PE		
5.2.2 d	Input power factor, double conversion mode			
	25-100% load	> 0,99		
	10-25% load	> 0,97		
5.2.2 c	Rated rectifier input current	754 A (400 V)	840 A (400 V)	916 A (400 V)
5.2.2 f	Maximum rectifier input current	908 A	1000 A	1000 A
	Bypass input current, recommended/maximum	722 A / 830 A	866 A / 996 A	866 A / 996 A
5.2.2 h and 5.2.2. i	Input current distortion at rated input current			
	Resistive load	< 3%		
5.2.2 e	In-rush current	<100% of rated current		

Manufacturer's declaration in accordance with IEC 62040-3

Appendix I,3

	MODEL RATING	500 kVA / 500 kW	600 kVA / 550 kW	600 kVA / 600 kW
5.2.2 k	AC power distribution system compatibility	TN-S, TN, TT, IT (4-wire or 3-wire)		
	Rectifier ramp-up, rectifier start and load step	Yes		
	Backfeed protection	Yes, for both rectifier and bypass lines		

ELECTRICAL CHARACTERISTICS

OUTPUT

5.3.2 k	Output power rating	500 kVA	600 kVA	600 kVA
	Output power factor	pf 1.0	pf 0.92	pf 1.0
5.3.2 f and 5.3.2 g	Number of output phases	3 phase + neutral + PE		
5.3.2 b	Rated output voltage	220/380 V; 230/400 V; 240/415 V, configurable		
5.3.2 b	Output voltage variation, steady state	< 1,5%		
5.3.2 i	Total voltage harmonic distortion 100% linear load 100% non-linear load	 < 2% < 5%		
5.3.2 q	Voltage unbalance at reference unbalanced load Phase displacement at reference unbalanced load	< 2,5% < 1,0 deg.		
5.3.2 j	Voltage transient (r.m.s) Recovery time to steady state	0% during transfer from stored energy to normal mode ±4% with 140 ms recovery from 100% load step		
5.3.2 c	Rated output frequency Maximum slew-rate when synchronizing	50 or 60 Hz, configurable 0,5 Hz/s		
5.3.2 l	Overload capability @ max temperature On inverter	10 min 120% load 30 sec 136% load 10 sec 165% load 300 ms >165% load	10 min 110% load 30 sec 125% load 10 sec 150% load 300 ms >150% load	10 min 110% load 30 sec 125% load 10 sec 135% load 300 ms >135% load
	Overload capability @ max temperature – On bypass	Continuous < 115% load 20 ms 1000% load		
5.3.2 m	Output current limitation, short-circuit capability	1600 A L-N, 300 ms 1520 A L-L, 300 ms		
5.3.2 o and 5.3.2 p	Load power factor, permitted range	From 0,7 lagging to 0,8 leading without de-rating		

ESS MODE CHARACTERISTICS

	Transfer time to double-conversion	
	Mains available	No break
	Mains failure	< 2 ms in normal transfer conditions, < 10 ms maximum

	MODEL RATING	500 kVA / 500 kW	600 kVA / 550 kW	600 kVA / 600 kW
	Output voltage variation setting	±10% of nominal voltage, default		
	Storm detection	UPS locks into double-conversion mode when three power line disturbances have forced the unit to double-conversion three times (user adjustable) within a one-hour period (user adjustable).		
	High Alert mode	UPS will stay on double-conversion for one hour (user adjustable), after which the unit will automatically return to operate on ESS.		
VMMS MODE CHARACTERISTICS				
	VMMS availability	Available for multi-module 9395P UPS system, both between internal modules and modules in an external parallel connected system.		
	VMMS operation	When load level per module is less than 55%, VMMS will automatically optimise the number of online modules for optimised operating efficiency. The extra UPMs will be set to ready state mode, capable to transfer online in < 2ms transfer time. The load will be fed in double conversion mode the entire time, even during and after a load step.		
	Redundancy level setting	Number of redundant online UPMs (system wide), configurable.		
	UPM module rotation	System will automatically rotate the ready state UPMs. Enabled by default, configurable.		
BYPASS				
	Type of bypass	Static		
	Bypass rating	600 kVA		
	Bypass voltage range	220/380 V; 230/400 V; 240/415 V tolerance -10% / +10% of rated voltage		
	Transfer time break	No break		
	Back feed protection	Integrated as standard		
	Rated conditional short-circuit current, I_{cc} Static bypass	100 kA (internal ultra-rapid fusing)		
	Internal static bypass ultra-rapid fuse	Bussmann, 170M6417, 1400A 690Vac		
BATTERY CHARACTERISTICS				
5.4.2.2 d	Battery technology	12 V, VRLA		
5.4.2.2 b	Battery quantity	38 - 41 battery blocks, 228 - 246 cells per string	40 - 41 battery blocks, 240 - 246 cells per string	
5.4.2.2 c	Battery voltage range	456-492 V	480 - 492 V	
5.4.2.2 f	Stored energy time	See separate declaration		
5.4.2.2 o	Recharge profile	Advanced Battery Management (ABM®) = 90% resting,10% floating/charging (typical) OR float charge		

Manufacturer's declaration in accordance with IEC 62040-3

Appendix I,5

	MODEL RATING	500 kVA / 500 kW	600 kVA / 550 kW	600 kVA / 600 kW
5.4.2.2 q	End of discharge voltage	1.67 VPC to 1.75 VPC Configurable or automatic (load adaptive)		
5.4.2.2 r	Charging current limit	240 A		
	Temperature compensated battery charging option	Yes (with Environmental monitoring probe)		
	Alternative backup power technologies	Lithium-ion batteries Wet cell batteries NiCd batteries Supercapacitors		
COMMUNICATION CIRCUITS				
5.6	Display	Touchscreen LCD, 4x LEDs for notice and alarm		
	Standard connectivity ports	4 x X-Slot ports for optional cards, 5 x building alarm inputs, 1 x relay output and a dedicated EPO		
	Optional	X-Slot cards: Web/SNMP, ModBus/Jbus, Relay, Hot Sync, ViewUPS-X remote display		
	Complete list of indications and interface devices	See User's Manual		
COMPLIANCE WITH STANDARDS				
IEC 62040-1	Safety Access	Restricted access		
	Degree of protection	IP20; protection against medium sized foreign matter (incl. finger)		
IEC 62040-2	Electromagnetic Compatibility			
	Immunity	EMC Category C3		
	Emissions	EMC Category C3		